Trinity College Dublin
Coláiste na Tríonóide, Baile Átha Cliath
The University of Dublin

The University of Dublin, Trinity College

On the Disaggregation of Optical Networks

Author:
Alan A. Díaz Montiel

Supervisor:
Prof. Marco Ruffini

This thesis is submitted for the degree of
Doctor of Philosophy

February 2021

Declaration

I declare that this thesis has not been submitted as an exercise for a degree at this or any other university and it is entirely my own work.

I agree to deposit this thesis in the University's open access institutional repository or allow the Library to do so on my behalf, subject to Irish Copyright Legislation and Trinity College Library conditions of use and acknowledgement.

I consent to the examiner retaining a copy of the thesis beyond the examining period, should they so wish (EU GDPR May 2018).

Signed: 

Alan A. Díaz Montiel, 24th May 2021

Summary

Optical network disaggregation is a novel technological paradigm enabling the mitigation of lock-in vendor constraints imposed within legacy systems, by aiming to standardise the control interfaces embedded in optical equipment to enable the development and deployment of technology-agnostic remote control systems. This has been mainly enabled by the Software-Defined Networking (SDN)/Network Function Virtualisation (NFV) paradigms, which have been deployed in recent years to operate on top of optical network systems. However, due to the complexity of disaggregating the control from optical networking equipment, the consolidation of fully software-defined optical networks has been rather slow. A major challenge has been the lack of testing platforms that enhance the evaluation of optical SDN control procedures. In this thesis, we propose an optical network emulation system to enhance the development of optical control plane research, and use this platform to investigate how to build intelligent optical control plane procedures in disaggregated optical networks.

Firstly, we developed a packet-optical network emulation platform, Mininet-Optical, to enhance the development, testing and prototyping of disaggregated, software-defined optical control plane procedures. Our emulation platform is the aggregation of two subsystems: i) an optical network simulation system, to simulate the physical performance of Optical Line Systems (OLSs); ii) a packet network emulation system, Mininet, which is a widely used emulation platform in the area of SDN in the packet-network domain. With our system we are capable of modelling state-of-the-art transport equipment such as Reconfigurable Add/Drop Multiplexers (ROADMs) composed of Wavelength-Selective Switches (WSSs) and Variable Optical Attenuators (VOAs), Single Mode Fibre (SMF) spans, Erbium-Doped Fibre Amplifiers (EDFAs) and Optical Power Monitors (OPMs). Thus, we can model a wide variety of optical network systems and topologies that may be complex and expensive to deploy in physical environments. By extending the internal composition of the Mininet emulator, we are able to abstract the transport equipment in virtual electronic components (i.e., ROADMs from open virtual switches), allowing us to extend the control plane emulation enabled in these. We then integrated Mininet-Optical with the well-known SDN Network Operating Systems (NOS) Ryu and Open Network Operating System (ONOS). Consequently, we were able to evaluate real control plane procedures (e.g., algorithms and systems) in large-scale scenarios.

Secondly, we evaluated the usage of the Ryu controller for building control plane systems and built our own system. Then, we integrated the SDN controller to Mininet-Optical to study the implications of transmission margins on network capacity. And, we evaluated how can these margins be mitigated by using Quality of Transmission Estimation (QoT-E) algorithms based on analytical modelling of the OLS. Moreover, we evaluate the use of active monitoring components to assist the QoT-E algorithms. For this, we propose three QoT-E models considering different types of monitoring capabilities: i) assuming the monitoring of signal power levels and Amplified Spontaneous

Emission (ASE) noise; ii) same as i), plus we use the signal power levels to correct the QoT-E prediction inaccuracies in the Nonlinear Interference (NLI) noise occurring at the optical fibre; iii) assuming monitoring capabilities of signal power levels, ASE noise, and NLI noise, such as reference receiver monitors. With these QoT-E models we also evaluated the issues in monitoring placement, focusing on the advantages of retrieving optical signal data at intermediate locations of an optical link.

Thirdly, we looked at the enhancement of QoT-E modules with Machine-Learning (ML) and deep-learning algorithms. We approached this by assessing the ability of ML algorithms to infer the wavelength-dependent operation of optical network components, with focus on the Wavelength-Dependent Gain (WDG) of EDFAs. For this, we propose the usage of the channel load as an input parameter to train the algorithms, in a feature that we label the active wavelength load. We thus used Mininet-Optical to generate large amounts of data to train and test the algorithms that we evaluated. We began our investigation with a thorough evaluation of the Support Vector Machine (SVM) algorithm, and then we also evaluated multiple algorithms, including: K-Nearest Neighbour (KNN), Linear-Support Vector Machine (L-SVM), Radial Basis Function SVM (RBF-SVM), Logistic Regression (LR), Decision Tree (DT), Artificial Neural Network (ANN), Naive Bayes (NB), and Linear Discriminant Analysis (LDA), Random Forest (RF), AdaBoost, and Bagging. We assessed these algorithms in terms of time to train them and F1 score.

Acknowledgements

The writing process of this thesis, as of many others, got impacted by the COVID-19 pandemic. At times, the global situation completely blurred the motivations and hopes for the present and the future, but as I write these last words for the completion of this work in isolation, I think of all the causal events, the serendipity and the people that surrounded me throughout the PhD journey.

I first want to thank the Mexican government and the people for supporting my academic and professional development through the National Council of Science and Technology (CONACYT, in Spanish). May the Mexican nation continue to support national talent.

I also want to thank Dublin the city and Ireland the country; the government, the people, the structure, the culture, the music, the football, the pubs. I salute the staff from The Gingerman and Kennedy's pubs, thanks for bringing the colour to the gloomy Irish sky. Accordingly, I think of the friends that became family and refuge at times: Anna Podczaska, Emily Roch, Cecilia Romero, Brianda Cebreros, Giacomo Politi, Julius Kaiser, Maxime Junak and Maxime Ferrera and their families.

I express my gratitude to the Trinity College Dublin staff from all the layers of its hierarchy, especially to the wonderful CONNECT Centre operational and executive staff: Colette Keleher and Lassane Ouedraogo, Monica Lechea, Catherine Keogh, Shirley Walsh, Andrew O'Connell, Mark Cooney and Linda Doyle. On a similar note, I thank the folks that made the office and my experience as a student a rich environment in one way or another, thank you: Boris Galkin, Jacek Kibilda, Jonathan van de Belt, Andrei Marinescu, Pedro Alvarez, Frank Slyne, Fadhil Firyaguna, Paco Martínez, Diarmuid Collins, Tom O'Dea, Eamonn Dillon and David Fitzpatrick.

As many PhD stories, mine includes the recollection of friendships that transcended cultural and professional barriers. Thank you: Merim Dzaferagic, Connor Sexton and Jernej Hibrar for your sanity and insanity, Erika Fonseca and Joao Santos for your spark of joy, Nima Afraz and Stefan Tonge for your guidance, mis-guidance and creativity. I thank Andrea Bonfante and Daniel Dempsey for your love, care and support. Francisco Paisana and Danny Finn, for your authenticity, spontaneity and curiosity: we will always have Lisbon.

I thank Prof. Marco Ruffini for his supervision and scolding, his mentorship and friendship, and for showing me different ways of approaching science. On a similar note, I also want to thank Prof. Dan Kilper and Prof. Luiz DaSilva for sharing their knowledge on science and life, their leadership and guidance. Moreover, I am grateful and thankful for my evolving team throughout the years: Prof. Christine Tremblay and Sandra Aladin, Yao Li, Weiyang Mo, Bob Lantz, Shengxiang Zhu, Jiakai Yu, Aamir Quraishy and Ayush Bhardwaj.

Of all the people, I am most grateful for having the unconditional love and support from a big extended family. I thank first my brothers from the formerly known Shawn Crew (SC) in Mexicali, Mexico, for their loyalty and support throughout the distance and through all these years.

Thanks to my *adoptive* brother Prof. Johann Márquez, without whom none of this would have been possible. Thanks to Christian Blumm, for his love and support through the darkest times. Thanks to Francisco Alarcón and family, also for their love and support throughout the years. Last but certainly not least, thanks to Kevin Fraser, for his love and support, for being the big brother at all times, and for pushing me through the finishing line.

At last, I thank my family nucleus for absolutely everything. I first thank Fam. Manduchi, Fam. Díaz, Fam. Montiel, Fam. Ramírez, for their love and support, and for being the home I would always come back to. Especially, I thank my grandmother, my parents and my sister: Armida Ramírez, the matriarch, Rosa Montiel, the artist, Arnoldo Díaz, the wise-man and Paulina Díaz, the genius. Thank you for being next to me at all times and for looking after me, everyone should be lucky to have a portion of their love. And of course, I thank Beatrice Manduchi, for being my rock, my best friend and partner, for the first to the last kiss of every day, and for the love that kept me sane when this journey pushed me overboard.

To my real hero,
my dad.

Contents

List of Acronyms

5G 5^{th} Generation

8QAM 8 Quadrature Amplitude Modulation

16QAM 16 Quadrature Amplitude Modulation

AI Artifical Intelligence

AGC Automatic Gain Control

ANN Artificial Neural Network

API Application Programming Interface

ASE Amplified Spontaneous Emission

BER Bit Error Rate

CAGR Compound Annual Growth Rate

CapEx Capital Expenses

CD Chromatic Dispersion

CIAN Center for Integrated Access Networks

CORD Central Office Re-architected as a Datacenter

CPqD Centro de Pesquisa e Desenvolvimento em Telecomunicações

DBM Database Management

DNN Deep Neural Network

DWDM Dynamic Wavelength-Division Multiplexing

EDFA Erbium-Doped Fibre Amplifier

EON Elastic Optical Network

FEC Forward Error Correction

GFF Gain Flattening Filter

GMPLS Generalized Multi-Protocol Label Switching

GN Gaussian Noise

gOSNR Generalized Optical Signal to Noise Ratio

IETF Internet Engineering Task Force

IoT Internet of Things

ITU International Telecommunication Union

KNN K-Nearest Neighbour

ML Machine-Learning

NB Naive Bayes

NBI Northbound Interface

NETCONF Network Configuration Protocol

NFV Network Function Virtualisation

NLI Nonlinear Interference

NOS Network Operating System

NTT Nippon Telegraph and Telephone

LDA Linear Discriminant Analysis

LR Logistic Regression

OCP Open Compute Project

ODTN Open and Disaggregated Transport Network

OIF Optical Internetworking Forum

OLS Optical Line System

OLT Optical Line Terminal

ONES Optical Network Emulation System

ONF Optical Network Foundation

ONS Optical Network System

ONSS Optical Network Simulation System

ONOS Open Network Operating System

OOPT Open Optical & Packet Transport

OpEx Operational Expenses

OPM Optical Performance Monitor

OSNR Optical Signal to Noise Ratio

PCE Path Computing Element

PMD Polarization Mode Dispersion

PON Passive Optical Network

PSD Power Spectral Density

QoS Quality of Service

QoT Quality of Transmission

QoT-E Quality of Transmission Estimation

QPSK Quadrature Phase Shift Keying

RF Random Forest

RBF Radial Basis Function

ROADM Reconfigurable Add/Drop Multiplex

RWA Routing and Wavelength Assignment

SBI Southbound Interface

SCI Self-Channel Interference

SDN Software-Defined Networking

SMF Single Mode Fibre

SRS Stimulated Raman Scattering

SVM Support Vector Machine

TAI Transponder Abstraction Interface

TCP Transport Control Protocol

TIP Telecom Infra Project

UI User Interface

VOA Variable Optical Attenuator

WDG Wavelength-Dependent Gain

WDM Wavelength Division Multiplexing

WL Wavelength Load

WRON Wavelength-Routed Optical Network

WSS Wavelength-Selective Switch

XCS Cross-Channel Interference

YANG Yet Another Next Generation

List of Figures

List of Tables

1 Introduction

In the past decade, the consolidation of the 5th Generation (5G) of Telecommunication standard technologies has driven the re-architecture of networking and communication systems. As envisioned by the Next Generation Mobile Networks (NGMN) Alliance in 2015, three key requirements have to be enabled in this type of network: enhanced mobile broadband (eMBB), massive machine type communications (mMTC) and ultra reliable and low latency communication (uRLLC) [4]. This in turn imposes technical challenges to the operational paradigms followed by contemporary telecom central offices. Traditionally, the central offices that orchestrate the provisioning of communication services are physically located at remote locations from the end-users. While this operation is appropriate to handle latency independent applications such as telephony or email, it is not suitable for use cases with strict latency requirements such as autonomous vehicles and a wide-range Internet of Things (IoT) applications, which fall under the umbrella of 5G technologies. Moreover, by enabling mMTC, central offices are required to process higher amounts of traffic requests demanding higher amounts of bandwidth. For instance, the rise of inter-communicated devices (i.e., smartphones and TVs) and the resurge of machine-to-machine applications such as video surveillance, healthcare monitoring and transportation, has been reflected in global increases of IP traffic, as shown in the global IP traffic forecast by Cisco [1] in Figure 1.1, which is a pattern that is expected to continue to grow at a pace of 14.1 zettabytes per year (since 2018). Consequently, in order to be able to provision high bandwidth and low latency services, telecom operators are trying to move their central offices closer to the end-users.

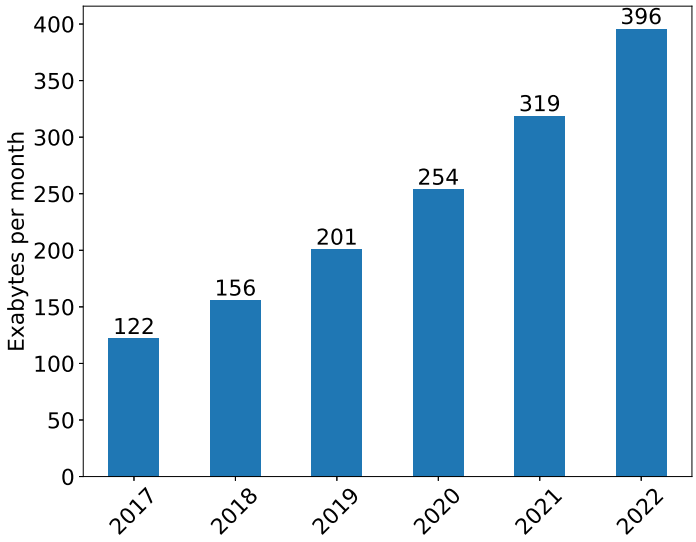

Figure 1.1: Cisco VNI Global IP Traffic Forecast, 2017 - 2022 [1].

However, the current architecture of central offices provides limited support for 5G services and business models. This is mainly because the legacy equipment that compose them are dedicated hardware systems developed to provide fixed networking functions, such as Passive Optical Networks (PONs). Consequently, telecom operators are looking at applying data centre architectural and operational principles, motivated by the fact that data centres are a cost-effective type of facility to process and deliver large amounts of data with commodity hardware (i.e., general purpose servers) [5]. Thus, the re-architected central office placed closer to the end-user is commonly refer to as the edge data centre. Today, the industry standard model addressing the technical and architectural challenges in migrating the central office to data centres is the Optical Network Foundation (ONF) Central Office Re-architected as a Datacenter (CORD) project [5–7], to which many operators have been subscribing since its foundation in 2017. In fact, in a 2017 survey by IHS Markit [8], 85% of operator respondents planned to create, or will have already deployed smart central offices (mini data centres) by 2018, as illustrated in Figure 1.2, and seven out of ten participants were planning to deploy CORD as their central offices.

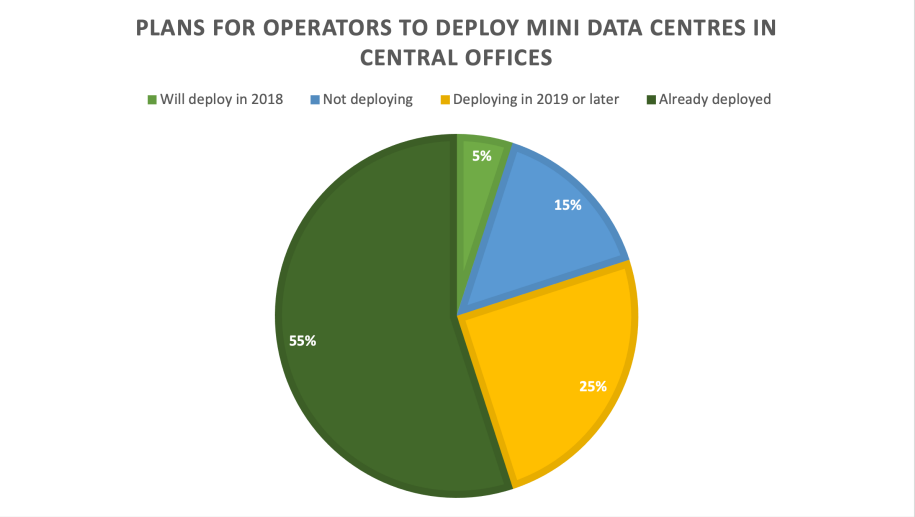

Figure 1.2: IHS Operator Survey.

At the backbone of central offices we find legacy optical network technologies such as PONs, Optical Line Terminals (OLTs), Reconfigurable Add/Drop Multiplexers (ROADMs), micro-electro-mechanical systems (MEMS) switches and arrayed waveguide grating routers (AWGRs), and broadband network gateways (BNG), that run physical networking functions to process traffic requests and provision services within the optical domain. These systems operate with fixed physical and operational configurations (i.e., fixed-grid transceivers) that limit the flexibility of optical networking control. Moreover, these systems are commonly designed to inter-operate with technologies developed by single vendors and manufacturers. In addition, given the operational complexity and specificity of legacy equipment, the physical upgrade (or "rip and replace") cycle of these is considered within a 10-20 year span, which is a challenging constraint that limits telecom operators to keep up with technological trends that evolve fast. Consequently, legacy optical equipment are not adequate candidates to be at the backbone of 5G networks, other than to provide support to older services (i.e., 4G, 4G-LTE), since the type of services envisioned in this type of network require the ability for optical network equipment to provide customised, flexible and easy-to-upgrade functionality.

To fill in this gap, the disaggregation of optical networking equipment enabled with Software-

Defined Networking (SDN)/Network Function Virtualisation (NFV) is an area receiving increasing attention in recent years, especially from operators who want to part from legacy vendor lock-in restrictions [9–11]. Thoroughly discussed in Chapter 2, optical network disaggregation is a paradigm that aims to standardise the fixed operational control embedded in optical equipment (i.e., transceivers, ROADMs, etc.) to enable the deployment of multi-vendor open interfaces that are run in a centralised controller that has a global view of the full network as well as the individual control of the equipment, enhancing greater autonomic network performance. The latter, also enables the development of sophisticated control plane procedures that were not possible with legacy equipment. Moreover, optical network disaggregation tackles the lack of flexibility of legacy systems, since disaggregated equipment is designed to enable customised operability (i.e., variable bandwidth and bandwidth on-demand), as well as the interoperability of devices from different vendors and manufacturers. Furthermore, disaggregation tackles the upgradability issues of legacy equipment, since the bare-metal infrastructure on which disaggregated systems run is more economic to replace, complying with data centre rip and replace cycles of 3-5 years. Moreover, the emergence of programmable (or software-defined) networking equipment is enabling the convergence of Telecommunication networks at all layers (i.e., wireless, packet and optical), which is an area of research that requires further investigation. As a result of the technological advancements for 5G networks and the new business models that these enable, according to a technological report by Markets and Markets [12], the global optical networking and communication market size is expected to reach USD $ 32.8 billion by 2030, at a CAGR of 6.2% from 2020 to 2030. This market was valued at $ 16.9 billion in 2019. In this report the authors considered as key factors the surging demand for high bandwidth, the heavy deployment internet of things (IoT) applications and machine-to-machine (M2M) technologies, as well as the rise in mobile data traffic.

Nonetheless, the migration of central offices to data centres, and in particular the transition from optical legacy systems towards disaggregated optical networking has been rather slow. This has been mainly because it is technically challenging to disaggregate the control of optical network equipment and to model their functionality at the control system, while at the same time enabling the inter-operability of multi-vendor systems with different requirements. The main areas that need to be addressed are:

- **Disaggregated equipment:** Firstly, the lack of optical disaggregated equipment has been a major limitation. In fact, only in recent years few working groups and companies have released their proposals of disaggregated optical equipment, such as the Voyager and Cassini open terminals from the Telecom Infra Project (TIP), which are fabricated by ADVA and Edgecore, respectively [13, 14]. However, as the race for entering the market of optical network disaggregation is tightening, more companies continue to release products that enable this type of operation. For instance, in February 2021, Cisco and Fujitsu released the Phoenix [15] and 1FINITY [16] projects, initiatives emerged from the OOPT-TIP [17] consortia, that consists in their own version of a white-box node and network operating systems.
- **Communication protocols and interfaces:** Moreover, the lack of interfaces to interconnect this type of device to the SDN controller has been another limitation. Also in recent years, communication protocols have emerged to support the development of this type of interface, such as OpenFlow [18] and Yet Another Next Generation (YANG)-based models OpenROADM [19] and OpenConfig [20], and, more recently, T-API [21] and Transponder Abstraction Interface (TAI) [22].

- **SDN controllers:** Additionally, only few SDN controller frameworks have been actively promoted within the optical networking and communications community: Ryu by Nippon Telegraph and Telephone (NTT) [23], OpenDayLight by The Linux Foundation [24] and Open Network Operating System (ONOS) by the ONF [25]. Although other customised solutions have been proposed, such as the ABNO controller [26, 27]. However, as more optical disaggregated equipment is becoming available in the market, more hardware demonstrations showcasing the real performance impact of SDN-controlled optical networks are being evaluated. We can conclude that as real control systems for disaggregated optical networks are coming together, there is a latent interest in multi-layer SDN control strategies and demonstrations, such as the optimisation of controller placement to improve network latency, resiliency, energy efficiency, load balancing, etc. [28]. For instance, Mayoral *et al.* [29] have proposed a partially disaggregated network architecture including multi-layer (L0-L3) and multi-vendor transport components. They have showcased a use case for multi-layer service provisioning in a real testbed. Sambo *et al.* [30] have proposed a restoration paradigm "delegated restoration", in a hybrid centralised and distributed SDN environment using YANG-based NETCONF interfaces for controlling the network devices and defining networking functions.

Evidently, since these technologies have only become commercially available within the past five years, the evaluation of optical control planes supporting them is an area of research that still requires further investigation.

A key question regarding the operation of the disaggregated optical control plane is its ability to add agility to the network while optimising the performance of resources. Due to the strict analog operation of optical network equipment, it is rather hard to model the physical performance of the optical layer at the control plane with high levels of accuracy, mainly because of the wavelength-dependent operation of devices such as ROADMs and Erbium-Doped Fibre Amplifiers (EDFAs). This complexity thus increases with the heterogeneity of functionality provided by the multi-vendor environment proposed in disaggregated optical networks. As a consequence, optical networks operate with transmission margins that allow them to guarantee service provisioning with strict Quality of Service (QoS) requirements. Unfortunately, the application of such margins can lead to the underutilisation of optical resources (i.e., optical spectrum) [31] limiting the overall bandwidth capacity. While practical considerations for designing and deploying near-zero margin networks have been proposed in recent years [32], operators and vendors have also been actively investigating the development of estimation tools capable of predicting the performance of individual optical network components and optical transmissions in technology agnostic scenarios, such as the GNPy Project [2]. More recently, cognition-assisted (i.e., Machine-Learning (ML)-based) solutions have been proposed to enhance the prediction of optical network performance [33–37, 37–56].

Furthermore, a major challenge that is faced by optical networking and communications research is the lack of testing and prototyping platforms that can assist the investigation of control plane procedures integrated within the disaggregated data and physical planes. This is a significant limitation because it constraints optical control plane research in the context of 5G networks to small testbeds that are hard and expensive to scale and consequently to be reproduced. Since the development of SDN in the electronic domain began earlier than in the optical domain (circa ’06 [57], though informally some scientist would consider studies from the ’80s as the pioneering time of SDN [58]), this field benefited from the extra years of experience. Among the strongest advantages in the electronic domain were the testing and development tools available to enhance the development

of packet SDN control systems. In particular, the SDN learning and prototyping tool Mininet [59], which is a packet network emulation system enabling the modelling of SDN scenarios in this domain, as well as assessing the performance of real control systems by emulating the operation of packet network components (e.g., links and nodes). Mininet has been widely used since its first appearance to the community in Lantz *et. al.* [60], and it was recently awarded the ACM SIGCOMM Test of Time Paper Award [61]. Because of the success of Mininet in the elctronic domain, we concluded that the optical networking and communications community would benefit from a similar emulation environment that would enhance the development of optical SDN control planes.

1.1 Research Questions

At the Optical Network Architectures (ONA) Laboratory, the vision of future 5G networks requires a multidimensional convergence for providing the overall architectural framework to bring together all the different technologies within a unifying and coherent network ecosystem [62]. In this thesis, we focus on the challenges encountered in the optical domain, particularly addressing the issues concerning the optical control plane in the context of optical disaggregated networks and its ability to add agility to the network management by exploiting the flexibility enabled in this type of systems.

How can novel optical SDN control systems be tested before deployment in an operational network?

As we have described above, the development of SDN control systems in the optical domain is limited due to the lack of equipment readily available supporting end-to-end disagreggation. Thus, it is highly relevant to have at hand an emulation/simulation platform that would enhance the development of real physical systems, and that would be robust to future trends in optical networking and communications research. Accordingly, we first investigated the definitions and uses of Mininet in the electronic domain, in order to identify similarities of network operation with the optical domain. We found that higher level networking functions such as routing could be easily migrated to the optical control plane. However, due to the analog nature of optical network components, lower level functions concerning the processing of connections would require a set of assumptions that are not shared with the packet domain.

Thoroughly discussed in Chapter 3, our primary aim is the development of a software system that enables the simulation of the transmission physics in optical networks, while simultaneously providing the emulation of disaggregated optical networks control. As we developed our emulation system and validated the optical networking transmission models, we were capable of addressing optical SDN open questions regarding the inner composition of disaggregated optical control systems. For instance, we examined:

What are the implications to network capacity of the use of transmission margins? How can a Quality of Transmission Estimation (QoT-E) module improve the configuration of these margins? And, how can active monitoring assist QoT-E modules in the optical control plane?

Our aim is to investigate what is the impact of receiver margins to the network capacity, and how in the context of optical SDN can a controller improve the management of resources to maximise network capacity utilisation by implementing a QoT-E module. Having information about the overall performance of the network could help to improve the management of resources. For instance,

optical network systems operate with transmission margins in the order of ± 3-7 dB, limiting the transmission capacity of the network [63].

Firstly, we considered monitoring procedures that require external equipment from the network topology to assess the performance of the network and the individual components (i.e., Optical Power Monitors (OPMs)). In this context, the use of monitoring equipment is thought to be included as a static element in the network, similar to a switch that once deployed could not change its physical position. Due to the fact that the costs of using monitoring equipment increase with the number of devices, understanding the optimal amount of monitoring equipment needed in a given network is an utmost important research topic [64]. Thus, we investigated how the optimal cooperation of QoT-E with active monitoring could help tackling the mitigation of margins and improvement of network capacity, while using a suboptimal amount of active monitoring at the same time. We then deepened our investigation on the suboptimal amount of active monitoring the could help with these issues. Our findings on these topics are discussed in Chapter 4.

In parallel to the early stage of the development of QoT-E subsystems in the context of disaggregated optical networks, in the Computer Science community, technologies from Artifical Intelligence (AI) such as ML and deep-learning started to gain attention from all scientific fields, due to the optimised computing performances to solve classification and estimation problems by looking at raw data [65–69]. Consequently, we examined the potential to use ML algorithms to improve the performance of QoT-E subsystems. We addressed this problem in the form of:

How can machine-learning algorithms assist QoT-E modules? And, how feasible is to implement supervised-learning algorithms in the optical control plane?

The uses of QoT-E modules aim to assist networking functions such as dynamic routing and fault management, as well as to mitigate the use of margins to improve network capacity. As mentioned above, an approach to enhance QoT-E modules is to use active monitoring equipment to keep track of the transmission. Unfortunately, this solution does not scale well with an increasing number of connections and network devices. Consequently, we investigated how a QoT-E could improve its performance by taking advantage of ML algorithms. Then, following the trends in exploring the application of cognition to the optical control plane, we investigated the potential of deep-learning to predict non-modellable optical transmission physics (i.e., wavelength-dependent operation of network devices).

To begin with, we limited the composition of the raw data available to the ML algorithms by using only the data that our simulation system could provide. Then, we chose a popular ML algorithm, Support Vector Machine (SVM), and evaluated the technical requirements to build the learning model and its implications to the optical control plane. Subsequently, we also evaluated the performance of multiple machine- and deep-learning algorithms for this task. These studies are discussed in Chapter 5.

Moreover, researchers continue to investigate to what extent could we benefit from including cognition-based control systems to operate over disaggregated optical networks, and achieve with that the development of autonomous control systems, enabling the maximum optimisation of performance of optical communications. However, because disaggregated optical network systems are currently under development, it is unclear how to determine the real potential of intelligent (cognitive) subsystems assisting the optical SDN control plane [70]. In modern literature, there exist a vast amount of efforts exploring these technologies, which rely on a number of assumptions and lim-

itations based on the current operation of quasi-static and partially disaggregated optical networks [32, 71]. As future trends continue to appear, the development of disaggregated optical networks and the technologies to enable them will continue to adapt to these. While optical control systems could benefit from ML algorithms, their performance is entirely dependent on the type of data that is possible to retrieve from a network system, the frequency in which this data can be retrieved, the amount and format of this [70]. As a consequence, it is utmost important to understand the features of monitoring equipment in optical networks, and how do these operate in the context of disaggregation. Thus, to what extent can control systems benefit from active monitoring.

1.2 Thesis outline

Chapter 2 - Background

In this Chapter we discuss the related work that motivated the research carried out for this thesis. We begin with a thorough description of optical network disaggregation and enabler technologies such as SDN/NFV. Additionally, we present the global consortia that has emerged in recent years to tackle the technical challenges encountered in this area. Subsequently, we discuss the work that has been disclosed in recent years concerning the disaggregated optical control plane, with special focus on active monitoring research works.

Then in section 2.2 we discuss the two main optical network optimisation and planning tools available today, Net2Plan [72] and GNPy [2], emphasising how the need for such tools is so strong that they have been widely accepted by industry to be deployed in commercial control systems [2, 25, 73]. Then, we contextualise the need for similar systems that enable the assessment of optical control plane procedures also.

In section 2.3 we review the state-of-the-art of QoT-E modules developed to assist optical networking functions such as dynamic wavelength allocation and fault management. We begin our discussion with estimation models mainly based on heuristic functions or statistical models, and then we also include cognition-based estimation models. We conclude this Chapter with a set of conclusions in section 2.4.

Chapter 3 - Mininet-Optical, an Emulation System

In Chapter 3 we present Mininet-Optical, the first SDN packet-optical network emulation system enabling optical control plane testing and prototyping. We begin with an architectural overview of the system and its integration with the Mininet project [59]. Then, we describe the transmission physics models that describe the physical operation of optical network equipment and optical transmissions in section 3.3. In section 3.4 we explain the integration of these physical models and their role in the context of Mininet-Optical. Similarly, in section 3.5 we present the architecture and algorithm of our emulation system. Since Mininet-Optical is based on its packet network counterpart, Mininet [59], we only explain how we do the integration of the optical network simulation system with Mininet. In section 3.6, we show the validation assessments of Mininet-Optical against the GNPy project [2] and the COSMOS testbed [74]. Lastly, we summarise our progress with our system in section 3.7.

Chapter 4 - Optical Control Systems

In Chapter 4 we present a set of studies regarding the operational challenges of optical control systems in a disaggregated context. We introduce the challenges of optical control systems and the architecture of our control system in sections 4.1 and 4.2, respectively. Then, we present a study evaluating the impact of the use of margins to optical network capacity in section 4.3. In section 4.4 we present our studies in the use of active monitoring to improve the performance of QoT-E systems. We summarise our work in section 4.5.

Chapter 5 - Cognitive-Assisted Control

In this Chapter, we present a set of studies with regard to the inclusion of cognition capabilities to the optical control plane. We introduce the scope and describe the problems that we address in sections 5.1 and 5.2, respectively. In section 5.3, we present a study evaluating the SVM ML algorithm in terms of its suitability to handle optical networking data. Due to the promising findings with SVM, in section 5.4 we deepen our assessment of ML by evaluating several algorithms. We discuss our conclusions and summarise our work in section 5.5

Chapter 6 - Conclusions and Future Directions

In Chapter 6, we discuss the current limitations of Mininet-Optical and present future directions in improving the system and facilitating its use for the community. Additionally, we discuss our view of the current context of disaggregated optical networks and give our view on what challenges require further investigation.

1.3 Contributions

The main contribution of this thesis is the design of intelligent control planes for highly dynamic disaggregated optical networks. To facilitate our studies, and due to the lack of optical control plane prototyping and testing tools, we thus developed the Mininet-Optical packet-optical network emulation system, which is another key contribution of this work, including:

- Development of optical network simulation system.
- Development of component interfaces to enable SDN control.
- Integration of a simulation environment with emulated network interfaces.
- Validation of our transmission physics models against the GNPy [2] simulation system.
- Validation of our transmission physics against the COSMOS testbed [74].

With this at hand, we have identified the potential of active monitoring to assist QoT-E monitoring, and found that it is possible to trade-off sophisticated monitoring equipment (i.e., capable of isolating nonlinear interference noise) with simpler monitoring equipment (i.e., capable of monitoring signal power only). For this, we have built and integrated a QoT-E algorithm into an optical SDN controller, and evaluated that by placing monitoring equipment at various locations in an optical link we can achieve comparable performance to sophisticated monitoring equipment.

Additionally, we have investigated the requirements to build QoT-E systems assisted with ML algorithms. For that, we have evaluated multiple ML algorithms and assessed their ability to improve their estimation performance by feeding active wavelength load information as a parameter to train these models. Additionally, we have evaluated the training times required to build these models, to provide a better understanding of their suitability to be deployed in the optical control plane.

1.4 Dissemination

Accepted papers

- Díaz-Montiel AA, Bhardwaj A, Lantz B, Yu J, Kilper D, Ruffini M. Real-Time Control Plane Operations for gOSNR QoT Estimation through OSNR Monitoring. In *Optical Fiber Communication Conference (OFC)*, 2021. Optical Society of America.
- Lantz B, Yu J, Bhardwaj A, Díaz-Montiel AA, Ruffini M, Quraishy A, Santaniello S, Chen T, Fujieda R, Mukhopadhyay A, Zussman G, Kilper D,. SDN-controlled Dynamic Fronthaul Provisioning, Emulated on Hardware and Virtual COSMOS Optical x-Haul Testbeds. In *Optical Fiber Communication Conference (OFC)*, 2021. Optical Society of America.

Published papers

- Díaz-Montiel AA, Lantz B, Yu J, Kilper D, Ruffini M. Real-Time QoT Estimation through SDN Control Plane Monitoring Evaluated in Mininet-Optical. In *Photonics Technology Letters*, 2021. IEEE.
- Díaz-Montiel, A. A., Ruffini, M. A Performance Analysis of Supervised Learning Classifiers for QoT Estimation in ROADM-based Networks. In *International Conference on Optical Network Design and Modeling (ONDM)*, 2019.
- Díaz-Montiel, A.A., Aladin, S., Tremblay, C. and Ruffini, M. Active wavelength load as a feature for QoT estimation based on support vector machine. In *ICC 2019 IEEE International Conference on Communications (ICC)*, 2019 (pp. 1-6).
- Díaz-Montiel, A.A., Yu, J., Mo, W., Li, Y., Kilper, D.C. and Ruffini, M. Performance analysis of QoT estimator in SDN-controlled ROADM networks. In *2018 International Conference on Optical Network Design and Modeling (ONDM)*, 2018 (pp. 142-147). IEEE.
- Lantz B, Díaz-Montiel AA, Yu J, Rios C, Ruffini M, Kilper D. Demonstration of Software-Defined Packet-Optical Network Emulation with Mininet-Optical and ONOS. In *Optical Fiber Communication (OFC) Conference*, 2020 Mar 8 (pp. M3Z-9). Optical Society of America.
- Zhu S, Gutterman C, Montiel AD, Yu J, Ruffini M, Zussman G, Kilper D. Hybrid machine learning EDFA model. In *Optical Fiber Communication (OFC) Conference*, 2020 Mar 8 (pp. T4B-4). Optical Society of America.

Other dissemination

- *April 2018/2019 - Strasbourg, France*: Present at the Symposium of CONACYT Scholarship Holders in Europe.
- *July 2019 - Ho Chi Minh City, Vietnam*: Seminar at the John Vonn Neumann Institute.

- *March 2020 - Mexicali, BC, Mexico*: Invited talk on: Postgraduate studies in optical communications.

1.5 Sponsors

The research work for this thesis has been financially supported by the following bodies, which are greatfully acknowledged:

- Financial support from Science Foundation Ireland (SFI) 15/US-C2C/I3132 and 13/RC/2077 (CONNECT) are acknowledged.
- Financial support from the National Council of Science and Technology (CONACYT, in Spanish) from Mexico is acknowledged.

2 Background

2.1 Optical network disaggregation

Today, a typical deployment of an integrated Optical Line System (OLS) can be represented by Figure 2.1. OLSs are commonly composed of transponders or line terminals to carry on the transmission and reception of optical signals, Reconfigurable Add/Drop Multiplexers (ROADMs) integrated with Wavelength-Selective Switches (WSSs) for multiplexing and de-multiplexing the signals, and Erbium-Doped Fibre Amplifiers (EDFAs) for boost, in-line and pre-amplification purposes. Each component is developed and controlled within an OLS control system that is provided by a single vendor or manufacturer. This architecture constraints the flexibility of network operators to acquire equipment from multiple vendors and limits the operational capabilities of these to the commercial offer of a single vendor. In recent years, optical network disaggregation has emerged as a networking paradigm to enable the use of multi-vendor components in optical equipment, and enhance the control operation of this type of systems. The logical architecture of disaggregated OLSs is represented in Figure 2.2. Here, the control of each network component can be carried out by controlling mechanisms (i.e., component interfaces) provided by different vendors. This in turn leads to multiple implications to business and operational models.

From a business perspective, optical network disaggregation emerges as an enabler technology to demonopolise the Telecommunication's market and to open competition for new network operators and vendors. In addition, it enables the emergence of novel business models such as providing services on-demand in a pay-as-you-go model (i.e., bandwidth on-demand), or even operational changes such as shared-infrastructure between network operators [11]. However, transport networks have operated for decades in isolated environments between operators, and the only times that sharing infrastructure has been enabled has been by the acquisition of one company by another, such as when Nokia bought Alcatel-Lucent in 2016 [75], and even then the control of the heterogeneous network elements needed to be carried out by different components and technologies. Because of this, in order to enable this type of novel networking use-cases that become possible in a disaggregated environment, network operators, vendors and service providers need to come to an agreement on the operational specifications of disaggregated equipment, and, to some degree, they also need to agree on the overall architecture of this type of network, from the control and data planes, to the physical layer composition.

From an operational perspective, the main implication faced in optical network disaggregation is in fact disaggregating the control from the network equipment to relay it to a software-defined control system. This in turn imposes multiple technical challenges. For instance, this requires an abstraction of the components' characterisation (i.e., bare-metal composition), as well as an abstraction of the

components' functional capabilities at the control plane. Due to the heterogeneity of optical network equipment in the market today, it has been challenging for vendors to agree on standard abstraction models and interfaces that satisfy each company system requirements. As a consequence, several consortia and working groups have come together in recent years, combining initiatives from both academia and industry, to tackle the development of optical network disaggregated technologies. These initiatives and the state of the art of their research outcomes are thoroughly discussed in section 2.1.2. In addition to these technical challenges, the enablement of both control systems and devices communicating in a common language needs to be addressed. That is, there is a need for novel communication protocols to operate on top of disaggregated networks equipment. Interestingly, disaggregating OLS control opens up a wide range of possibilities to enhance the control plane by re-architecting its composition and by extending the functionality. For instance, by opening up the configuration interface of networking equipment and centralising the control of these, it is possible to build analytical information of the overall network performance that can assist networking functions such as dynamic resource allocation and fault recovery. In recent years, the integration of these heterogeneous technologies has been facilitated with the standardisation efforts in Software-Defined Networking (SDN) and Network Function Virtualisation (NFV), as well as cloud open-source software and commodity hardware.

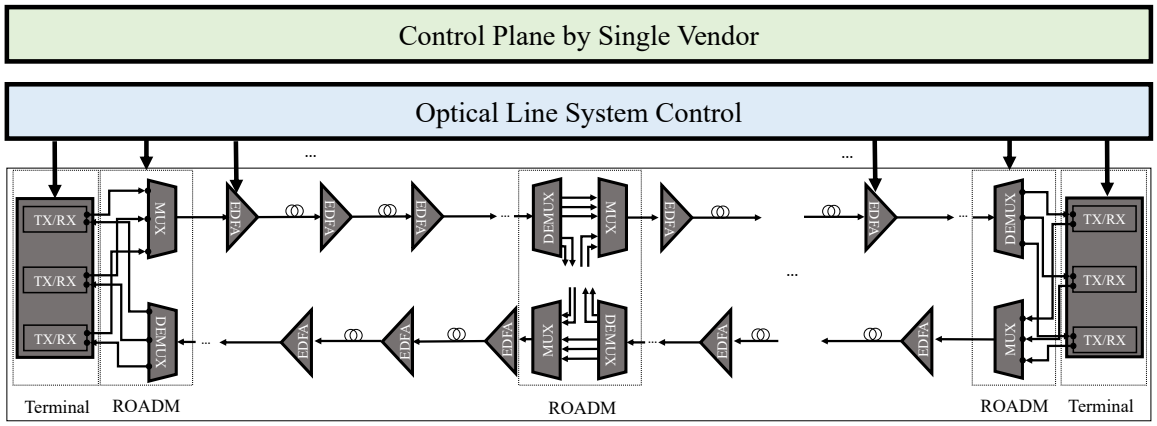

Figure 2.1: Typical deployment of an integrated optical line system today.

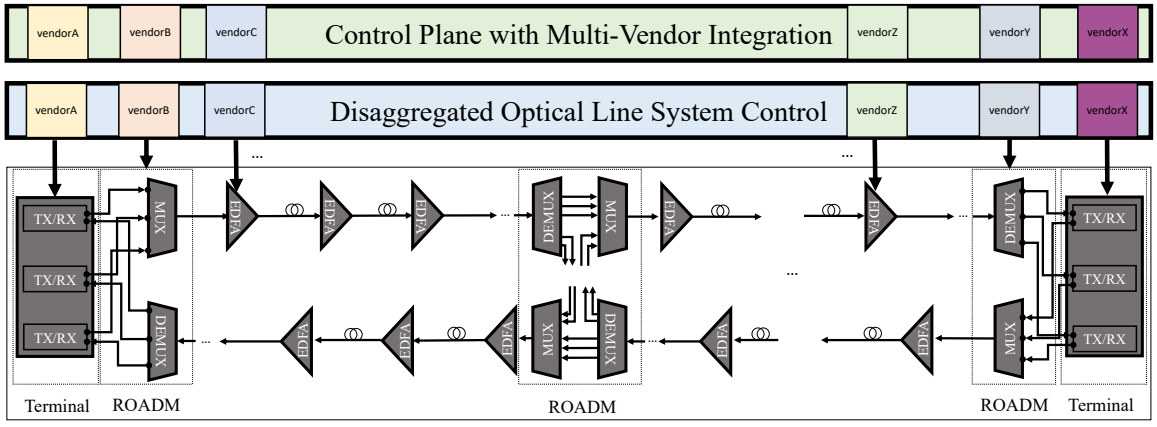

Figure 2.2: Disaggregated deployment of an integrated optical line system.

2.1.1 Software-defined networking: the paradigm

As illustrated in Figure 2.2, by disaggregating the control from the OLS components it becomes possible to have several tools enabling the control of these, all aggregated in a centralised control system. Thus, we can think of the control environment as a separate plane from the network that it is controlling. This architecture can be better described with the SDN paradigm. SDN as described by the Optical Network Foundation (ONF) is a network "architecture [that] decouples the network control and forwarding functions enabling the network control to become directly programmable and the underlying infrastructure to be abstracted for applications and network services, [which] is dynamic, manageable, cost-effective, and adaptable, making it ideal for the high-bandwidth, dynamic nature of today's applications." [6]. NFV addresses instead the architectures for virtualising the networking functions that become part of the SDN control plane. A baseline SDN architecture is shown in Figure 2.3.

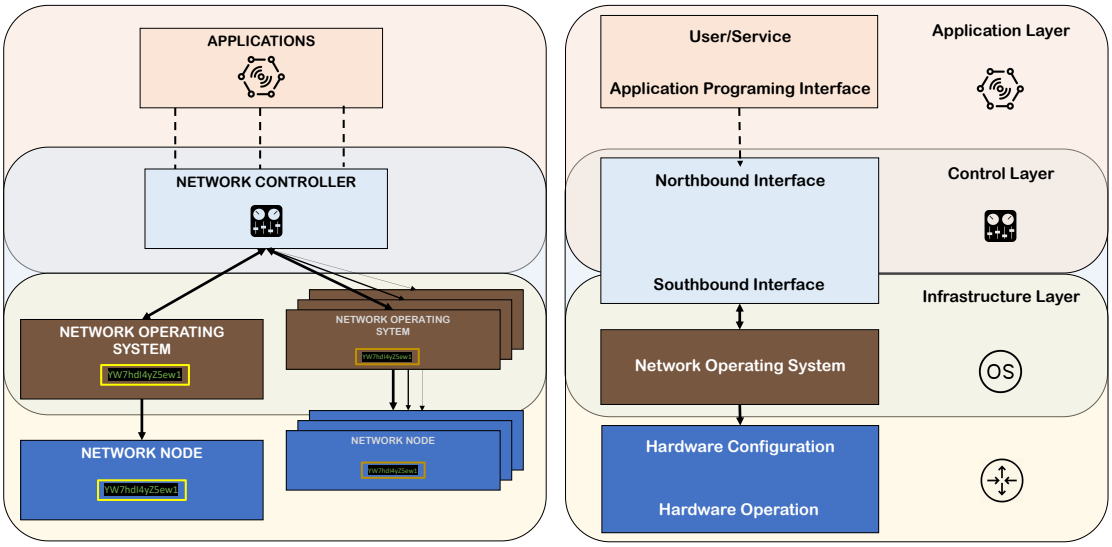

Figure 2.3: Logical architecture of the SDN paradigm.

On the left-hand side, top to bottom, we have applications that are run by a centralised network controller, which are in charge of configuring devices to fulfill the service demands from users (i.e., resource provisioning, guaranteeing Quality of Service (QoS), etc.). To do so, the controller connects to the network nodes by accessing a Network Operating System (NOS) that is embedded within the nodes. The NOS contains the policies and procedures enabled by a network node. Recently, several research efforts have been proposed to address the numerous technical challenges that are encountered at each layer of the SDN architecture [76–78]. In fact, according to the 2020 forecast by Markets and Markets [79], the global SDN market size is expected to grow from USD 13.7 billion in 2020 to USD 32.7 billion by 2025 at a Compound Annual Growth Rate (CAGR) of 19.0%. According to this analysis, the major growth drivers are the automation of network infrastructure, which leads to a significant reduction in Capital Expenses (CapEx) and Operational Expenses (OpEx), the increasing demand for cloud services, data center re-architecting, and server virtualisation, and the increasing demand for enterprise mobility to enhance productivity for field-based services. As a consequence, several companies are investing in research efforts to investigate the development of SDN-based Telecommunication networks. Today, there are persistent issues within the optical

domain that are being addressed by multiple global consortia.

2.1.2 Global consortia

Historically, the Internet Engineering Task Force (IETF) [80], International Telecommunication Union (ITU) [81] and Optical Internetworking Forum (OIF) [82] are the three main organisations that have had formalised the evolution of transport networks. Thus, the operation of legacy OLS systems is well defined through standardisation efforts within these bodies. Because optical disaggregated networks is vanguard research, only standardisation efforts within the electronic domain (e.g., packet networks) have become available, since the networking operations of this domain have evolved faster than within its counterpart optical domain. Because of this, numerous research groups have been formed around the world to tackle the formalisation efforts in the optical domain. Undoubtedly, the two key consortia that are leading the future of optical network communications are the ONF [6] and the Telecom Infra Project (TIP) [13]. In this section, we discuss the main research efforts that have emerged from both initiatives during the past decade, commencing with the ONF.

The ONF is a "non-profit operator led consortium driving transformation of network infrastructure and carrier business models, serving as the umbrella for a number of projects building solutions by leveraging network disaggregation, white box economics, open source software and software defined standards to revolutionize the carrier industry" [6]. It was founded in 2011 by Deutsche Telekom, Facebook, Google, Microsoft, Verizon, and Yahoo!, and today it counts with the collaboration of over 150 members distributed along companies, universities and research centres, as well as re-known open-source groups such as the Linux Foundation [83] and the Open Compute Project (OCP) [84]. Since its foundation it has been leading SDN developments in the packet, optical and wireless domains. The most impactful projects that have been developed during the past decade by the ONF are: the OpenFlow communication protocol [18], enabling the SDN control of packet-switches (although it also supports now transport configuration); the Open Network Operating System (ONOS) [25], which has become the industry standard for SDN controllers providing scalability, high availability, high performance and abstractions to create apps and services when controlling a network; and the Central Office Re-architected as a Datacenter (CORD) [7] platform that leverages SDN, NFV and Cloud technologies to build agile data centers for the network edge. Nonetheless, the ONF also counts in its portfolio projects that are being thoroughly supported within its community: Stratum [85], Trellis [86], next generation SDN (NG-SDN) [87], P4 [88], XOS [89], Open and Disaggregated Transport Network (ODTN) [73], Open Transport Configuration & Control (OTCC) [90], Information Modeling [91] and Mininet [59]. Most of the work investigated within the ONF focuses on next generation data centre networks.

Separately, the Facebook initiative of TIP [13] is another ecosystem of projects and working groups. In fact, TIP describes itself as a "global community of companies and organizations that are driving infrastructure solutions to advance global connectivity." Today, it counts with over 450 members, also ranging between academia and industry profiles, and has dozens of working groups on a wide range of Telecommunication networks topics [92]. Within TIP, the working group that is in charge of researching next generation optical networking communications is the Open Optical & Packet Transport (OOPT) group [17], which is an operator driven group that will "allow to reimagine how we can innovate and do business" [93]. This working group is divided in 4 sub-groups that investigate the elements of packet-optical transport networks including OLS, disaggregated

transponder and chip (DTC), physical layer simulation environment (PSE) and common-APIs.

In addition to ONF and TIP, in the last decade other working groups have formed to address individual aspects of optical networks disaggregation. For instance, there is the OpenROADM group [19], which is a Multi-Source Agreement (MSA) that has the goal of defining interoperability specifications for white-box ROADMs. Their specifications consist of both optical interoperability as well as Yet Another Next Generation (YANG) data models. Additionally, there is the OpenConfig group [20], which is "an informal working group of network operators sharing the goal of moving our networks toward a more dynamic, programmable infrastructure by adopting software-defined networking principles such as declarative configuration and model-driven management and operations [20]." Both OpenROADM and OpenConfig are currently being evaluated by different groups around the globe [14, 94, 95].

While the implementation of SDN and NFV is not novel in the context of electronic networks (i.e., packet networks), especially in the area of data centre networks, optical networking systems, which operate with strict analog constraints, have only begun to implement these paradigms for commercial purposes in the past decade. As we have discussed in section 2.1.1, the main challenge of enabling SDN in the optical domain concern the communication between the controller and the devices. However, enabler-technologies such as communication protocols and hardware prototypes have been around since the '80s. In 1988 the Consultative Committee on International Telephone and Telegraph (CCITT) Study Group XVIII released the first recommendation, G.707 [96], to introduce network node interfaces for the synchronous digital hierarchy (SDH) technologies, and, consequently, synchronous optical networking (SONET) technologies. This motivated the worldwide development of pioneering work of SDN in the optical domain. For example, Fujimoto *et al.* [58] from Fujitsu Laboratories LTD, Japan, presented the concept of software-defined optical shuttle nodes with a demonstration of one of the first system controllers operating on top of a SONET network back in 1988. Since this initial period, the control plane of optical networks has been re-designed and re-architected extensively, and formalised in the ITU-G series: Transmission systems and media, digital systems and networks [81], as well as through other standardisation bodies and initiatives (e.g., IETF [80] and OIF [82]). In particular, the ITU-T Recommendation G.709 Interfaces for the optical transport network [97], first approved in 2001, has been formalising the integration of optical network elements, as well as providing reference models for the principles of operation of these and the interfaces to control them. Since 2009 this ITU-T recommendation has been revised annually with incremental advancements towards enabling more agile and flexible Dynamic Wavelength-Division Multiplexing (DWDM) optical networks, which have come to slowly replace legacy transport technologies relying on SONET/SDH systems.

Naturally, the evolution of optical transport networks has been heavily influenced by the advancements in network disaggregation of packet-networks, which due to their digital nature have evolved at a faster pace than analog systems such as optical networks. For instance, also in 2009, the ONF released the first version of the OpenFlow [18] protocol to enhance the Southbound Interface (SBI) of SDN electronic switches. This communication protocol simplified the disaggregation of the control of this type of switches to be handled by a system (software) controller, enabling more sophisticated traffic management and routing procedures at this layer of communication. This also motivated the emergence of several OpenFlow standardisation activities as well as the development of network operating systems (or SDN controllers), which have already been surveyed by Kreutz *et al.* in [76]. Today, OpenFlow has become the industry standard for disaggregated electronic net-

works. Due to the tremendous success that OpenFlow achieved within few years, in the early years of the '10s it was thought of as the favourite candidate to replace the Generalized Multi-Protocol Label Switching (GMPLS) protocol [98], which can still be found operating on top of optical transport networks [99]. As a result, in 2014 the ONF released a set of requirements to be considered to extend OpenFlow to transport networks in [100], but it was not until 2015 that they released the first official version of OpenFlow supporting these requirements [101]. Also in 2014, the ONF released the first version of their ONOS project, already integrating OpenFlow and other south-band communication protocols, i.e., Network Configuration Protocol (NETCONF) [102], which has since then become the preferred SDN controller also for electronic networks. However, due to the lack of readily-available programmable (white-box) transport equipment, it is yet unclear whether OpenFlow will have the same success in the optical domain.

In parallel to the ITU activities of the past decade, several IETF Request for Comments (RFC) have been proposed to enable SDN support in the optical domain. For instance, in 2009 Zhang *et al.* proposed the RFC-7062: Framework for GMPLS and Path Computing Element (PCE) Control of G.709 Optical Transport Networks [103], providing the guidelines for telecom operators to introduce control plane capabilities based on GMPLS to optical transport networks. Built on top of RFC-7062 and RFC-4657 [104], in 2012, King and Farrell proposed the RFC-7491: A PCE-based Architecture for Application-based Network Operations (ABNO) [105], which has served as a template for optical SDN research since it was first proposed as it allows to implement complex workflows and compute time consuming optimisation algorithms in the optical control plane [26, 27, 106–108]. This line of research motivated the assessment and development of other SBI communication protocols such as NETCONF and YANG-based models like T-API [21], as alternatives to OpenFlow.

2.1.3 Disaggregated optical control plane

Software-defined control

As we have already mentioned, only during the past decade the area of disaggregated optical networks has been thoroughly researched. In this section, we review the key research efforts and initiatives that have resulted from this movement. For instance, Liu *et al.* [109] have demonstrated an in-field OpenFlow-based unified control plane for multi-layer multi-granularity optical switching networks. They have virtualised a layer of control of WSSs that are physically controlled with the TL1 protocol, so that they can be controlled through an OpenFlow controller. This was the first demonstration of such a controller that enabled them to quantitatively evaluate the latencies for end-to-end path creation and restoration through a field trial between Japan, China, and Spain.

Choi *et al.* [110, 111] have demonstrated the implementation of adaptive transceivers that were controlled with an SDN controller that enabled OpenFlow. The authors developed an extension to the OpenFlow protocol to enable the control of the adaptive transceivers. They were capable of dynamically, with the controller, adapt the modulation format of their optical transmitters. Their controller was based on the architecture of the PCE architecture [112]. The PCE architecture as a framework for disagreggated optical networks has been extensively reviewed in: Casellas *et al.* [113], Casellas *et al.* [114], and Muñoz *et al.* [115].

Sambo *et al.* [116] have also developed an extension to the OpenFlow protocol in order to be able to control optical network equipment to set transmission parameters (e.g., code rate) at

the transmitter and the receiver ends. They have reported the creation of super-channels (i.e., flexi-grid) with their SDN controller. In fact, the evaluation of flexi-frid networks (also referred to as Elastic Optical Networks (EONs)) with OpenFlow-enabled SDN controllers gain significant attention [117–127].

With the release of the ABNO architecture (RFC-7491 [27, 105]) a boost of optical SDN research resurged following this design. For instance, Muñoz *et al.* [128, 129] have demonstrated a transport network orchestration for end-to-end multi-layer provisioning across heterogeneous SDN/OpenFlow and GMPLS/PCE control domains. Casellas *et al.* [130] have proposed a multi-domain and multi-vendor network SDN control architecture that uses GMPLS to control the network elements of an optical network. Morover, other international efforts have been done to demonstrate the SDN control of remote testbeds across the globe. For instance, Vilalta *et al.* [131, 132] proposed methods for using NFV to deploy OpenFlow-controlled virtual optical networks (VON). They have interconnected international optical SDN testbeds from Japan, U.K., Germany and Spain. Also, Li *et al.* [133] have demonstrated a customised multi-domain transport SDN control using the OpenFlow protocol and a customised controller. Yoshida *et al.* [107] have shown an OpenFlow-based SDN control of interconnected testbeds physically located in Japan, the U.K. and Spain.

Recently, there have been multiple efforts to evaluate the performance of different communication protocols to control optical disaggregated equipment. For instance, Oda *et al.* [134, 135] have evaluated a control system that through OpenROADM was capable of retrieving live-information about the optical performance of the network, allowing them to improve the transmission margins. Also, Kundrat *et al.* [136] have evaluated the use of YANG-based models to control programmable ROADMs networks. Similar evaluations of YANG-based models have been analysed by Velasco *et al.* [137]. Recently, Campanella *et al.* [138] have disclosed the aim and architectural details of the Open and Disaggregated Transport Network (ODTN) project from ONF, which makes use of the ONOS SDN controller to manage an OLS system with the protocols NETCONF/RESTCONF and models OpenConfig/TAPI. And, more recently, Sgambelluri *et al.* [94] have investigated the real potential of OpenConfig and OpenROADM to be used in real deployments.

Disaggregated optical equipment

As we have briefly commented on Chapter 1, despite the research outcomes in recent years, the assessment of disaggregated optical networks are limited to testbeds that integrate few network components that are SDN-enabled. As a result, the optical networking community has been looking at the well-established white-box solutions proposed by the OCP [84] for data centre networks, and have come up with novel designs. At the first TIP Summit in November 2016 the OOPT project announced the industry's first networking white box, called Voyager, which is a packet-optical solution combining a switching ASIC with coherent DWDM modules [93]. Also in 2016, Edgecore Networks released their optical terminal with SDN control capabilities, the packet/optical Cassini [139]. After these official releases multiple companies started to produce their own versions of white-box switches, such as the Czech Light ROADM [140] and the Lumentum ROADM Graybox [141].

Consequently, multiple research efforts have been investigating the performance enabled by white-box solutions. For instance, Kushwaha *et al.* [142] have performed a 400 Gb/s carrier-class SDN white-box design and demonstration, based on protocol-agnostic YANG-based models for the

optical SDN control. With this tool the authors proposed a bitstream, low-latency, source-routing based scheme. Velasco *et al.* [137] have proposed a control architecture and a NETCONF YANG-based data model, as well as a customised white-box architecture for data centre networks. They have used a customised CASTOR controller interconnected to ONOS in order to control multi-vendor international testbeds in Spain and Italy. More recently, white-box studies from academia have emerged. For instance, Sgambelluri *et al.* have built a photonic integrated switch matrix including 1398 circuit elements interconnected in a 3-D stack that is controlled through Open-ROADM NETCONF/YANG Agent and experimentally validated in an ONOS-based SDN testbed encompassing OpenConfig-driven 100G pol-mux transponders [95]. Also, Lopez *et al.* [22, 143] have recently presented the Transponder Abstraction Interface (TAI) project, which is yet another TIP initiative to investigate the development of white boxes in the optical domain.

Evidently, the assessment of the control system frameworks and technologies (i.e., network operating systems and communication protocols) are becoming more present. For instance, Campanella *et al.* [144] have disclosed the recent advancements of the ONF-ODTN project, demonstrating dynamic multi-layer (data and control) provisioning of data connectivity services and advanced automatic failure recovery. Their experiments continue to exploit the ONOS framework, as well as the YANG-based models of OpenConfig and OpenROADM. Also, Sgambelluri *et al.* [94] investigated the optimisation of provisioning and fault management scenarios. Their experiments also use ONOS, OpenConfig and OpenROADM, as well as enabled telemetry monitoring capabilities.

2.1.4 Active monitoring

Active monitoring has been a capability of the optical control plane that has gained much attention in recent years, as it can improve the management of lightpath installation, fault management and dynamic routing. In conventional network deployments today it is common to account for monitoring of the physical layer with Optical Performance Monitor (OPM) solutions. For example, it is typical to install OPM nodes at the receiver-end of a point-to-point optical connection, that use coherent receivers to estimate lightpath Quality of Transmission (QoT) given the characteristics of the optical link, which can effectively provide performance monitoring (i.e., Bit Error Rate (BER), Generalized Optical Signal to Noise Ratio (gOSNR)) as well as other power anomaly detection measures through digital backpropagation [145, 146]. This can be part of a larger research area developing control methods that combine real-time data collection with Quality of Transmission Estimation (QoT-E) and lightpath provisioning [147]. This approach involves the use of real-time control plane operations to gather OPM information and run algorithms for the correction of QoT-E functions.

For instance, Pointurier *et al.* [148, 149] have proposed through simulations a strategy to select which lightpaths to monitor in order to compute an accurate estimation of the overall spectrum performance by means of network kriging solutions that compute the BER of unmonitored channels. Their monitoring capabilities assumed the extraction of power levels and Amplified Spontaneous Emission (ASE) noise levels at the end of an optical link. Additionally, they have also evaluated the impact of placing monitoring nodes at different locations in a network, in order to estimate the performance of lightpaths across a network. Thus, the placement of monitoring nodes has also been a topic of interest in recent years.

Angelou *et al.* [64, 150] have proposed an optimisation algorithm to allocate OPM nodes at different locations of an optical network with the objective function of minimising the amount of

equipment required that can help to accurately estimate the QoT of lightpaths that share connection links. They have reported that for optical networks of different scales, their algorithm can reduce the amount of OPM equipment by a 1/4 or a 1/3 of the total monitoring (theoretical) capacity.

Sartzetakis *et al.* [151] have evaluated the monitoring of probing channels only, in order to accurately estimate the performance of active channels. Their algorithm enabled to reduce the amount of monitoring equipment by 60% when compared against integer linear programming algorithms, with the objective function of reducing transmission margins. Sambo *et al.* [152] have performed a demonstration of a QoT-E module mounted on a real SDN controller, that was used to allocate optical traffic in a single and multi-domain scenario. They made use of NETCONF agents to retrieve online data that was later used to improve their QoT-E module. Yan *et al.* [153] have proposed an SDN-based monitoring framework to build multi-layer analytical information of the optical link performance. They have extended the OpenFlow protocol to retrieve physical layer information from the nodes that their OpenDayLight controller managed. Paolucci *et al.* [127] have demonstrated a scalable solution based on the subscribe and publish model, to build a SDN controller using the gRPC protocol to enable on-demand streaming of real-time monitoring parameters. Their optical control is enabled through YANG-based models. Gifre *et al.* [154] have proposed a monitoring and data analytics (MDA) architecture, integrating data analytic capabilities with telemetry. Their study considers a YANG-based data model that is used to retrieve information from the network nodes. Seve *et al.* [155] have developed an SDN control plane developed with ONOS, where they have integrated monitoring capabilities with coherent receivers at the end of an optical link, and have been able to identify different types of fibre anomalies (i.e., chromatic dispersion without traffic interruption).

Evidently, the use-cases enabled by the disaggregation of optical networks enhance the applicability of active monitoring strategies. However, this is an area that requires further investigation.

2.2 Optical network design and modelling

At this point, we can conclude that it is desirable to be able to model optical networks before deploying them because this allows you to benchmark potential faults, system functionality, etc. As we have already mentioned, disaggregating optical networks assumes the inter-operability of heterogeneous networking equipment. As a consequence, the proprietary networking modelling solutions carried out by network operators in legacy systems are not suitable for modelling network scenarios including the components from multiple vendors. Thus, it has become of interest to account for modelling tools that are capable of aggregating the physical performance of disaggregated optical networks. Today, there are two main initiatives that have been considered by the community: the Net2Plan Project [72] and the OOPT-GNPy Project [2].

2.2.1 Net2Plan

Net2Plan is a project developed at the Universidad Politécnica de Cartagena (Spain) and it was first released in 2015 [72]. It is an interactive platform that enables the modelling of IP networks, Wavelength Division Multiplexing (WDM) networks, and NFV elements, enabling the creation of nodes, links, traffic unicast and multicast demands, routes, protection segments, multicast trees,

shared-risk groups, resources and network layers. It was designed to be useful for laboratory sessions as an educational resource, or for a visual inspection of a network. It is developed as a Java library as well as a command-line and graphical user interfaces. Net2Plan counts with four main features: offline network design, traffic matrix generation, online simulation and reporting. This tool has been used to investigate a variety of interesting research works in the optical domain, including blocking issues in noncontentionless ROADMs [156], assessing IP vs optical restoration [157], fault management procedures [158], as well as dynamic operations of IP/MPLS-over-WDM networks [159]. Net2Plan has also been integrated with the SDN controller OpenDayLight [24, 160].

2.2.2 GNPy

GNPy is a project developed by the 2017 OOPT - Physical Simulation Environment (OOPT-PSE) working group from the TIP consortium [17]. It is an open source and vendor-neutral library of applications capable of assessing optical impairments in OLSs. It relies on the estimation of an optical transmission by evaluating the accumulation of both the ASE noise generated by EDFAs and the Nonlinear Interference (NLI) noise introduced by nonlinear signal propagation in an optical fibre. This tool has been validated against physical testbeds in [161] and, more recently, also in [162]. Today, it is the optical network planning and optimisation tool that has been widely accepted within the optical networking and communications community, and has been used in a variety of research works. Barzegar *et al.* has used it to study soft-failure localization and time-dependent degradation detection for network diagnosis [163]. Borraccini *et al.* [164] have used GNPy to assess open line controlling and modulation format deployment. Also, Triki *et al.* have integrated GNPy to an OpenROADM compliant network [55]. This tool has also been integrated with the ONOS SDN controller from the ONF [165].

2.2.3 Emulation systems: the missing piece

As of today, a major challenge in doing research in the area of disaggregated optical networks is testing the real-time control plane aspects, as real testbeds, especially in academia, are of limited size, typically composed of only few ROADM nodes. Indeed, a lack of testing platforms and reference systems, similar to the recirculating loops used in transmission system development, has limited this area of research primarily to customised, often not scalable solutions, as we have shown in the examples presented above. Optical controllers such as ONOS/ODTN [166] could benefit from rapid and flexible development on reliable emulated environments, in addition to testing on hardware testbeds, just as Mininet [59] helped the development of OpenFlow and SDN control planes.

As we aim to automate the control of optical networks, network planning and optimisation tools such as GNPy [2] aim to cover the network management functions of the control system, and to assist decision-making processes (i.e., lightpath installation). However, they operate as a closed simulation environment designed for planning and optimisation, leaving the assessment and development of optical SDN control systems in real-time an open issue. While these systems enable the assessment of a transmission even upon network deployment, there are no tools enabling the assessment of the communication mechanisms (i.e., interfaces and protocols). As a consequence, the development and testing of optical control plane systems requires the physical prototyping of the devices and their NOS. In the electronic domain, the emergence of the Mininet Project

enhanced the development, testing and prototyping of electronic software-defined networks and their control planes [59]. Mininet allows to deploy a virtual electronic network composed of virtual Linux hosts (servers), virtual Ethernet links and programmable electronic switches. Consequently, at the ONA Laboratory, in collaboration with the University of Arizona, we have designed and developed an emulation platform to support the optical networking and communications community in the assessment of optical control planes, which is one of the key contributions of this thesis, and it is thoroughly described in Chapter 3.

2.3 Quality of Transmission Estimation

As we have mentioned in section 2.2, the hardware heterogeneity of the disaggregated network components is hard to model with network modelling systems for proprietary systems. As a consequence, in recent years, it has been of great interest to the optical networking and communications community the development of control plane NFV compounds in charge of computing performance estimations of the physical layer transmissions that traverse disaggregated optical networks, i.e., predicting the Optical Signal to Noise Ratio (OSNR) levels of a point-to-point optical link transmission. The current research approaches could be divided in two classes: 1) estimation models based on analytical modelling and 2) estimation models based on cognitive techniques (i.e., Machine-Learning (ML)-assisted). A distinctive feature of cognitive techniques is that they require large amounts of data points in order to operate at optimal levels. This in turn poses a great limitation, since the collection of optical data information is a limiting action, as academic research testbeds tend to be of lower sizes with respect to commercial deployments, usually composed of few nodes and monitoring capabilities. Also, this type of estimation requires constant updates of the status of the ground-truth performance that it is trying to model in order to perform with great accuracy. On the other hand, estimation models based on analytical modelling do not depend on active monitoring procedures, but require instead great levels of detail of the OLS that it is trying to model, which can be hard to represent due to the wavelength-dependent operation of optical network equipment, such as the case of the wavelength-dependent gain of EDFAs. Thus, this type of estimation model tend to not scale well with a big number of network nodes and transmission channels. Here we discuss the most relevant research contributions disclosed in recent years with regard to the development of QoT-E modules to be integrated in the control plane of disaggregated optical networks, with the intention of highlighting the variety of strategies developed for analytical modelling estimations and the popularity of ML algorithms for cognitive estimations, such as Support Vector Machine (SVM) and Artificial Neural Network (ANN). The analytical models from Net2Plan and GNPy are not included here, since they have been described above in sections 2.2.1 and 2.2.2.

2.3.1 Analytical models

Zami *et al.* [167] studied the impact of OSNR levels of a signal towards near channels for a given set of connections. While they did not consider the addition of optical noise in the in-line optical amplifiers, the interest of a QoT-E was first raised, considering some of the physical impairments in an optical network system. The idea of a QoT function was later introduced in Morea *et al.* [168], which, in combination with a customised routing algorithm, provided simulated performance studies on the feasibility of including these type of functions into the control plane. By consider-

ing a non-heterogeneous model of network elements, they evaluated transmission performance for different wavelengths based mostly on the Chromatic Dispersion (CD) optical impairment. Since high computational resources are inappropriate for Routing and Wavelength Assignment (RWA) functions in the control plane, they determined it was necessary to quantify the estimation error when using the routing tool as a function of the network. Also, Morea *et al.* [168] proposed the possibility to combine the QoT-E with monitoring functions, by retrieving information from the optical nodes at fixed periods of time.

Leplingard *et al.* [169] proposed to use QoT-E as a function of the CD map, to help derive appropriate margins on the dimensioning of an optical network. Under these considerations, they used the estimated results to determine the number of regenerators needed for a given network, as a function of the applied margins. In this study knowing the CD of the system helped reduce the errors of the QoT-E.

Subsequently, Leplingard *et al.* [170] analysed the application of adaptive margins to a QoT-E, based on the amount of residual CD and non-linear phase experienced by a signal. In this study it was found that the utilisation of adaptive margins decreases the number of misestimations. Nonetheless, according to the authors, while the application of margins guarantees safer dimensioning, it is at the expense of including additional equipment.

Following a more statistical approach, the authors in Morea *et al.* [171] considered the introduction of confidence levels for adding margins in both fixed and adaptive manners. They also used the QoT function to determine the number of regenerators needed at a given transmission. However, it was concluded that comparing the required regenerators is not enough to assess the advantages related to a QoT-E.

Sambo *et al.* [172] have proposed three signaling and multi-layer probe-based schemes that can estimate QoT, the Multi-layer Probe Scheme (MPS), the Signaling-based Multi-layer Probe Scheme (S-MPS) and the Signaling-based Conditional Multi-layer Probe Scheme (SC-MPS). Their simulation results showed that the use of QoT-E procedures in a GMPLS-based network can improve blocking probability and lightpath setup time. Also, Pinart *et al.* [173] make use of probing signals to verify QoT-E, enabling the optimisation of impairment-aware wavelength assignment.

Pointurier *et al.* [174] have investigated the use of a Q-tool for impairment aware routing and wavelength assignment. The latter, served as a baseline for the work developed by Sambo *et al.* [175], which proposed a lightpath establishment framework based on this estimation tool that was then implemented as part of a PCE-based demonstration [176].

Azodolmolky *et al.* [177, 178] have proposed a RWA procedure that aimed to mitigate the inaccuracies caused to QoT-E, which are attributed to inaccuracies in modelling, as well to a lack of monitoring capabilities in an OLS. In their evaluations, they were able to allocate 40% more lightpaths in a 10-channel system, thanks to their lightpath allocation method improved with QoT-E.

Qin *et al.* [179, 180] have proposed a hardware accelerated QoT-E procedure used in the DICONET impairment-aware optical network [181]. The authors have reported a considerable performance achieved with the hardware acceleration processes.

Zami *et al.* [182] have proposed a QoT-E-based routing algorithm that considers the accumulation of uncertainties in the physical parameters along a path during the route selection process. They presented an analysis based on a U.S.-wide core network. In general they showed that the number

of regenerators deployed in an optical network can be reduced by implementing QoT-E modules, and, that the receiver margins required to guarantee successful lightpath installation could also be reduced. This study coincided with the findings of Garcia-Manrubia *et al.* [183], who also evaluated the impact on the reduction of network equipment (i.e., regenerators) required to be deployed.

Bottari *et al.* [184] have proposed an evolutive lightpath assessment to evaluate the QoT of unestablished lightpaths. Their algorithm mixes quality estimations and in-field measurements of the transmitted channels. They have also reported a reduction in the amount of regeneration required to be deployed.

Perellò *et al.* [185] have performed a demonstration of a QoT-E module mounted on an FPGA module. Interestingly, their lightpath allocation strategy using the QoT-E system required 1.36 seconds to execute for the high priority traffic.

Today, the evolution of coherent optical transmission has made it possible to easily recover from CD and Polarization Mode Dispersion (PMD) using digital signal processing at the receiver, so that accurate QoT-E for these impairments has become redundant. However, Zami *et al.* [186] proposed that it is still relevant to consider the OSNR levels and crosstalk attenuation of signals, as input parameters for QoT functions. In addition, it is mentioned that analysing the performance of a transmission channel from a bandwidth perspective is important, especially when considering multiple physical impairments of a system. They proposed that the accumulated uncertainties along the lightpaths must be also considered, e.g., as the aggregated noise caused by amplification systems.

Sartzetakis *et al.* [187] proposed an analytical framework for a QoT-E considering spectrum dependent parameters. While assuming OPM functions capable of reporting the state of the network, the MATLAB simulations presented in this study demonstrated that they were able to approximate the prediction of the network behaviour with high-accuracy. Although the analysis presented there lacks consideration of physical layer models, it provides an insight on how novel statistical techniques could improve the precision of a QoT function for signal performance in an optical network.

Bouda *et al.* [188] proposed a prediction tool that is dynamically configurable considering optical physical impairments as these changed through the network. They included both linear and non-linear effects, such as Q-factor and non-linear fibre coefficients, for predicting accurate QoT. The authors were able to reduce the Q-estimation error to 0.6 dB. However, they believe the accuracy of the parameters in their model could be improved by considering more data variability, e.g., by changing the launch powers or considering measured OSNR levels.

In Panayiotou *et al.* [189], a data-driven QoT-E is analysed from a theoretical perspective. The authors commented on the advantages of approaches based on data analysis, in-gather than based on Q-factor estimation, overcoming the dependency of the consideration of physical layer impairments, eliminating the requirement of specific measurement equipment, as well as extensive processing and storage capabilities. While this approach presented high accuracy (between 92% and 95%) the neural network approach taken in this study presented high computational complexity, which is typically unsuitable for the management of all-optical networks.

Cantono *et al.* [190] developed a QoT-E system capable of modelling nonlinear interference generation with Stimulated Raman Scattering (SRS), showing errors within 0.5 dB on the gOSNR estimation. This integration of the SRS effect was later added to the GNPy project [162].

Delezoide *et al.* [191] have demonstrated a QoT-E method that is capable of estimating the filter penalty to QoT when WSSs are presented in cascade and reported the reduction of margins to up

to 1.7 dB for optical links with high number of hops, with estimation errors between 0.1 and 3 dB.

Zhang *et al.* [192] have integrated a novel analytical model of both ASE and NLI noise to a WDM control plane, enabling real-time updates of the estimations. Their model is based on a single transmission figure of merit applied to every line span and lightpath in a WDM network. Their figure of merit consists in the line span OSNR degradation that is first computed by the QoT-E module analytically from a number of input parameters that are periodically monitored by their controller.

Zhao *et al.* [193] have proposed a spectrum allocation scheme using a QoT-E system that partitions the spectrum to be allocated in sections that prioritise based on the transmission time of these. Their approach outperforms conventional QoT-E systems when looking at the improved blocking probability.

Vincent *et al.* [194] have artificially evaluated a RWA algorithm that focuses on the fact that wavelength packing can enhance overall traffic whilst giving only slight penalties for latency and the required transceivers.

Virgillito *et al.* [195] have proposed an analytical model of NLI noise, which is spectrally disaggregated, by separating the single-channel - self-phase modulation (SPM) - from the multi-channel effects - cross-phase modulation (XPM). They used the GN model to validate their split-step simulations. They have reported that by separating the SPM and XPM occurrences from the analytical models, it is possible to improve the estimation of NLI noise.

D'Amico *et al.* [49] have proposed a method to evaluate the equivalent SPM component of NLI noise of fibre spans, which are independent of the history or configuration of the optical network.

Ferrari *et al.* [162] have used the GNPy project to build an estimation model that is sensitive to connector loss uncertainties. They have evaluated their results in a core Microsoft testbed and have reported errors of up to 1 dB.

Evidently, there are too many considerations to be taken in the modelling of physical effects encountered in optical networking systems. Fortunately, recent proposals such as the ones presented in [49, 162, 195] are reporting significantly lower QoT-E inaccuracies with respect to a decade ago, which can enhance the optimisation of transmission margins and the overall optical control plane operation. Moreover, the evaluation of ML techniques have emerged to further mitigate the inaccuracies carried out by analytical modelling and build cognition-assisted QoT-E models.

2.3.2 Cognition-based estimation models

As briefly mentioned in Chapter 1, the re-emergence of cognitive control supported with virtualised instruments pose design challenges to the implementation of future optical control systems. In recent years, studies have reviewed the potential of Artifical Intelligence (AI) techniques (i.e., ML), to support intelligent software-defined optical control systems in enhancing the overall network capacity [65, 70].

Several studies have addressed this problem from various perspectives. For instance, Barletta *et al.* [196] considered the use case of determining whether unestablished lightpaths meet a required BER threshold. Synthetic data was used for their experiments. They implemented a Random Forest (RF) classifier with 100 estimators. The features used for training their model were: the number of links of lightpaths, lightpath length, longest link length, traffic volume, and modulation

format. Datasets were collected from a single topology, enabling RF to perform with high accuracy with only 1000 training data samples, although they also trained the model with 90 thousand samples. The findings were extended in Rottondi *et al.* [197] where they included a deeper analysis of the challenges imposed by network components in optical networks to the development of cognitive control systems.

In a different study, Bouda *et al.* [188] studied the learning capabilities in a multi-vendor scenario. They collected and trained synthetic data *on-the-fly*, representing the case of an online control system. The learning model used for their studies was based on maximum likelihood principles, correlated with the monitored data. They used many physical layer parameters (i.e., launch powers, fibre span losses of certain links, etc.). An emulated 88-channel system was used to generate data traversing all the spans in their network topology. QoT prediction with 0.6 dB Q-factor accuracy was achieved. Then, they extended their research in Bouda *et al.* [146], presenting an analysis of the network capacity gain due to the implementation of the Q-estimation tool.

Mata *et al.* [198] have reviewed the potential of SVM to classify lightpaths into high or low quality categories in impairment-aware Wavelength-Routed Optical Networks (WRONs), in long-haul communication networks. Their results favor SVM with respect to the high accuracy for binary classification. A dataset with 11 thousand samples was used to train the learning model. Nonetheless, they have pointed out the main pitfall of SVM is the extensive time to train the model, which is indeed a considerable limitation for future control systems. They extended their findings in Mata *et al.* [199] by comparing the previously implemented SVM model against RF and Bagging Trees. This time, the new models outperformed SVM in computational time while maintaining a classification accuracy of 99.9%. Contrasting the results from Mata *et al.* [198], Aladin and Tremblay studied the potential of an SVM model to classify lightpath QoT into good or bad according to BER thresholds [200]. They also compared the performance of SVM with K-Nearest Neighbours (KNNs) and SVM in terms of computational time and prediction accuracy. By training the learning models with more than 25 thousand data samples, their SVM implementation outperformed the other two candidates in classification accuracy, but with the tradeoff of longer computation time with respect to KNN and RF. As input features for the learning model they considered: total link length, span length, channel launch power, modulation format and data rate. In Tremblay *et al.* [201], they show a comparative analysis between the three classifiers, where the results favor SVM with 99.15% accuracy. Similar to Aladin *et al.* [200], Morais *et al.* [202] compared an SVM model against KNN, logistic regression, and an ANN model, also with the aim to predict the QoT of unestablished lightpaths. They considered 13 different features to train their learning model (i.e., number of hops, spans, link length, span attenuation, etc.). Around 5 thousand samples were used to carry out the learning model training. Their results favored ANN because they achieved 99.9% prediction accuracy with this model. Nonetheless, the other two algorithms performed with an accuracy of 95%. They extended their research work in Morais *et al.* [203]. This time they concluded that SVM models, KNN and logistic regression could classify correctly 90% of the lightpaths, and ANN continued achieving a classification accuracy of 99.9%.

From the literature presented above, it is clear that supervised-learning algorithms are capable of dealing with optical domain data with outstanding performance. Nonetheless, these studies mainly used synthetic data, and it is also clear that in order for these to perform best they required large amounts of data. This is a major complication for optical networks, since state-of-the-art monitoring equipment cannot extract the amount of data required in a fast manner. This motivated

the investigation of this type of algorithms when dealing with real data in physical testbeds. In Meng *et al.* [204], they used a learning model based on Markov Chain Monte Carlo, achieving a Q-factor estimation error of 0.5 dB. This was a testbed experiment consisting of the integration of a QoT-E as a module in the control plane of a software-defined small optical network system.

Liu *et al.* [205] presented an end-to-end testbed with a QoT-E tool with performance accuracy above 90%. In this study, the learning model used was ANN. The small testbed demonstrated the potential of cognition on software-defined elastic optical networks.

In Mo *et al.* [206], they studied a Deep Neural Network (DNN) to predict the power dynamics of a 90-channel ROADM system. In their study, a comparison between DNN, ridge regression and RF is presented, favoring DNN with the lowest maximal error (0.8 dB). They performed online training with 6720 training samples. The experiments were carried out in a small testbed, analyzing the effects of power excursions encountered in the amplification process of EDFAs.

Seve *et al.* [207] have proposed a learning process for reducing uncertainties on network parameters and design margins, based on the correlation of input parameters to network components (i.e., amplifiers and receivers), and using machine-learning techniques to reduce the uncertainties from these.

Proietti *et al.* [208–210] have demonstrated a control system assisted with a ML-based QoT-E in multi-domain elastic optical networks with alien wavelengths, capable of recognising modulation format, QoT monitoring, and cognitive routing. They have reported an OSNR prediction accuracy of 95% when using 1200 data points. Then, an experimental demonstration of this was introduced in Liu *et al.* [205], showing hierarchical machine-learning network management framework for impairment-aware end-to-end elastic optical RMSA service provisioning across multi autonomous domains. In this physical demonstration they reported QoT-E deviations below 10%.

Salani *et al.* [211] have proposed a ML-assisted QoT-E system, that is capable of detecting lightpaths with unacceptable QoT and improve spectrum allocation. They have reported spectrum allocation savings of up to 30% when compared to Integer Linear Programming modelling.

Sartzetakis *et al.* [212] have proposed a QoT-E method based on monitoring the QoT of existing connections, to learn the actual physical conditions of the network. They then feed this information to their ML algorithm, reporting good estimation performance with the use of a small dataset.

Curri *et al.* [213] have proposed a scheme to combine an analytical model with ML models, in order to improve the overall QoT-E performance. They proposed that the ASE noise estimation should be carried out by a ML algorithm, whereas the NLI noise modelling can be performed by analytical models (i.e., GN model), when estimating the gOSNR.

Evidently, ML algorithms have a strong potential to assist QoT-E processes in the optical control plane. However, as more disaggregated testbeds are coming together, it is necessary to further evaluate the performance of these in real large-scale deployments.

2.4 Conclusion

We have reviewed that the disaggregation of optical networks is pushing vendors, manufacturers and network operators to rearchitect the implementation and operation of optical networking systems. We have also shown that only during the past decade multiple global consortia have emerged to tackle

the technical and operational challenges encountered in this area of research, and we can conclude that as of 2021 disaggregated networks are reaching a new level of maturity. For instance, with regard to the integration of heterogeneous technologies following a SDN architecture, research is focusing in enabling multi-layer (L0-L3) control as more testbeds are proving the manageability of all-optical networks in a disaggregated environment to be cost-effective [214]. Also, SDN controllers such as ONOS are becoming to be operatable in more commercial deployments. Moreover, communication protocols such as OpenFlow, OpenROADM and OpenConfig continue to be examined as more disaggregated optical equipment is becoming available in the market.

We can thus conclude that there are some research areas that are of high interest for the following years. For instance, there is a need for assessing more optical performance monitoring capabilities in the context of disaggregated optical networks, as it is becoming more cost-effective to collect physical layer data, other than the power and ASE noise levels, that can be used to build analytical information useful to enhance networking operations such as dynamic resource provisioning and/or fault management. In particular, the estimation and monitoring of NLI noise is a topic that is gaining significant attention [190, 215]. And, while several applications of ML algorithms assisting networking functions such as QoT-E [66, 216] have been demonstrated, it is still unclear to quantify the real benefits and uses of these technologies to boost optical SDN control.

3 Mininet-Optical, an Emulation System

3.1 Introduction

As we have reviewed in Chapter 2, Telecommunication networks in the optical domain are transitioning from closed to disaggregated networking systems [217]. This implies that most (if not all) of the optical network devices composing this type of networks today, will be controllable by control systems capable of dynamically reconfiguring their operation by means of software-based processes, described as Network Function Virtualisation (NFV) [62]. One of the key issues of control plane design is that hardware testbeds offer ground truth and line rate performance, but they are often expensive, hard to reconfigure, and limited in size. The development of innovative optical Software-Defined Networking (SDN) systems such as Open and Disaggregated Transport Network (ODTN) - Open Network Operating System (ONOS) [166] could benefit greatly from a flexible and scalable open source software emulator that emulates the physical, data, and control planes for packet-optical networks. However, research on the development of these systems and their controllers is limited by a dependence on expensive, small-scale testbeds, and emulation systems that do not currently model the physical, data plane, and control plane behavior. In packet networks, it is possible to emulate networking capabilities by virtualising the network card/interface of a computer or device (i.e., a switch), and make them available to other computers or devices [59]. While it is impossible to emulate the behaviour of light beams (i.e., it can only be simulated), it is possible to emulate the control capabilities of the equipment that compose optical networks, since these operations rely on software systems. At the ONA laboratory, we came up with the idea of integrating optical networking models of the physical effects with networking interfaces that emulate the control of optical networking devices, as well as SDN-controlled optical transmission and switching planes, to develop the world first packet-optical network emulation system: Mininet-Optical. The development of this system has been done in collaboration with the Center for Integrated Access Networks (CIAN) at the University of Arizona and the open-source Mininet project [59]. We first developed the simulation system for the transmission physics models, and then we integrated it with Mininet [59], a widely used emulator that supports disaggregated packet network emulation and is often used to develop and test SDN controllers and that it is being supported and developed by the Optical Network Foundation (ONF). By integrating optical network modelling with Mininet's existing emulation of IP and Ethernet networks, we can provide a complete platform for testing cross-layer operation of SDN control planes. Thus, Mininet-Optical simulates the physical behavior and impairments of the analog optical network, emulates the data plane of both packet and optical networks, and exposes SDN control Application Programming Interfaces (APIs) to SDN controllers (i.e., ONOS).

3.1.1 Scope and contributions

This Chapter aims to provide a clear understanding of all the components that form Mininet-Optical, our emulation system for prototyping optical network SDN control planes.

The main contributions of this Chapter are:

- Introduction of the architecture of an optical network simulation system.
- Design and implementation of an algorithm to model physical layer transmissions in the optical domain.
- Introduction of the architecture of an optical network emulation system, Mininet-Optical.
- Design and implementation of an algorithm to handle the models composing Mininet-Optical.
- Implementation of validation studies of Mininet-Optical against various models and testbeds.

3.2 Mininet-Optical Overview

In Figure 3.1 we show the architectural diagram of Mininet-Optical. At the bottom we show how the virtual network runs in a single Linux kernel. The middle layer shows how Mininet-Optical is integrated with Mininet. Mininet has been extended to use our optical transmission simulator as a built-in API that allows the instantiation of the optical network elements in a virtual network environment. While Mininet continues to operate as a packet-network emulator, we abstract the optical domain functionality within the electronic emulated network elements. For instance, Line Terminals and Reconfigurable Add/Drop Multiplexers (ROADMs) are abstracted from real ovs-switch instances, for which we have extended the Switch models from Mininet to distinguish between electronic and optical classes. Optical fiber links between ROADM nodes, together with Erbium-Doped Fibre Amplifiers (EDFAs) and Variable Optical Attenuators (VOAs) are abstracted from virtual-Ethernet (v-eth) links. Then, optical network transmissions are abstracted from the emulated packet transmissions by encapsulating parameters of the optical transmission models in the packet headers, which are processed at each Switch node model in Mininet. With this design, we can take advantage of the built-in southbound control plane Mininet interfaces to enable the SDN control of the emulated network elements. Also in Figure 3.1 the top layer shows the control plane interface for SDN controllers. To a control plane, Mininet-Optical appears as a Southbound Interface (SBI), so that commands from the controller are forwarded to the virtual optical elements, and their behavior reproduced by the physical layer simulation. The same southbound interface is used by the SDN controller to retrieve Optical Performance Monitor (OPM) information. Currently, we have deployed a REST server written in Python to enable the SDN control of the emulated devices, matching requests to individual networking functions with the OpenFlow protocol. However, our design supports future implementation of standard APIs such as T-API, OpenROADM or OpenConfig for plug-and-play compatibility with hardware networks.

By enabling the simulation of optical transmission impairments, Mininet-Optical enables the modeling of optical components behavior, while managing their operation through an SDN control plane. Elements modeled by Mininet-Optical include: transceivers; colorless ROADMs with Wavelength-Selective Switches (WSSs), and VOAs for channel power leveling purposes; EDFAs for boost-, inline- and pre-amplification; and OPM devices. In Mininet-Optical, OPMs can in principle provide any information that is simulated by the physical transmission layer. Concretely,

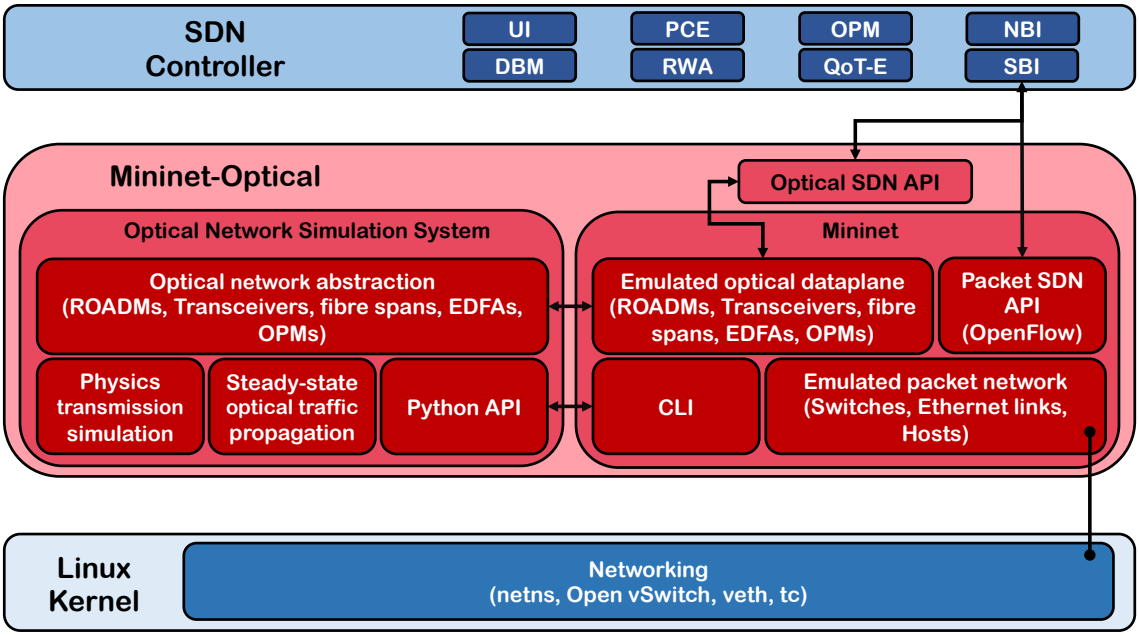

Figure 3.1: Mininet-Optical - Architecture Diagram.

the enabled monitoring capabilities allow us to collect optical signal power, Amplified Spontaneous Emission (ASE) and Nonlinear Interference (NLI) noise data of individual channels and study collective effects that can manifest over an optical link. Also, OPMs emulate Optical Signal to Noise Ratio (OSNR) monitors or reference receivers that can recover estimates of the full Generalized Optical Signal to Noise Ratio (gOSNR), either of which can be interrogated through a control plane interface.

3.3 Transmission Physics Simulation

Depicted in the centre-left of Figure 3.1, a simulation subsystem models the optical transmission physics using analytical models (such as the GN-model for fibre nonlinearities). In our design, each modelled network component is abstracted as a software-object that take as input the abstracted representation of optical signals (e.g., optical signal objects), process them according to an algorithm (i.e., switching), and then relay these to other objects. Optical signal objects are described by their wavelength, frequency, symbol rate, modulation format, power levels and noise levels, and keep track of their steady-state processing at each point of a network, which then can be easily monitored by the OPM components enabled in the system. A key feature from our implementation design is that it allows for customised configuration of the network elements individually. For example, it is possible to set wavelength dependent noise figure functions in the EDFAs and to set specific wavelength-dependent gain functions, to then evaluate its performance in optical transmission systems with signal power behaviour modeling physical testbed performance. Table 3.1 lists the specific physical models that are used to simulate the optical transmission for each network element. Due to the modular design of this system, it is possible to extend and modify the transmission physics models

to evaluate different performances.

Table 3.1: Transmission Physics Models of Network Elements

Network Component	**Transmission Physics Model**
ROADM	Component Insertion Losses Wavelength-Dependent Attenuation Channel Power Leveling
Optical Fibre	Optical Fibre Linear Attenuation Optical Fibre Dispersion Stimulated Raman Scattering [218] Self-Channel Interference Noise [219] Cross-Channel Interference Noise [219]
EDFA	Wavelength-Dependent Gain Optical Power Dynamics [220] Amplified-Spontaneous Emission Noise

3.3.1 Physical models

Transmission physics models such as the component insertion losses of ROADM nodes are the simplest to model, since these consist in defining an insertion loss per component and use it as the attenuation value inflicted to the signal power and noise levels. Thus, we do not include the analytical representation of these. However, the rest of the models listed in Table 3.1 operate as independent subsystems that compute the multiple physical effects. These models are described as follows:

Stimulated Raman Scattering

The Stimulated Raman Scattering (SRS) effect is a property of optical fibre that is well understood today. It consists of the increase or decrease of wavelengths by means of energy exchange. In Mininet-Optical, we implement the model proposed by Zirngibl in [218]. Zirngibl determined that to be able to describe the SRS effect with a simple model the following three assumptions must be met. First, the Raman gain coefficient has a triangular profile. Second, we can neglect the energy that is lost whenever a short wavelength photon is transformed into a long wavelength photon (i.e. $\lambda_i/\lambda_k \sim 1$). Third, we consider uniform loss and negligible noise. Considering these, we can then describe the Raman coefficient in single-mode fibres (SMFs) with Equation 3.1:

$$\beta = \frac{r}{2 \times A_{eff} \times B} \tag{3.1}$$

Where $r[m/W]$ is the Raman fibre gain, $A_{eff}[\mu m^2]$ effective core area and the factor of 2 is due to random polarisation, and $B[THz]$ is the Raman amplification band (commonly 15 THz for SMF). Consequently, it is possible to describe the Raman gain/loss of each signal (λ) with Equation 3.2:

$$R(\lambda) = \frac{\beta P_0 L_{eff} \left(\lambda_{\max} - \lambda_{\min}\right) \exp\left\{\beta P_0 L_{eff} \left(\lambda - \lambda_{\min}\right)\right\}}{\exp\left\{\beta P_0 L_{eff} \left(\lambda_{\max} - \lambda_{\min}\right)\right\} - 1} \tag{3.2}$$

Where λ is the frequency of the signal of interest, $P_0[mW]$ is the total power given by all signals in the fibre, $L_{eff}[km]$ is the effective length of the fibre. Thus, the variation in frequencies as established by λ_{max}, λ_{min} and λ is also expressed in [Hz].

Gaussian Noise Model of Non-Linear Interference in Coherent Optical Transmission Systems

The nonlinear interference noise due to Self-Channel Interference (SCI) and Cross-Channel Interference (XCS) is the most complex of the models in our simulation system. This is due to the fact that its randomised physics nature is hard to model in a closed-form formula. However, in the past decade these phenomena have been investigated in detail, and it has been demonstrated by Poggiolini *et al.* [221] that by assuming a Gaussian (normal) behaviour of this type of noise, an accurate approximation with a closed-form formula can be given by Equation 3.3:

$$G_{\bar{E}_{NLI}}\left(f_{ch,i}\right) \approx \frac{16}{27}\gamma^2 L_{eff}^2 \sum_{n=1}^{N_{ch}} G_{ch,n}^2 G_{ch,i} \cdot \left(2-\delta_{ni}\right)\psi_{n,i} \tag{3.3}$$

In this Equation, the factor $\frac{16}{27}$ is attributed to dual-polarisation fibre effects and it can be obtained from the full derivation of this closed-form expression [221]. The fibre non-linearity coefficient is given by $\gamma[1/(Wkm)]$, $L_{eff}[km]$ is the effective length, and the factors determined by G ($G_{\bar{E}_{NLI}}$, $G_{ch,n}$, $G_{ch,i}$) correspond to the Power Spectral Density (PSD) of the channels. δ accounts for SCI or XCS, since it takes the value of 1 when $n = i$ and 0 otherwise. Last, the ψ coefficient is described by Equations 3.4 and 3.5, which compute the XCS (3.4) and SCI (3.5), respectively. For a full derivation of this model we refer to Poggiolini *et al.* [221].

$$\begin{aligned}\psi_{n,i} \approx N_s \frac{\operatorname{asinh}\left(\pi^2[2\alpha]^{-1}|\beta_2|[f_{ch,n}-f_{ch,i}+B_{ch,n}/2]B_{\mathrm{ch},i}\right)}{4\pi(2\alpha)^{-1}|\beta_2|} - \\ -N_s \frac{\operatorname{asinh}\left(\pi^2[2\alpha]^{-1}|\beta_2|[f_{ch,n}-f_{ch,i}-B_{ch,n}/2]B_{\mathrm{ch},i}\right)}{4\pi(2\alpha)^{-1}|\beta_2|}, \quad n \neq i\end{aligned} \tag{3.4}$$

$$\psi_{i,i} \approx N_s \frac{\operatorname{asinh}\left(\frac{\pi^2}{2}|\beta_2|\left[2\alpha\right]^{-1}B_{ch,i}^2\right)}{2\pi|\beta_2|\left[2\alpha\right]^{-1}} \tag{3.5}$$

EDFA System Gain

The wavelength-dependent characteristics of network components in optical network transmission systems result in wavelength-dependent impairments on the transmitted optical signals. In particular, the Wavelength-Dependent Gain (WDG) when EDFAs operate in Automatic Gain Control (AGC) mode can lead to unequal channel power compensation, often referred to as channel power divergence. This effect is commonly mitigated by vendors through Gain Flattening Filter (GFF). However, the GFF solves the problem only in part, as there is a residual WDG due to component-specific behaviour, amplifier operation point changes, nonlinear gain effects, which can be of the order of ±0.5-1.0 dB [220], resulting in power divergence that can accumulate between nodes and reduce the Quality of Transmission (QoT) [222]. To compensate for the WDG effect, it is common practice to deploy VOAs at system level (i.e., at the ROADM). For Mininet-Optical, we model this WDG operation in EDFA by representing the WDG as a function of channel wavelength, that we refer to as $f(\lambda)$. To model these, we consider WDG functions that have been retrieved from physical systems. Thus, we can simply model the EDFA system gain with Equation 3.6:

$$G_{sys} = G_t \times f(\lambda) \tag{3.6}$$

Where G_{sys} is the EDFA system gain (mean gain), G_t is the target gain (configuration gain) and $f(\lambda)$ refers to the ripple function of the amplifier.

EDFA Amplified Spontaneous Emission Noise

In addition to amplification, EDFAs also add noise to the optical signals. This type of noise is known as ASE noise, and it is due to photons that are emitted independently (i.e., without being stimulated) by the incoming signal, and it has been studied thoroughly over the past decades. In our system, we use a simplified model. The model is described as follows:

$$P_{ASE} = P_{ASE} \times G_{sys} + NFh\lambda_f(G_{sys} - 1)B \tag{3.7}$$

Where P_{ASE} is the aggregated noise at a given point, G_{sys} is the gain of the EDFA in mW, NF is the noise figure, h is the Planck's constant, f is the centre frequency of the optical signal and B is the bandwidth for which the amplifier has been configured.

EDFA Power Excursions

The power excursions that occur in EDFAs are because the AGC algorithms tend to neglect the gain ripple and tilt of these systems. For an AGC–EDFA, the ratio of the total output power to the total input power needs to be maintained to guarantee operational QoT. By neglecting the ASE noise gain ripple and tilt, we can use Equations 3.8–3.10 to approximate the effect of power excursions, as explained by Mo *et al.* [220]:

$$P_{o,k} = \left(\sum_{j=1}^{N} P_{i,j} / \sum_{j=1}^{N} G_j P_{i,j} \right) G_T G_k P_{i,k} = G_k P_{i,k} \tag{3.8}$$

$$P'_{o,k} = \left(\sum_{j=1}^{N'} P'_{i,j} / \sum_{j=1}^{N'} G_j P'_{i,j} \right) G_T G_k P_{i,k} = (G_k \Delta G)\, P_{i,k} \tag{3.9}$$

$$\Delta P_{o,k}(dB) = 10 \times \log_{10} \left(\frac{P'_{o,k}}{P_{o,k}} \right) = 10 \times \log_{10}(\Delta G) \tag{3.10}$$

Where G_T is the target gain setting for the AGC EDFA, G_j is the WDG for channel j. $P_{i,j}$ and $P_{o,j}$ are the input power and output power for channel j. N and N' are the number of channels input to the EDFA before and after wavelength reconfiguration. $P_{i,k}$ and $P_{o,k}$ are the input power and output power for channel k before wavelength configuration, and $P'_{o,k}$ output power for channel k after wavelength reconfiguration.

3.3.2 Operational features

Channel Power Leveling

Our ROADM nodes are composed of WSSs for providing direction to the signals that are traversing, and VOAs at each output port of the WSSs to provide means of variable attenuation to the optical signal. In the operational design, we have considered a control circuit at the ROADM nodes that adjusts the optical spectrum to ideal operational power levels, enabling all channels in the spectrum to have approximately equal power levels. This process consists in attenuating all channels traversing a ROADM node by a fixed value (i.e., 3 dB), additional to the component insertion loss attributed to the WSSs (i.e., 7 dB). Both values are customisable. After the signals are muxed into the output ports, we consider the inclusion of a boost EDFA to compensate for the ROADM losses. We monitor the output ports of the boost amplifier, to feed power level data to the control circuit in the ROADM nodes, in order to calculate the individual channel attenuation to mitigate with the VOAs, and consequently compensate for these. This control circuit exits when it detects that the spectrum has been flattened, which occurs approximately after 1 circuit loop. The computation of the leveling factors for individual channels are described in Equations 3.11 and 3.12.

$$\Delta P = P'_{out}/P'_{in} \tag{3.11}$$

$$P'_{in} = P_{out} \times \Delta P \tag{3.12}$$

Where $\Delta P[mW]$ is the variation in power level given by the difference between the output power at the EDFA (P'_{out}) and the input power at the EDFA (P'_{in}). Then, we correct the output power at the ROADM (P_{out}), by applying this correction factor to it (Equation 3.12).

3.4 Simulation system

At the ONA laboratory, we have developed the Optical Network Simulation System (ONSS) system, including the validation of physics transmission models, as well as the integration to the other subsystems (i.e., emulation). The simulation system is the backbone of Mininet-Optical. As we have explained above, it contains the models that describe optical network elements such as optical fibre spans, transceivers, colorless ROADMs with WSSs and VOAs for switching and channel power leveling purposes, EDFAs for boost-, inline- and pre-amplification, and OPM devices. Also, it contains the models that describe the physical impairments to optical signals associated to each of the network elements in an optical transmission, such as the nonlinear effects from optical fibre. This simulation system is developed as an independent piece of software, entirely written in Python, and can also be used as a stand-alone system for offline simulations. Additionally, and for the purposes of disaggregated optical control plane prototyping, it can be used as a library of APIs, providing access to the descriptive models of the network elements, enabling active reconfiguration. This feature is key to the development of disaggregated optical networking scenarios, since it allows the reconfiguration of devices *on-the-fly*. This latter concept will be further explained in section 3.3.2, together with a detailed description of the mathematical models of the physical effects of

the optical network elements. In this section, we present the architecture design of the simulation system including each individual network component.

3.4.1 Architecture

The architecture diagram of the ONSS is illustrated in Figure 3.2. The ONSS (parent entity in green) is the virtual environment that orchestrates the definition and execution of optical networking scenarios. It comprises the model definitions for optical network elements and their associated physical effects. For that, it relies on a steady-state propagation subsystem enabling a dynamic interaction with the simulation system. Also, it provides the interfaces to remotely interact with the network components. The latter is provided in the form of Python APIs that can be called as third-party software when using the ONSS. The key component of the ONSS is the Optical Network System (ONS), which can be understood as a single entity within the ONSS. The ONS acts as a wrapper for the definitions that compose a network scenario, containing the information about the network components, the network topology and the state of the network. However, the elements that compose the ONS are not constrained to fixed and direct management from this entity, but are detached as independent components as each element is an independent object.

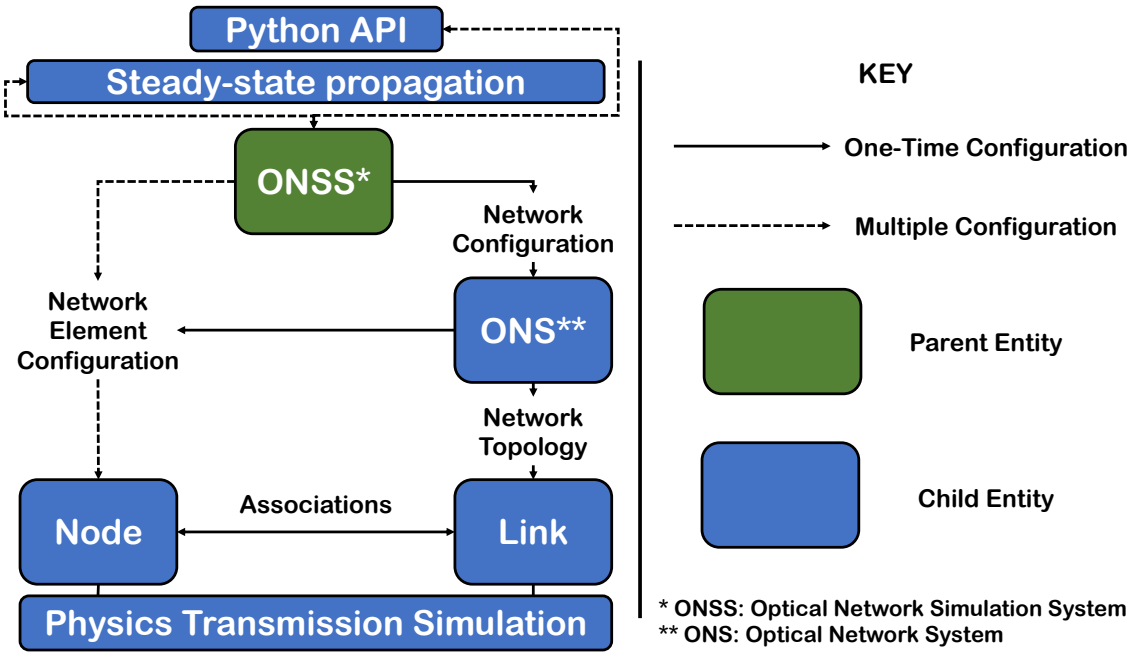

Figure 3.2: Optical Network Simulation System - Architecture Diagram.

These components are divided into two main types. Firstly there are the nodes, which can be defined as elements of the network that can be programmable by the ONSS or by an external source (i.e., remote controller). Secondly, there are the links, which are static elements comprising the connections between nodes and define the topology. Upon transmission (steady-state propagation), the transmission physics simulation models are triggered for each component and aggregate as a pipeline according to the flow of the transmission.

3.4.2 Simulation process

The algorithm of the simulation system follows a simple process. It is embedded in the steady-state propagation subsystem, already presented in Figure 3.2. Its simplicity is enabled by the modular design of the components and the interactions between them. Then, it is possible to describe the algorithm as follows:

1. The first thing that is needed is to declare the components in the optical network model. That is, instantiating the line terminals with their transceivers for transmission and reception, the ROADMs with their WSS–VOA, as well as the monitoring capabilities enabled within these nodes.
2. Once the main nodes are created, it is possible to inter-connect them with optical links to build the network topology. Optical links are declared in two steps: *i)* instantiation of the link between two elements, and *ii) decorating* the link object with elements such as optical fibre spans and EDFAs.

The next algorithm models the signal transmissions. Due to the modular design of our system, managing optical transmissions is a rather logical process that only requires the inclusion of an external model from the network, which is the optical signal. Within the ONSS, optical signals are instantiated as regular objects that carry physical properties such as the central frequency or the channel spacing and symbol rate for which they have been encoded. The algorithm used for the transmissions operates as follows:

1. The first step in this process is to instantiate the signals that are going to be transmitted (i.e., wavelength, launch power levels, signal encodings, etc.).
2. Once the optical signals are declared, the next step consists in configuring the devices to transmit and mux/demux the signals. Intuitively, the first device that must be configured is the terminal and the transceivers that would be used for launching the signals. Subsequently, it is necessary to configure the ROADM nodes to create switch-tables with the information of the expected input and output signals at a given node. However, it is possible to declare routing functions within the ROADMs at any point. Furthermore, it is possible to reconfigure the EDFAs to set the mean system gain to the desired one at the various locations these are placed.
3. After all the devices have been configured, it is then possible to 'turn on' the transmitters, enabling the signals to traverse the network.
4. Traversing the network consists in each network component processing the signals (i.e., attenuating or amplifying) as they are relayed to each of them, to then pass them to the next element according to their configuration. Intuitively, if the network elements are not configured properly, the transmission will be unsuccessful. However, these errors are easily detectable with the monitoring interfaces provided in the system, and due to the simplicity of the reconfiguration processes they are easily solvable.

The main advantage of using the simulation system is in the ease of network deployment and reconfiguration of elements. When trying to test simple features or executing quick transmission runs, the fastness of these processes alleviate the time consuming tasks when dealing with physical testbeds. However, our tool is not intended to be a replacement for these types of testbeds, since validation against hardware systems must always be addressed. In section 3.6, we discuss the limitations of the system, and show how we validated its performance against a hardware testbed.

3.5 Emulation system

The simulation system provides the means to evaluate transmission physics performance at the optical layer following a defined set of assumptions. However, it is incomplete to assess data plane management, control plane procedures, and system interconnection outside of the simulation environment (i.e., interoperability with third-party systems). Because of this, we merged the control APIs from the ONSS to comply with that of Mininet. With this extension, we were able to develop the first packet-optical network emulation system, providing network planning and optimisation capabilities at the optical layer, simultaneously enabling the development of control plane procedures in a wide range of scenarios such as optical link failure or optical device failure. In addition, it enables the development of control plane procedures for hybrid optical-electronic networks. The architecture diagram of the emulation system is illustrated in Figure 3.3. Noticeably, the parent entity from Figure 3.2 (ONSS) has been replaced by the Optical Network Emulation System (ONES), which in our system is equivalent to the Mininet environment.

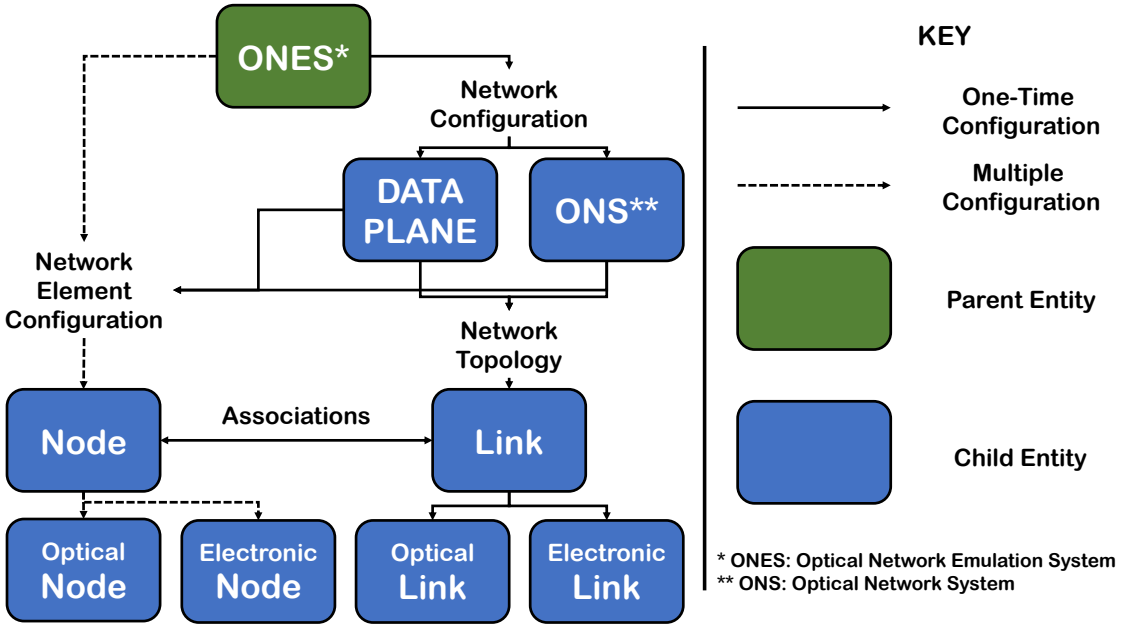

Figure 3.3: Mininet-Optical, an Emulation System - Architecture Diagram.

3.5.1 Architecture

The intent of including the ONES as a separate system is to present the operation as seen from the emulation environment. This is because within Mininet-Optical, the management of the control plane interfaces is a task enabled by the system itself, which is further explained in Chapter 4. Similar to the ONSS, the ONES is the parent entity in charge of describing, configuring and deploying the virtual optical network. The main difference is there is a way to use both optical and electronic devices. Additionally, there is a different way of establishing connections among devices, as well as launching optical transmissions. Mainly, there is a higher level of detail that is included, which enables the management of real electronic data, i.e., bit transmission sensitivity.

3.5.2 Emulation process

The key element of the emulation is the dataplane block depicted in Figure 3.3. Mininet has been extended to use the ONSS as a built-in library of APIs that enables the instantiation of the optical network elements within the virtual (emulated) environment. While Mininet continues to operate as a packet-network emulator, we abstract the optical domain functionality within the electronic network elements. For instance, Line Terminals and ROADMs are abstracted from real ovs-switch instances, enclosing information of the optical domain within packet headers. As the electronic packets are relayed across the network, Mininet extracts the optical information from the packet headers and processes them with the simulator. Once processed, the packet headers get updated and relayed to the next node as instructed by the switching rules in the optical and electronic domains. A REST server is deployed to enable the SDN control of the devices in the optical domain, matching requests to individual networking functions. However, as we have mentioned above, our design supports future implementation of standard APIs such as OpenROADM or OpenConfig for plug-and-play compatibility with hardware networks.

The algorithm of Mininet-Optical in emulation mode is almost identical to that of the simulation system. While the network deployment is performed similarly (i.e., declaration of network topology), configuring the devices is no longer performed by the same subsystem (e.g., ONS), but it is implemented with an external control system, completely independent of the underlying simulation system, as depicted at the top of Figure 3.4. This is described as follows:

- Mininet orchestrates the communication interfaces of the devices that it emulates via OpenFlow protocol, so that the elements that are being declared from the control system are abstracted within Mininet and the ONSS. An example of the installation of flow-rules to the virtual (packet) switches to be reflected in the optical (simulation) system is depicted in Figure 3.4. Currently, we use basic OpenFlow commands (e.g., add-flow) to configure the virtual electronic switches. As our dataplane processes the packet headers, the relevant information (i.e., ports and channels) is relayed to the simulation system.
- Upon transmission, optical signal objects are no longer just relayed among the virtual elements of the simulation system, but are capsuled within the real electronic packets that are passed between the electronic switches. Every time a packet arrives to an electronic switch, the switch decouples the optical signal object from the packet header, then passes the relevant optical transmission parameters to the underlying transmission physics simulation, in a similar sequence of events as for the installation of flow rules.
- At the physical layer simulation, the signals are processed according to the abstracted network representation. For instance, the physical effects attributed to ROADMs, optical fibre links, EDFAs, are computed at this point, and the steady-state of each abstracted optical signal gets updated.
- Lastly, these signals are relayed back to the Mininet dataplane environment to capsule the appropriate parameters in the packet headers, and continue the electronic transmission (i.e., packet switching). At this point, we update the packet headers with OpenFlow commands such as flow_mod, which are processes embedded in our extension to Mininet.

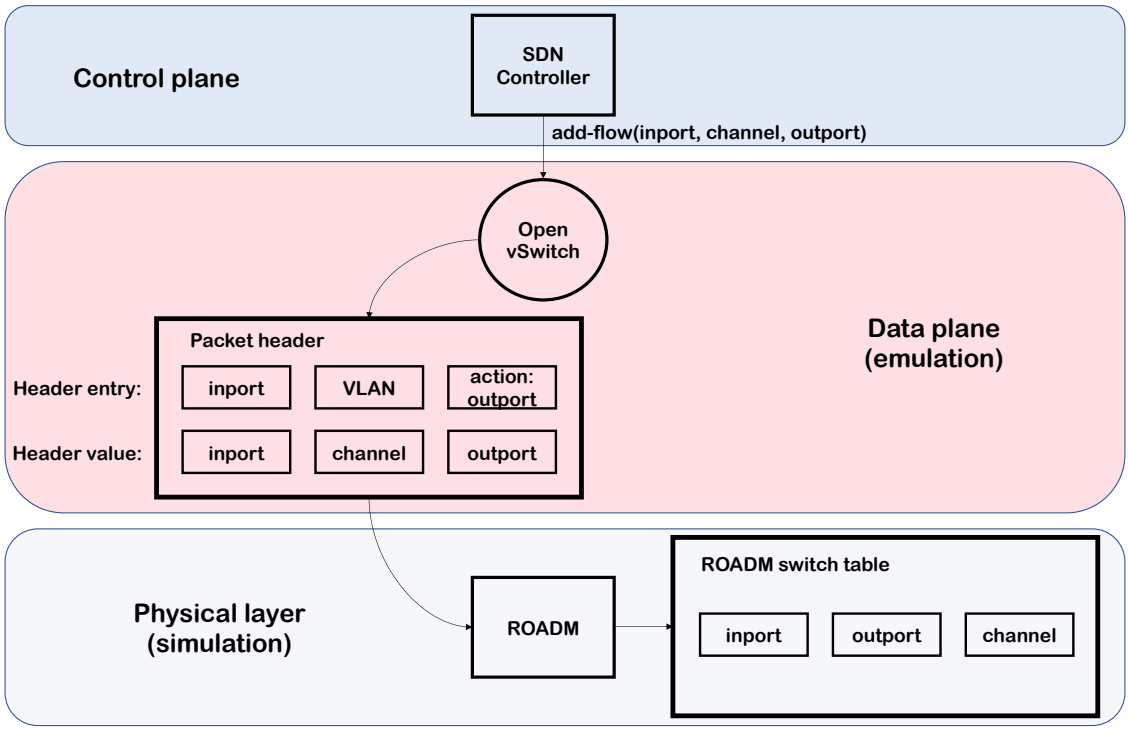

Figure 3.4: Installation of flow rules in Mininet-Optical.

3.6 Validation and demonstration

3.6.1 Evaluation of analytical models

We begin with a performance validation of our system against the OOPT-GNPy Project [2]. For this assessment, we have modeled a linear topology, following the topological composition of Figure 3.5, with 5 ROADM nodes connected by SMF-28 optical fiber links of 240 km, made up of 3 x 80 km spans. Boost EDFAs at each ROADM output compensate the 17 dB mean ROADM loss, and inline EDFAs compensate the 17.6 dB fiber span loss. We also apply channel equalisation at each ROADM, by setting the VOAs appropriately. The total end-to-end distance is 960 km. Virtual OPM devices are applied at the EDFA outputs depending on the monitoring strategy described below. For the purposes of these studies, we consider OPM devices capable of separately measuring signal power, ASE noise and NLI noise levels.

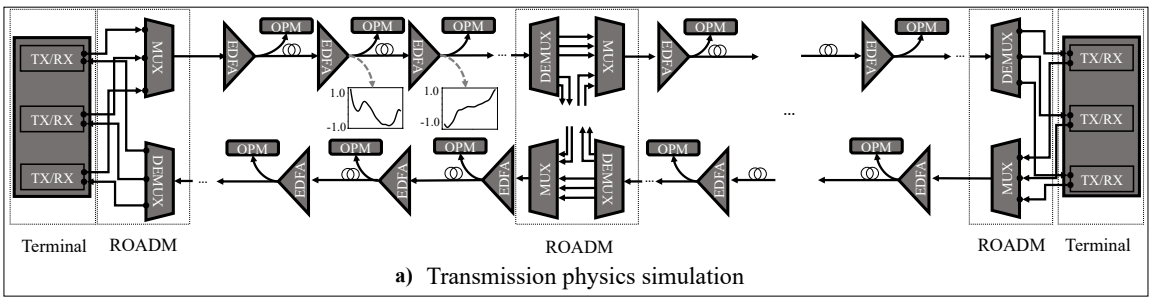

Figure 3.5: Linear topology composition example.

Then, we evaluated multiple transmissions at different power levels, [-8, 8] dBm at a 2 dBm power step, with 90 C-band channels and monitored the centred channel at the end of the link. In Figures 3.6a and 3.6b we show the OSNR and gOSNR performance, respectively. We can see that both OSNR and gOSNR modelling of Mininet-Optical perform closely to the OOPT-GNPy Project in the light-blue and red curves, respectively, when we do not include other physical effects such as the SRS [218]. Mininet-Optical performed with an OSNR mean absolute error (MAE) of 0.13 dB and a gOSNR MAE of 0.16 dB when comparing the centred channel at the different power levels. The dark blue curves show the impact of including SRS on the same 90 channel transmission, when monitoring at the first channel in the transmission (solid), the centred channel (dotted) and the last channel (dashed). As we have explained above, the SRS effect produces an exchange of energy from the lowest frequency channels to the highest. Thus, in Figure 3.6a we can observe that as the highest frequency channel (channel 90) gains energy, its OSNR levels increase. The opposite behaviour is seen at the lowest frequency channel (channel 1). In Figure 3.6b we can observe that the gOSNR levels of channel 90 increase when the power levels acquire more energy and when the ASE noise dominates the gOSNR (e.g., power levels < 0 dBm). Accordingly, the gOSNR levels of channel 90 drop rapidly as the power levels increase. The inverse effect is seen at the lowest frequency channel.

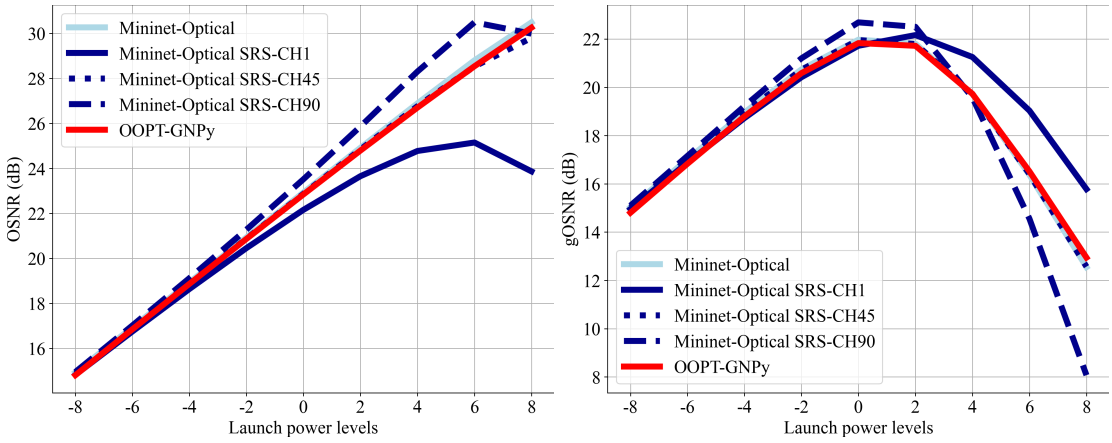

(a) (b)

Figure 3.6: (a) OSNR and (b) gOSNR performance comparison between the OOPT-GNPy Project [2] and Mininet-Optical (red and lightblue curves, respectively), and Mininet-Optical with SRS modelling (darkblue curves) for the first, centre, and last channels in a 90 C-band channel transmission.

Evaluation of the optical fibre SRS effect

In general terms, the SRS effect results in the passing of energy from the lowest wavelengths to the highest wavelengths in the optical spectrum, as the signals composing the spectrum interact with an optical fibre medium. Here, we evaluate the performance of the model described by Zirngibl [218], integrated with the other models, by looking at transmissions considering multiple channel loadings (as this is an effect that varies with the channel load), using the same topology described for the previous example. This time, we sequentially transmitted the number of wavelength channels 8, 16, 32 and 64 at 0 dBm launch power. The impact on different signals is depicted in Figure 3.7.

First, in Figure 3.7a, we observe the performance of the last wavelength channel for the different loadings. As expected, the higher number of channels (sequentially) allocated in a transmission, the higher the exchange of energy from lower wavelengths to higher wavelengths [218]. We can see

that as the number of transmitted channels increase, the excitation perceived (energy acquired) at the last channel in the transmission, which is also the channel with the highest frequency, is increasing. Additionally, we can also see the evolution of SRS as it accumulates in an inter-node link, which in Figure 3.7a is given by the interval from one OPM node location to the next one. For example, we can see a cumulative pattern from OPM locations 1-4, and the location 5 the power levels are flattened down to 0 dBm. The latter, is because at location 5 we are looking at the boost amplifier compensating for the first ROADM node in our linear topology, which performs the channel equalisation process.

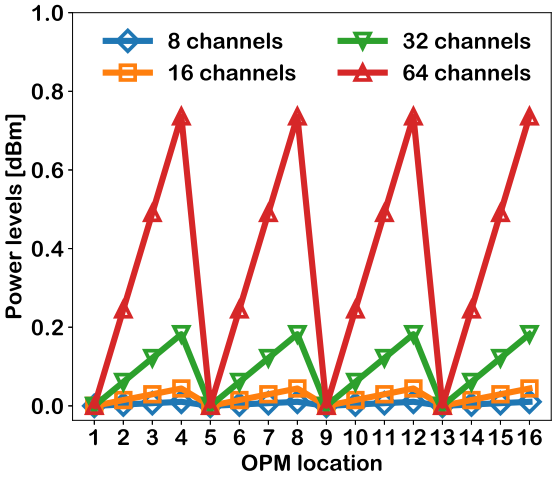

(a) λ's: 191.7, 192.1, 192.9, 194.5 [THz].

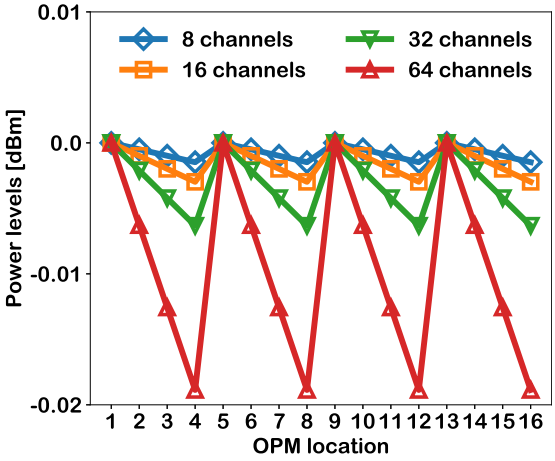

(b) λ's: 191.45, 191.65, 192.05, 192.85 [THz].

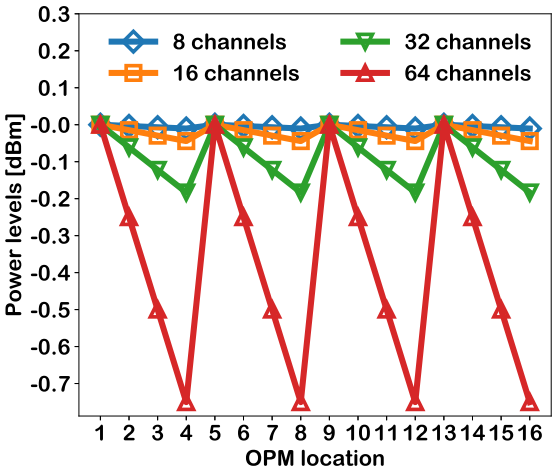

(c) λ: 191.35 [THz].

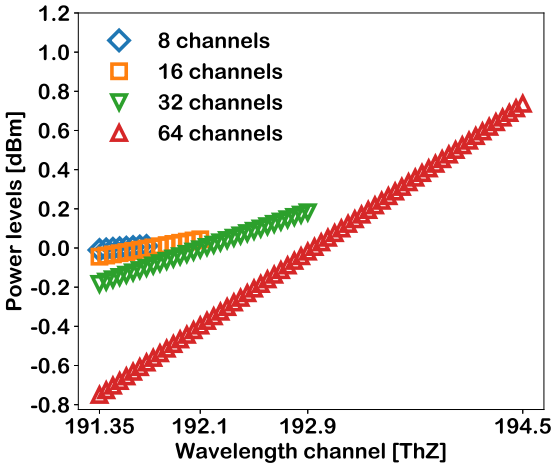

(d) λ: 191.35 - 194.5 [THz].

Figure 3.7: Evolution of the power levels due to the SRS effect at different monitoring locations.

Next, we also look at the centred channel for the different channel loadings, and show this in Figure 3.7b. By looking at the vertical axis it is noticeable that the effect of SRS is significantly smaller. This is because these channels do not suffer from drastic energy perturbations, as their energy levels remain balanced by the channels at each end of the spectrum. However, it is also noticeable that a pattern occurs in decreasing the power levels in a cumulative form as the signals traverse the linear topology. This is because we monitor the shortest frequency closest to the centre of the transmitted spectrum (i.e., when transmitting 8 channels, we monitor channel 4 instead of

channel 5). Thus, the patterns observed in Figure 3.7b confirm that the exchange of energy always goes from shortest to highest frequency/wavelength. These perturbations are again compensated at each ROADM node with the VOA nodes.

We also look at the first channel for all transmissions (e.g., frequency 191.35 THz). The performance of this channel is shown in Figure 3.7c. The interesting feature of these three figures (3.7a, 3.7b, 3.7c) is that, as reported in Zirngibl [218], the exchange of energy is a rather symmetrical phenomenon. Thus, comparing Figures 3.7a and 3.7c, we can see that the impact of the first and the last channel in a transmission is inversely proportional. This symmetry is much better depicted in Figure 3.7d, where we show the exchange of energy across the full transmitted spectrum. It also becomes evident that by increasing the number of channels in a transmission, the higher the impact on the edge-channels due the SRS effect.

Evaluation of the optical fibre NLI noise

We now look at the evolution of the NLI noise with a similar approach to the one used for the assessment of the SRS effect. This is depicted in Figure 3.8b. The contribution of the NLI noise perceived at an optical signal is dependent on its power level intensity. Because the NLI noise is the result of the combination of SCI and XCS, the impact on a given signal is also dependent on the performance of the neighbouring signals. We have already shown in Figure 3.6b that our model matches that of the OOPT-GNPy project when we do not consider the SRS effect or the wavelength-dependent operation of the network components. Thus, this time we consider the presence of the SRS and the NLI noise at the same time. Consequently, the power levels of the transmitted channels would also experience an energy exchange due to this effect.

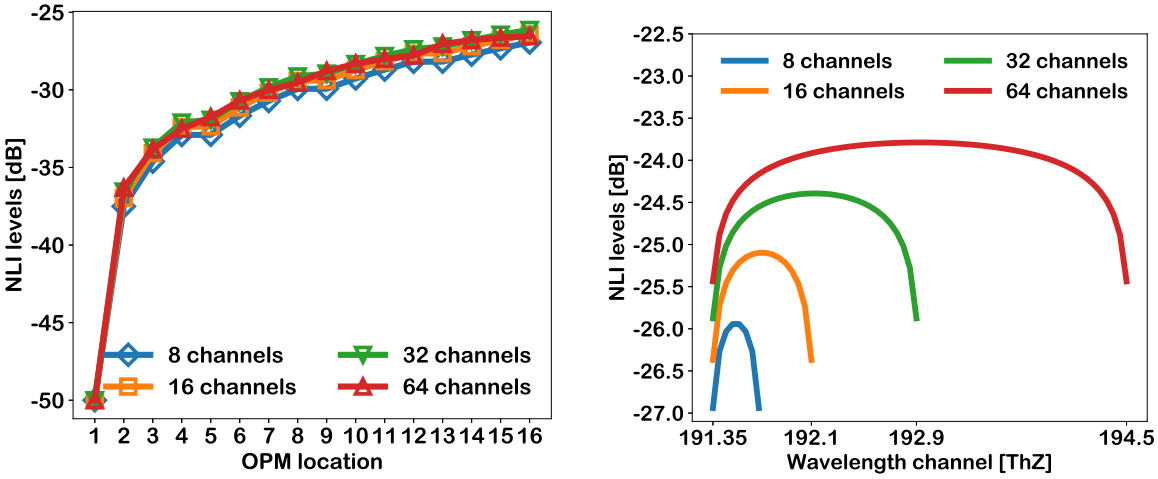

(a) λ: 191.35 [THz].

(b) λ's: 191.35 - 194.5 [THz].

Figure 3.8: (a) Evolution of the NLI noise levels considering the XCS and SCI nonlinear effects as a function of the monitoring locations. (b) Spectral NLI evolution at the receiver end for different channel loading strategies.

As described in Equations 3.3, 3.4 and 3.5, in addition to the dependence of channel-power levels, the occurrence of NLI noise is dependent on the length of a fibre span. Consequently, and because in our linear topology all the spans are of equal length, the contribution of the NLI noise at each stage is the same. The only exceptions are the ROADM nodes where no NLI noise is generated.

It is important to remark that the NLI noise, as the ASE noise, accumulates as it occurs at the producing elements of the network aggregate (i.e., cumulative optical fibre links). As such, neither type of noise can be eliminated as it appears, but they can be controlled by processing the signal power levels, for example, by means of channel equalisation.

Also, the main assumption of the GN model described by Poggiolini *et al.* [219, 221] (Equation 3.3) is that the occurrence of noise follows a Gaussian (normal) behaviour. To illustrate this effect, we show the occurrence of NLI noise as a function of the transmitted spectrum when looking at the receiver end of our linear topology. As we can observe, this type of noise becomes higher as the number of transmitted channels increases, and becomes more prominent at the centred sections of the transmitted spectrum, due to the Gaussianity assumptions.

Evaluation of the ROADM channel equalisation

The effect of the ROADM channel equalisation process is described by Equations 3.11 and 3.12. Here we look at the same transmission setups from the past two examples, only this time we look at the minimum and maximum OSNR levels from the transmitted signals. To remark the effect of this model, we first show the minimum OSNR levels without and with the equalisation process, as shown in Figures 3.9a and 3.9b, respectively. Because of the flattening impact onto the spectrum due to this process, we see a similar power evolution of the signals when considering the equalisation (Figure 3.9b), leading to an improvement of the OSNR at the receiver end (OPM location 16). The results from the analysis of the maximum OSNR are presented in Figures 3.10a and 3.10b. Because of the SRS effect, we see the contrasting behaviour between Figures 3.9a and 3.10a, where the different number of channels affects directly the OSNR of these cases. Another important point is the similar performance achieved in Figures 3.9b and 3.10b. Consistently, the minimum OSNR remains close to the maximum performance when the equalisation is performed at the ROADM nodes.

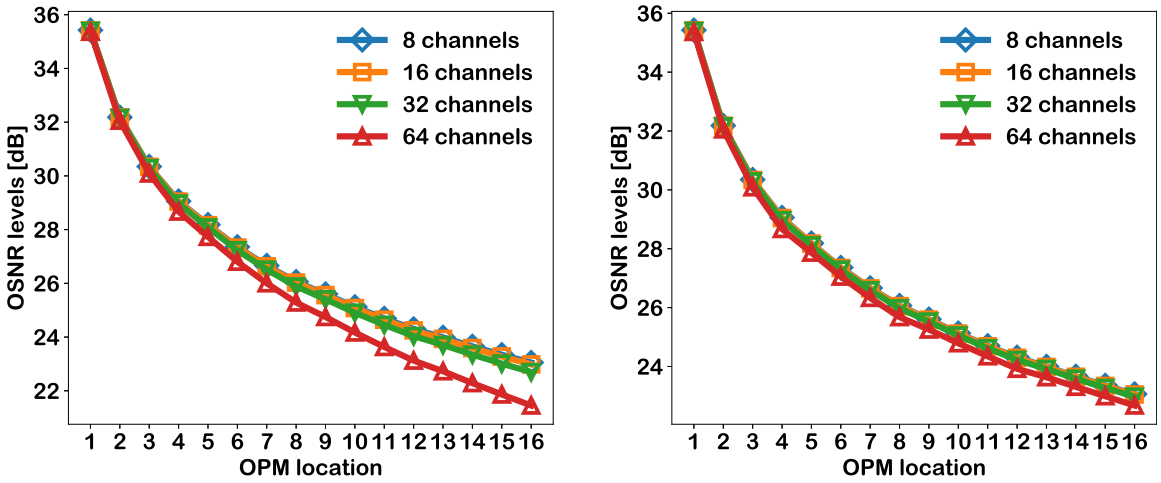

Figure 3.9: Minimum OSNR (a) without and (b) with equalisation at every ROADM.

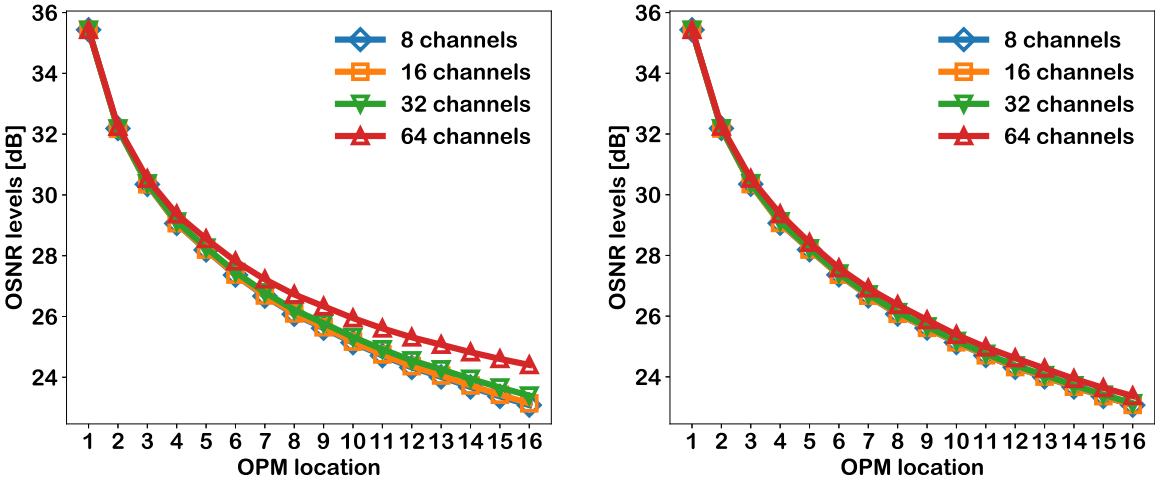

(a) (b)

Figure 3.10: Maximum OSNR (a) without and (b) with equalisation at every ROADM.

Evaluation of the EDFA-WDG model

The last model that we present is the one related to the EDFA–WDG effect. This is shown in Figures 3.11a–3.12b. To do that, we configured all EDFAs in the network with individual WDG as depicted in Figure 3.5. With that, we enable uneven EDFA system gain amplification, resulting in higher power divergences. Intuitively, as the WDG effects are produced in cascade, their impact aggregates, resulting in a spectrum behaviour that resembles the WDG $f(\lambda)$ functions.

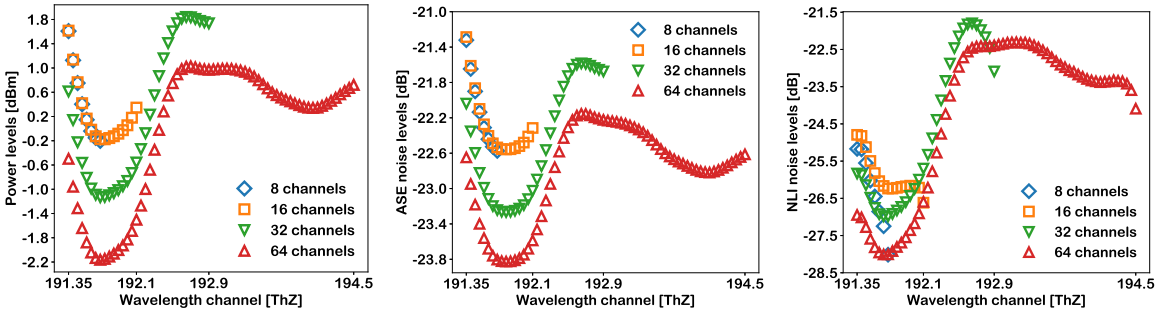

(a) Performance of power levels. (b) Performance of ASE noise. (c) Performance of NLI noise.

Figure 3.11: Performance evaluation of the EDFA-WDG: (a) Power levels, (b) ASE noise and (c) NLI noise.

Because this is an effect occurring at the EDFAs, the impact of the WDG functions are perceived similarly in the power and ASE noise levels, as seen in Figures 3.11a and 3.11b. For this evaluation, we only consider one WDG function for all EDFAs. As a consequence, the resemblance to this function of the channel metrics (i.e., power and noise levels) is rather sharp. However, in a real testbed all EDFAs would operate with different ripple effects, leading to an accumulation of uneven amplification gains that can significantly decrease the performance of the transmitted channels. As we have explained in previous sections, the NLI noise is dependent on the power. Thus, the effect of the WDG functions is perceived differently when observing this phenomenon. This is depicted in Figure 3.11c. While the pattern form by these curves resemble that from Figures 3.11b and 3.11a, it is noticeable that at the edges of the transmitted spectrum the NLI noise levels tend to vary less

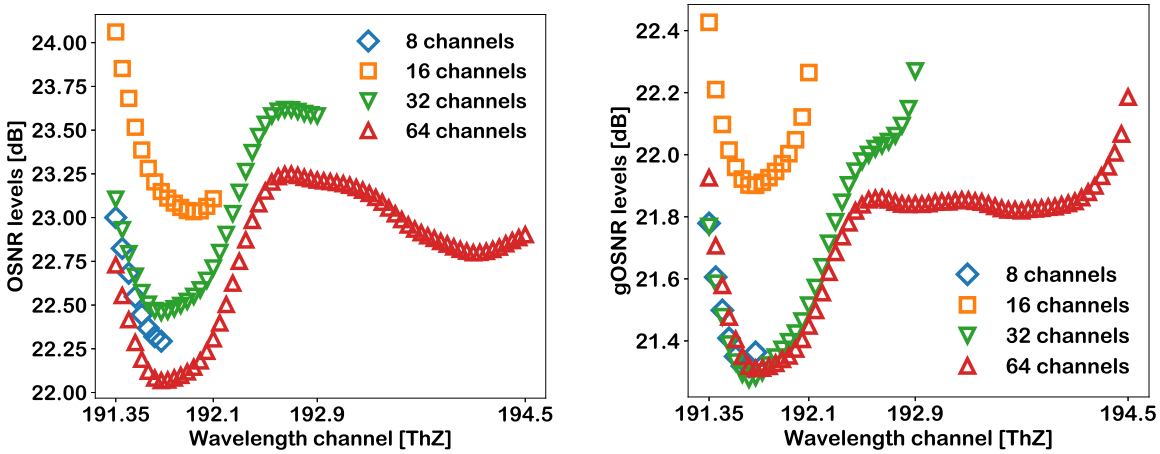

(a) Performance of OSNR levels.

(b) Performance of gOSNR levels.

Figure 3.12: Performance evaluation of the EDFA-WDG: (a) OSNR and (b) gOSNR.

between the channels found at these edge sections. This is due to the Gaussian assumptions of the GN model. The latter, can also be seen when comparing the performance of the OSNR and the gOSNR levels, shown in Figures 3.12a and 3.12b, respectively. As expected, a minor divergence between the gOSNR and the OSNR is noticeable.

3.6.2 Validation against physical testbed

We used the COSMOS testbed to validate the transmission physics models from Mininet-Optical. COSMOS is the Cloud Enhanced Open Software Defined Mobile Wireless Testbed for City-Scale Deployment in Manhattan, it is a "city-scale programmable testbed for experimentation with advanced wireless" [74]. This testbed, currently being developed and deployed in upper Manhattan, includes software-defined radio (SDR) nodes along with edge and cloud compute nodes, connected via a flexible, disaggregated, optical x-haul (front/back/cross-haul) network. The optical x-haul testbed [223] for COSMOS consists of ROADMs, optical terminals and transceivers, fibre spools, and optical amplifiers, connected to a programmable optical patch panel, all under SDN control. We had access to this testbed through the CIAN centre from the University of Arizona, which has been our main academic partner in the development of Mininet-Optical. As described by Yu *et al.* [224], the optical networking architecture of COSMOS can be customised to develop isolated experiments. Thus, we have deployed a ring topology as illustrated in Figure 3.13, composed of Cassini white-boxes with transponders for transmission and reception, ROADMs composed of two WSSs for mux and demux processes, EDFAs compensating for 22 and 25 km fibre spans. Additionally, we used optical channel monitors at the input and output interfaces of the ROADM nodes, that were capable of checking the power levels of individual channels. With this data it was then possible to estimate the ASE noise attributed to each EDFA, by means of interrupting transmitted channels and checking their performance.

COSMOS supports the transmission fully-transparent and flexi-grid channels for 10 Gbps and 100 Gbps transmissions. For our evaluation, we have considered four channels that we have labeled CH-25, CH-35, CH-45 and CH-55, that correspond to the frequencies 192.55, 193.05, 193.55 and 194.05 THz, respectively. These channels were configured with a modulation format of Quadrature Phase

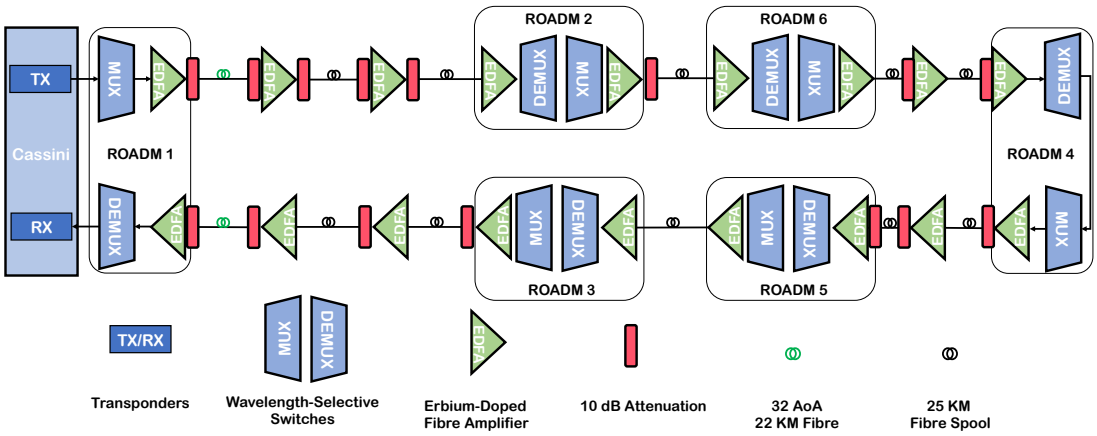

Figure 3.13: COSMOS testbed topology.

Shift Keying (QPSK). The transmitting transponders from the Cassini white-box were configured with a launch power level of -0.5 dBm. To launch our transmission, we configured the ROADM nodes to create the path ROADM-1, ROADM-2, ROADM-6, ROADM-4, ROADM-5, ROADM-3, and back to ROADM-1. It took approximately 1 min to collect the power levels of each channel.

Accordingly, we modelled the same network topology in Mininet-Optical and tried to replicate the scenario described above. However, the migration of the physical testbed to Mininet-Optical was not a straightforward process. This was mainly due to the wavelength-dependent operation of the multiple components in the network, which we could not monitor accurately. For instance, the occurrence of ASE noise in the physical testbed, which we could accurately monitor, differed from our simplified models due to the intrinsic wavelength-dependent operation of the EDFAs. Thus, in order to effectively replicate the performance of each EDFA, we would have had to monitor the individual performance of each EDFA under all possible channel combinations, which is an extremely time consuming and expensive task. However, we were able to collect EDFA-WDG ripples for fully-loaded systems, that we included in the models of the EDFAs. Moreover, we had no means to monitor the occurrence of the NLI noise as an isolated parameter, since the monitoring nodes enabled in our testbed were only capable of monitoring the power levels. In addition to the physical limitations imposed by the individual components, we had to develop the extra attenuation elements in Mininet-Optical, in order to comply with the network protection measurements enabled in the physical testbed, which are depicted in Figure 3.13 as the 10 dB attenuation red blocks. We present the validation of the Mininet-Optical simulation compared to the COSMOS testbed in Figures 3.14 and 3.15.

In Figure 3.14, we show the performance of channels CH-25, CH-35, CH-45 and CH-55 at the input interfaces of the ROADMs. It is noticeable that, with the exception of CH-35 (Figure 3.12b), the rest of the channels behave rather similar to the COSMOS testbed. Although, the behaviour experienced by CH-35 mimics that from the physical system. As a consequence, we attribute this divergence to the wavelength-dependent operation of the network components that impact CH-35 differently than the other channels. Also, we can notice that Mininet-Optical is capable of modelling the power level fluctuations due to the aggregation of fibre spans, EDFAs and attenuators, even in cases where performance would not be obvious, as it is the hop from ROADM6 to ROADM4 in the circular network. We calculated the power MAE of Mininet-Optical for the seven input monitoring

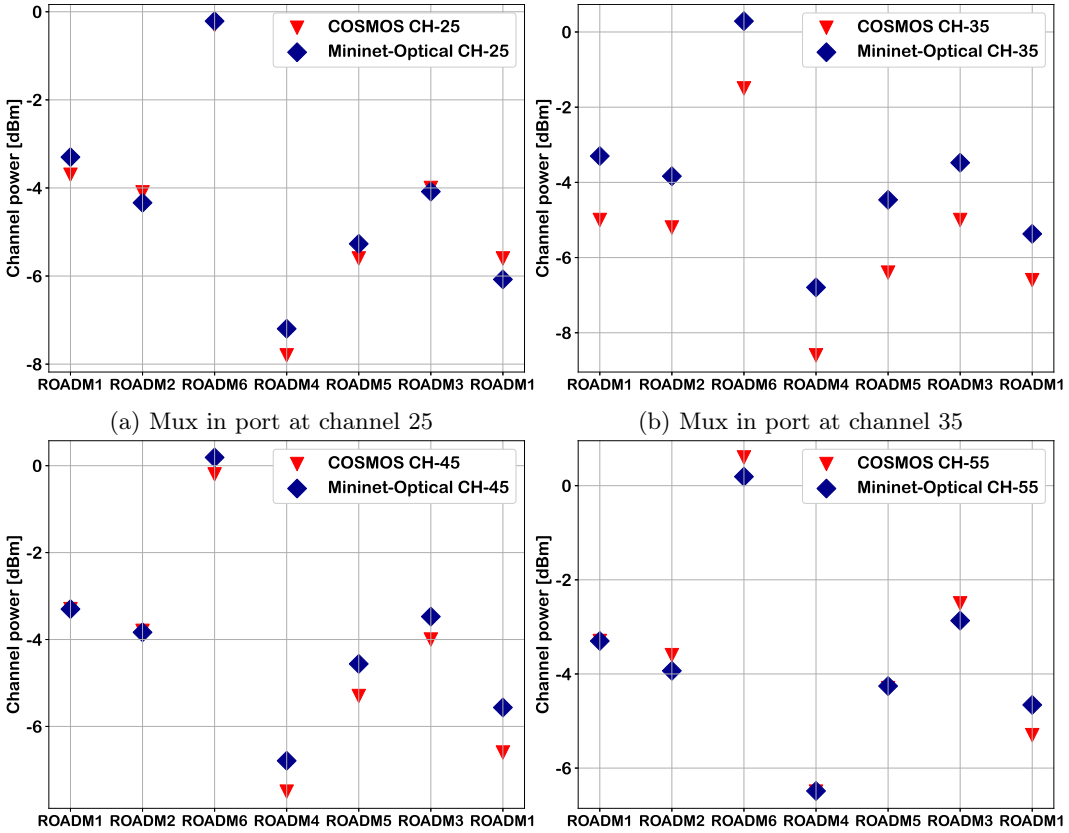

(a) Mux in port at channel 25

(b) Mux in port at channel 35

(c) Mux in port at channel 45

(d) Mux in port at channel 55

Figure 3.14: Mininet-Optical vs. COSMOS testbed at the input ports of the ROADMs.

locations with 0.31 dBm, 1.62 dBm, 0.49 dBm, 0.25 dBm for CH-25, CH-35, CH-45 and CH-55, respectively. In Figure 3.15, we show the performance of channels CH-25, CH-35, CH-45 and CH-55 at the output interfaces of the ROADMs.

Interestingly, this time the performance of CH-35 present smaller divergences with respect to those at the input interfaces. When signals are processed by a ROADM node, they perceive a rather linear attenuation effect due to the mean insertion loss produced by the components of the ROADM. However, this attenuation takes place at the WSSs that compose the ROADMs, which can also produce wavelength-dependent attenuation effects. Thus, we attribute the seemed improvement of Mininet-Optical when evaluating CH-35 at the output interfaces of the ROADMs to be a result of the wavelength-dependent operation of this particular network component. Thus, we can conclude that the wavelength-dependent operation of the ROADMs is an effect that needs to be controlled, otherwise it could lead to a detrimental management of optical channels when performing the mux/demux operations (optical switching). We calculated the power MAE of Mininet-Optical for the seven output monitoring locations with 0.50 dBm, 1.59 dBm, 1.04 dBm, 0.67 dBm for CH-25, CH-35, CH-45 and CH-55, respectively.

This preliminary validation study was limited to four channels and one set of EDFA-WDG. Consequently, we want to collect further data for more channels and combinations of these, to continue to assess the performance of Mininet-Optical. Nonetheless, our results demonstrate that our model is capable of performing closely with respect to the physical testbed, with MAE below 0.5 dBm for the input monitoring locations, with the exception of CH-35.

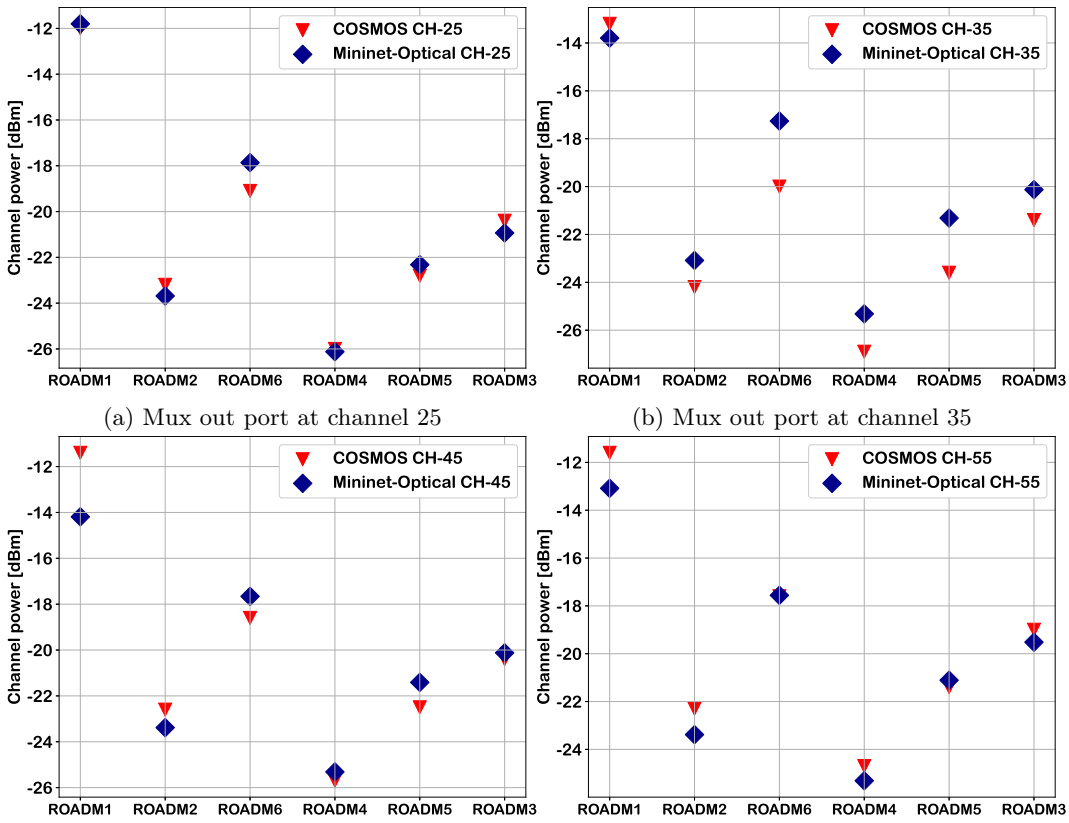

(a) Mux out port at channel 25

(b) Mux out port at channel 35

(c) Mux out port at channel 45

(d) Mux out port at channel 55

Figure 3.15: Mininet-Optical vs. COSMOS testbed at the output ports of the ROADMs.

3.6.3 Demonstration

We have showcased the integration of Mininet-Optical with the ODTN-ONOS [25] controller at the 40th edition of the Optical Networking and Communication Conference & Exhibition (OFC), 2020, that took place in San Diego, CA, USA. We have performed a live demonstration of the ability to model and prototype OPM, impairment-aware wavelength provisioning, and failure recovery in a software-defined, emulated packet-optical network environment. This work was also done in collaboration with the University of Arizona.

We have demonstrated several new and important capabilities for open source optical network emulation, including:

- End-to-end, interactive emulation of an SDN-controlled packet-optical network.
- An emulated optical switching and transmission layer, including a model of the transmission physics.
- Discrete emulated optical components such as transceivers, amplifiers, optical fiber spans, and ROADMs.
- SDN control and monitoring interfaces for emulated optical network devices.
- Scalability to topologies with dozens of optical nodes.
- Compatibility with the Mininet emulator for packet networks.
- Connecting an emulated packet-optical network to a widely used, open source SDN controller (ONOS) that is deployed in the commercial Internet.

We have modelled a mesh topology with 6 points-of-presence (POPs) and 8 bidirectional links, as illustrated in Figure 3.16. The POP node architecture results from the aggregation of the emulated packet-network elements (e.g., virtual hosts and routers) with the abstracted optical-network elements (e.g., line terminals and ROADMs). Similarly, the links between nodes are built from the aggregation of the virtual Ethernet links and the abstracted optical link composition, including fibre spans and EDFAs. For this demonstration, we have assigned different WDG functions to all the EDFAs modelled in the links between POPs. Consequently, we were able to demonstrate the impact on QoT imposed by this physical effect. Moreover, these POP nodes emulate the control interfaces from Mininet with the extensions to build Mininet-Optical as explained in section 3.2. For this demonstration, we have integrated our customised RESTful/OpenFlow APIs to support the SBI of the ONOS controller, and we have also integrated our APIs for enabling the monitoring capabilities of Mininet-Optical. For the latter, we have enabled monitoring interfaces at each POP node, which can be queried by the controller.

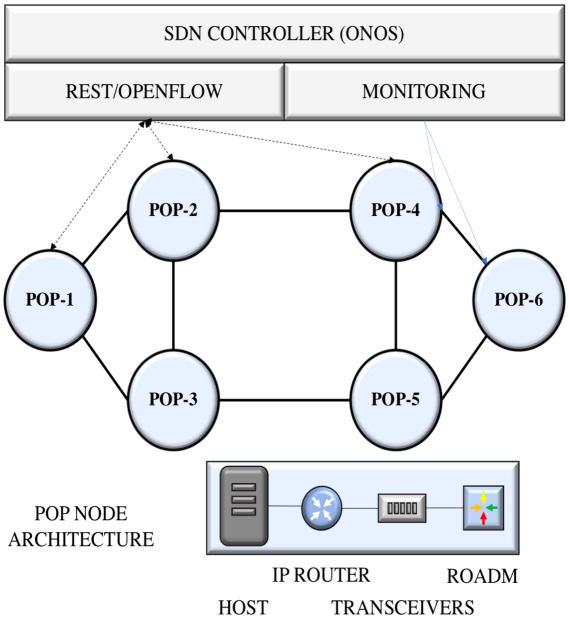

Figure 3.16: Emulated demonstration network.

In Figure 3.17 we show the ONOS GUI interface when connected to our Mininet-Optical topology. On the right-hand side of this figure, we can see that from virtual Ethernet links (top) we are abstracting the optical network topology (bottom), and as such ONOS is capable of detecting a virtual optical network composition. We then list the ROADM nodes and the established links on the left of the figure, demonstrating that ONOS is indeed managing optical devices (e.g., ROADMs), instead of the electronic switches that are deployed. We also show how ONOS is capable of monitoring the OSNR and gOSNR information of some channels that we have launched in the network, for a use case that we describe below.

Our use case consisted in a live fault recovery procedure handled by ONOS when controlling Mininet-Optical. For this, we considered six channel groups (CGs) of 5 channels each as depicted in Figure 3.18a. We have configured the modelled ROADM nodes to establish the traffic represented by the different colours in this figure. CG-1 (dark blue) traverses POP1, POP2, POP4, POP5; CG-2 (green) traverses POP1, POP2, POP4, POP6; CG-3 (black) traverses POP3, POP2, POP4; CG-4

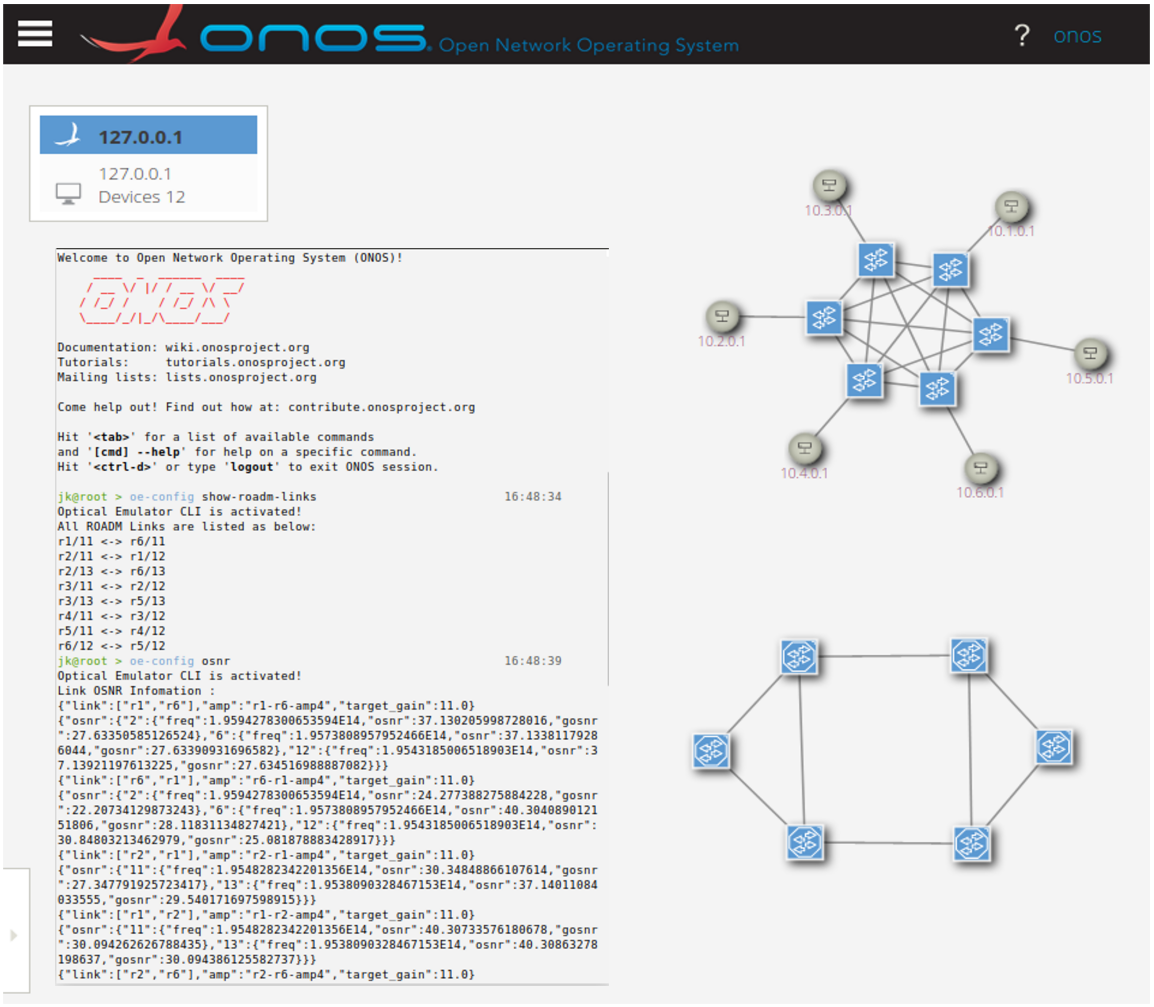

Figure 3.17: ONOS CLI and GUI showing monitoring and visualization of optical and packet layers in the Mininet-Optical network.

(yellow) traverses POP2, POP4, POP6; CG-5 (magenta) traverses POP1, POP3, POP5, POP6; and, CG-6 (cyan) traverses POP4, POP5. The purpose of this traffic was to model common links between CGs, enabling us to study the impact on QoT performance due to channel interference. For example, in Figure 3.18b we show the OSNR and gOSNR monitored values at the input interface at POP4 when traffic is coming from POP2. Thus, we can see that CGs 1, 2, 3 and 4 are being detected by ONOS.

For our use case, we artificially configure the system gain of an EDFA in the link between POP1 and POP2 (also through ONOS), in order to degrade the performance of the CGs that traverse this node, CG-1 and CG-2. Consequently, at a subsequent stage, in this case also the input monitoring interface from POP4, we can detect that the performance of these channels has been degraded and that this has also affected the performance of the channels that share the common link (CG-3 and CG-4), as illustrated in Figures 3.19a and 3.19a.

Consequently, the ONOS reconfiguration procedure that we have opted to demonstrate consisted in re-routing CG-1 and CG-2 to traverse the path POP1, POP3, POP5, POP6, instead, as illustrated in Figure 3.20a. Then, in Figure 3.20b we show the monitored gOSNR of these channels when

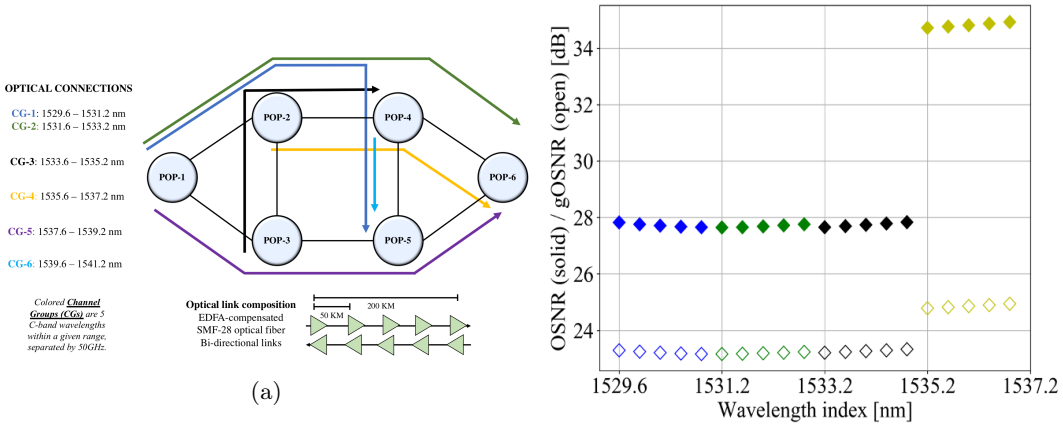

(a) (b)

Figure 3.18: (a) Traffic setup and optical link composition. (b) Controller monitors OSNR (solid) and gOSNR (open) of all channels entering POP-4 (via POP-2) during the initial transmission.

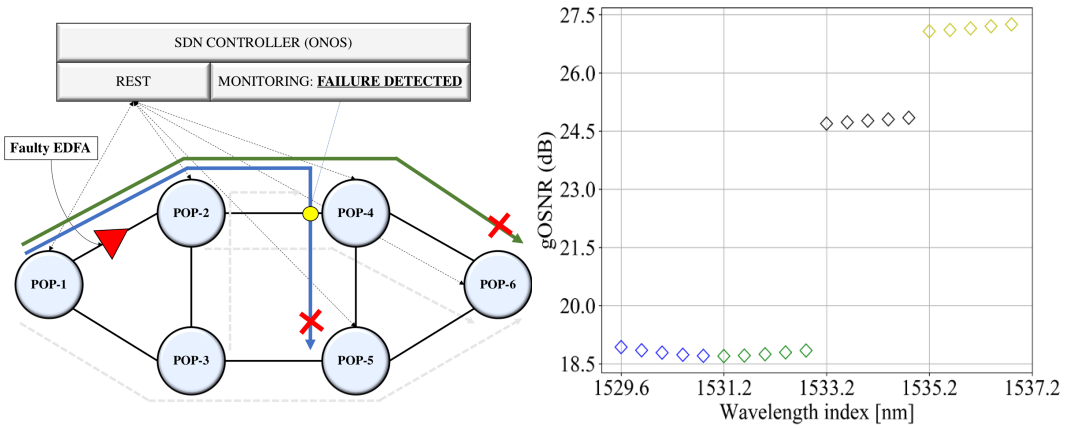

(a) (b)

Figure 3.19: Faulty EDFA degrades CG-1 and CG-2; controller observes low monitored gOSNR for signals entering POP-4 (via POP-2).

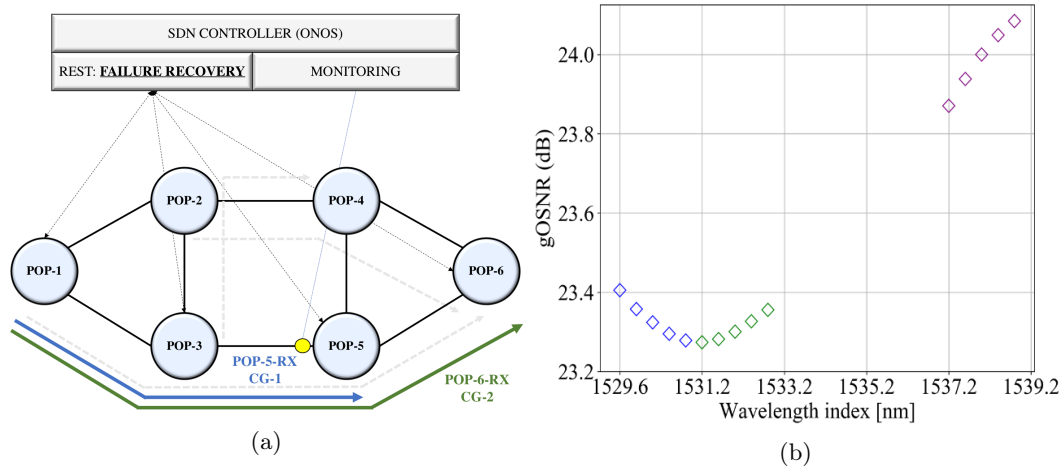

(a) (b)

Figure 3.20: Controller re-routes CG-1 and CG-2, resulting in high monitored gOSNR for signals entering POP-5 (via POP-3).

checking the input interface of POP5 when traffic is comming from POP3, and demonstrate that the gOSNR performance of the channels has been recovered, that the behaviour of these has changed due to the wavelength-dependent operation of the devices encountered in the new path, and that the new path is shared with CG-6.

3.7 Summary

In this Chapter, we have introduced Mininet-Optical, the first packet-optical network emulation system supporting both physics transmission simulation and optical disaggregated control emulation, enabling real-time disaggregated control testing and prototyping of the optical network elements. We have presented all the subsystems that compose Mininet-Optical, as well as a detailed description of the transmission physics models used to simulate optical transmissions, and how these are integrated. We have also provided the algorithms required for the subsystems to interact with each other and enable the modelling of almost any networking scenario. This is allowed by the customisation of the network topologies and the individual configuration of the optical network components within the system. Additionally, Mininet-Optical allows for the configuration of wavelength-dependent operation of the network components, aiming to represent the behaviour of realistic amplified systems. Then, we have also presented a detailed explanation of the emulation system developed with Mininet, as well as the algorithm required for this to interoperate with the simulation system.

Furthermore, we presented evaluation studies of the transmission physics models that compose Mininet-Optical, demonstrating the aggregated nature of our algorithms. We have shown that our system performs accordingly to well-known models such as the SRS from Zirngibl [218] and the GN-model from Poggiolini *et al.* [221], by comparing our tool against the OOPT-GNPy project, showing comparable performance with OSNR MAE of 0.13 dB and a gOSNR MAE of 0.16. Then, we have provided a validation study against the COSMOS testbed. For that, we replicated an experiment performed in a hardware testbed in Mininet-Optical. We have shown that our system assimilates with high accuracy the behaviour of the physical testbed, with the only errors attributed to the wavelength-dependent operation of the network components found in the network, which are device dependent. In Figure 3.15, we show the performance of channels CH-25, CH-35, CH-45 and CH-55 at the output interfaces of the ROADMs. We computed the power MAE for CH-25, CH-35, CH-45 and CH-55 with values 0.31 dBm, 1.62 dBm, 0.49 dBm, 0.25 dBm, respectively. And, we also calculated the power MAE of Mininet-Optical for the seven output monitoring locations for CH-25, CH-35, CH-45 and CH-55, respectively with values 0.50 dBm, 1.59 dBm, 1.04 dBm, 0.67 dBm. Because our analysis was limited to four channels, we plan to extend our analysis to more channels and scenarios. Additionally, we plan to further inspect this operational effect from all the devices (i.e., extract the WDG functions from some EDFAs), so that we can include these in the models of Mininet-Optical, in order to have a better representation of the COSMOS testbed, enabling a tighter integration between the two systems. This last step will allow us to develop control plane procedures with Mininet-Optical that could be directly migrated to operate on top of the physical testbed.

Last, we have also presented the integration of Mininet-Optical with the ODTN-ONOS controller. For this, we have shown a use-case for fault recovery procedures, based on active monitoring of the optical links with the OPM capabilities enabled in our emulator, and the SDN control with ONOS of the ROADM nodes to dynamically allocate and remove traffic from a virtual network.

4 Optical Control Systems

4.1 Introduction

The development and implementation of optical control systems is transitioning from quasi-static to fully-dynamic autonomous systems [62]. It is mainly due to the lack of communication protocols and standards that the development of this type of systems remains an open issue. In addition, the composition of optical networks and the standard methods to operate them consider limitations that must be addressed to complete this transition. For instance, we have reviewed in Chapter 2 that due to the unpredictable wavelength-dependent operation of optical network components, receiver margins must be introduced to launch optical transmissions within a safe range of operation, ranging in the ± 3-7 dB [63]. The latter, imposes constraints to the network capacity that require further investigation to understand the real impact in performance and costs.

In Ghobadi *et al.* [225] and Filer *et al.* [31], the authors studied the benefits of applying elastic modulation gains in the Microsoft's optical backbone network in the US. They found that a capacity gain of at least 70% is achievable via elastic modulation. Also, they demonstrated how different wavelengths performed differently across the network, looking at multiple segments of it. From the latter, the authors concluded that different wavelengths might benefit from different modulation formats even while sharing paths.

To solve the problem of unknown optical path performance, Optical Performance Monitor (OPM) equipment is commonly used. Unfortunately, these devices are not easily deployed and are usually included in the network at times and points of interest only. The latter, is mainly due to the high costs of these (ranging in the tens of thousands of US dollars). On top of that, the processes to operate OPM equipment requires having human-in-the-loop interventions that are costly (engineering costs) and time consuming, requiring several hours and days, including the interpretation of observation points. Also, state-of-the-art OPM devices have limitations, as it is the case for the number of channels they can observe simultaneously; and, the accuracy of the measured points. For instance, it is possible to measure optical signal power intensity (dBm) and use this metric to estimate the accumulated noise due to amplification, but points of error will remain because of the artificial computation. As a result, it has become a necessity to improve monitoring equipment, as well as the methods to operate these. In recent years, estimation methods have been evaluated to assist monitoring equipment in order to tackle the unpredictable operation of network components [146, 184–188, 188, 189, 196–198, 198, 199]. We further discuss these models in Chapter 5.

In this Chapter, we investigate the implications of receiver margins into the overall network capacity. Additionally, we delve into the implementation of Quality of Transmission Estimation (QoT-E) processes to assist the mitigation of margins, and also evaluate the implications of margins

to the QoT-E functions. For that, we review the composition of optical control systems. Initially, it is necessary to understand the role of the control system in the networking environment: we must determine what are the main processes required to control and how these are developed and implemented. With that at hand, it is then possible to understand how all the network elements interact with each other. In the current state-of-the-art, the main challenges emerge from the management and deployment of monitoring equipment and the investigation of the benefits that these would bring into the network operation [133]. In an attempt to fill in this gap, we investigate the implementation of QoT-E methods into the management of optical network traffic, and the benefits that they add specifically to optimising the installation of optical paths.

First, we show these effects over a simulated optical network based on the Telefonica Spanish national topology, emphasising the reduction in capacity due to the incomplete knowledge the network controller has on the exact wavelength gain and system gain variation of Erbium-Doped Fibre Amplifier (EDFA) due to Automatic Gain Control (AGC). We consider this to be of high relevance, as it allows for further experimentation on the use of sparse OPM to provide data that can be used to improve the QoT-E from the control plane of a Software-Defined Networking (SDN)-based system. The simulation used is based on a predecessor tool to the Mininet-Optical system introduced in Chapter 3 [226], also based on the Mininet [59] framework. This provided the advantage of testing SDN control planes that can be then utilised on experimental Reconfigurable Add/Drop Multiplex (ROADM) networks. In order to link SDN controller and the extended Mininet emulation environment, we developed an optical agent capable of emulating the control operation of ROADM systems. We used the Ryu framework from Nippon Telegraph and Telephone (NTT) to develop our control system for this study, enabling the control of all network devices.

Also, we present the use of the Mininet-Optical system, to evaluate a SDN-controlled QoT-E system based on the deployment of monitoring nodes at periodic locations in an optical transmission system. The controller used in this case was a customised control system written in Python, supporting the required APIs to communicate with Mininet-Optical. This SDN controller running on the emulated system achieves a reduction in the QoT-E absolute errors based on active monitoring of the OPM devices. We run our experiments over a linear topology. Our results show improvements of over 3 dB for short distances, and between 0.8 dB and 2 dB for links of approximately 2,000 km.

Lastly, we present another scenario for the use of active monitoring procedures with Mininet-Optical. This time, we have modelled the Cost239 topology and also analysed the placement of OPM nodes at different locations of an optical link. Only this time we have used the physical layer monitored information to enhance the performance of our QoT-E system. Our results show that by taking advantage of OSNR monitors, it is possible to improve the QoT-E performance at intermediate locations of an optical link.

4.1.1 Scope and contributions

This work addresses the analysis and design of the QoT-E module of an optical control system. Additionally, we investigate the development process, as well as its implementation and assessment. In this Chapter, we address heuristic models assisted with the monitoring capabilities of the controller (i.e., active monitoring). In Chapter 5, we investigate cognition-based solutions to assist this module.

The main contributions of this Chapter are:

- Implementation of an optical SDN control system with the Ryu framework from NTT to interact with the Mininet emulator and to a customised optical agent via the OpenFlow protocol.
- Performance analysis of the impact on network provisioning capacity due to the usage of receiver-margins in coherent transmission systems in the optical domain, circumstances of origin and directions towards the mitigation of these.
- Implementation of a customised optical SDN control system entirely written in Python to interact with Mininet-Optical via customised RESTful APIs.
- We present a demonstration of the ability to test control plane operations on large-scale networks with Mininet-Optical.
- We present a QoT-E strategy based on active monitoring of lightpaths in an optical SDN environment that mitigates estimation inaccuracies produced by wavelength dependent power dynamics.
- We analyse the error that OSNR vs generalized-OSNR (gOSNR) monitoring produce in estimating QoT for different numbers of OPMs deployed in an optical link.
- We demonstrate how real-time OSNR monitoring information can be used to improve the QoT-E and monitoring functions, even when only OSNR types of OPM are available.

4.2 Control system

In this Section, the architectural design and model composition of the proposed control system and its implementation is described. Initially, a Ryu-based controller is described, which is used for the implementation of a study addressing the investigation of network capacity constraints due to receiver margin utilisation. In addition, a customised Python-based controller is introduced, which is used for the studies on the advantages of active monitoring in the context of optical disaggregated networks. Finally, we expand on the Open Network Operating System (ONOS) controller presented in Chapter 3, which is the current system considered to operate with Mininet-Optical.

4.2.1 Architecture

The architecture diagram of the control system is presented in Figure 4.1, highlighted in blue. The internal composition of a control system is dependant on the requirements of a system. Because of that, multiple frameworks such as ONOS from the Open Networking Foundation [25], Ryu from the NTT [23] and OpenDayLight from the Linux Foundation[24] are extensible, meaning that they provide control applications for basic functions such as traffic installation and overall traffic management, and also enable network engineers to develop customised modules for control (i.e., virtualised networking functions). For the purposes of our research, the ideal SDN controller is composed of the modules presented in Figure 4.1. The detailed consideration of these, as well as the key role the play in the control system is described below.

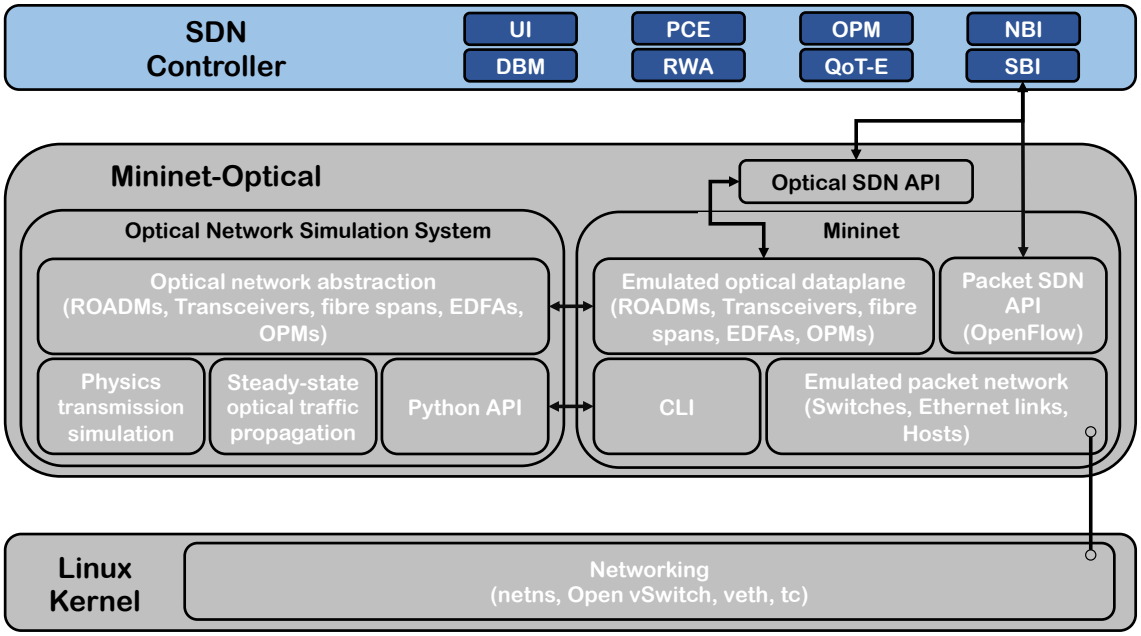

Figure 4.1: Optical Control System - Architecture Diagram.

4.2.2 Components

User Interface

The User Interface (UI) is commonly presented as a command-line interface providing customised configuration and troubleshooting of the controller by a network engineer, in a similar fashion of that of a network management system. The key role of the UI is to enable active engineering to intervene in the live operation of the network. It can be presented as a functional module of the controller or as an external (third-party software) module. This only becomes available when the network is live. In the controllers that we have developed, the UI was developed in three different ways. First, for the Ryu-based controller, this consisted in a software program that we attached to the Ryu framework, capable of performing basic querying commands for the purposes of lightpath provisioning, restoration and optical performance monitoring. Second, for the customised Python-based controller, we omitted the inclusion of a UI, evaluating the potential of a fully software-defined optical control plane. Last, for the ONOS controller, we used the command-line interface provided by this project, which is a sophisticated UI enabling the management of the traffic, querying of all the devices in the network, as well as the manipulation of the traffic and devices.

Database Management

The Database Management (DBM) system is a decentralised entity that monitors the state of all modules within the controller. The key role of this module is to record the state of the components of the network. This is to be able to build analytical data of the performance of the network and assist in decision-making processes at a control and management level (i.e., dynamic routing). For instance, it is designed to keep track of the processing of traffic requests, system calls and lightpath allocation. However, due to the fast response requirements for optical network systems,

mainstream DBM systems relying in technologies such as SQL or Oracle are not feasible tools. As a result, the development of DBM technologies for disaggregated optical networks is left to customised methods, often relying in the creation of memory-exhaustive log-files. For the three controllers used in our studies, our DBM system operated to write log-files on the configuration of the network (i.e., topology composition) and the active traffic at the observation times, storing individual information on the transmitted channels including: power intensity, Amplified Spontaneous Emission (ASE) and Nonlinear Interference (NLI) noise levels, as well as estimated Optical Signal to Noise Ratio (OSNR) and Generalized Optical Signal to Noise Ratio (gOSNR) levels.

Path Computing Element

In our design, the Path Computing Element (PCE) is not to be confused with the IETF RFC [104]. Upon traffic request, our PCE determines the path(s) a signal or group of signals must follow, thus it acts as a high-level routing algorithm. The key role of this module is to compute end-to-end paths following specific requirements. For example, the PCE can be designed to compute shortest-paths with the least connection hops (i.e., number of traversed nodes). Intuitively, this is an algorithmic-problem that can be implemented in a variety of ways. In our studies, we have (for the most part) relied on shortest-path computations based on the Dijkstra and breadth-first search (BFS) algorithms.

Routing and Wavelength Assignment

Assisted by the PCE, the Routing and Wavelength Assignment (RWA) function is in charge of determining the optical spectrum resources that will be allocated for fulfilling a traffic request. It is not unusual to find PCE and RWA used interchangeably in the literature. However, a main distinction of the RWA module is the management of optical network resources, and specifically the wavelength allocation. While the PCE has a higher-level view of the network on which operates, the RWA operates closer to the transmitters and receivers (e.g., transceivers). We have found through our research that the RWA module is the key element that could benefit from the inclusion of cognition in optical control systems, as we explain in Chapter 5. For the purposes of our research, this module has been implemented with the PCE module mentioned above, with the extension to keep track of the wavelengths (channels) that have been assigned at different times of operation.

Optical Performance Monitoring Interface

The OPM interface module is a software system that actively retrieves state-data from the signals being transmitted at a given time. The key role of this module, as part of a control system, is to provide querying procedures to be accessed by the other modules in the system. For the purposes of our studies, we investigate the potential interaction between the OPM and the QoT-E (discussed below), to assist the RWA module. A thorough discussion on the OPM has been presented in Chapter 2, and its usage and implementation continues to be in the backbone of this thesis. The monitoring capabilities of our system allow us to collect optical signal power, ASE and NLI data of individual channels and study collective effects that can manifest over an optical link. Also, OPMs emulate optical OSNR monitors or reference receivers that can recover estimates of the full gOSNR.

Quality of Transmission Estimation

The QoT-E module is the main subsystem introducing cognition to the controller. It collaborates with the OPM, PCE and RWA processes to help optimise the usage of resources. Its key role is to learn from the network components and their performance upon operation to provide reference models on the future operation of these. This is the main element of study within this thesis. As such, we also have implemented offline QoT-E modules as part of all the controllers used in our studies.

North-Bound Interface

The Northbound Interface (NBI) enables the interaction between a controller and third-party systems (e.g., services and applications) running over the network. This type of interface is commonly deployed with simple REST-API tools. The NBI is not to be confused with the UI, since the user does not have direct access to the NBI and its operation. The NBI is a set of Application Programming Interfaces (APIs) that enable the orchestration of the controller's decisions to fulfill the requirements of all services and applications.

South-Bound Interface

The Southbound Interface (SBI) enables the interaction between the controller and the network elements that it manages. We have reviewed in Chapter 2 that popular protocols enabling this type of communication in the optical domain are Network Configuration Protocol (NETCONF)/Yet Another Next Generation (YANG) and OpenFlow, and more recently, OpenConfig and OpenROADM. This is an area that requires further investigation to consolidate the standardisation of protocols. As disaggregated optical networks continue to evolve, the usage of different tools to build SDN architectures is also changing.

4.3 QoT Estimator in SDN-Controlled ROADM Networks

4.3.1 Implications of the use of margins

Dynamic add, drop and routing of wavelength channels can generate optical power dynamics which may result in signal quality degradation. This becomes even more complex in mesh networks, hence, the research community has been recently working on solutions for controlling dynamic optical switching, both in proprietary [227] and open systems [19]. One of the key elements for enabling dynamic switching in ROADM networks is the presence of OPM functions [217], so that the control plane can operate on a feedback loop that takes into account the state of the active optical channels. Recent studies have shown the beneficial impacts of OPM at intermediate nodes, enabling dynamic management decisions to reconfigure and optimise network channels [228]. While SDN approaches introduce a high level of flexibility for managing network resources, there is a lack of standardised interfaces for optical networking devices (i.e., optical switches), not to mention the absence of open interfaces in the OPM equipment, which leads to high-cost, complex solutions for monitoring in real-time the state of a network. Real-time analysis is crucial for dynamic lightpath provisioning

and network adaptation, overcoming the suboptimal solution of over-provisioning network resources for system-specific purposes [229]. Furthermore, the additional information provided by the OPM mechanism could not only assist reconfiguration and optimisation of the network performance, but also enable a better use of resources upon service setup (i.e., OSNR estimations, based on distance vs. modulation formats) [217]. However, on-site signal monitoring is still difficult to achieve, mainly because of the high Capital Expenses (CapEx) and Operational Expenses (OpEx) it generates.

In modern optical networks, the most common monitoring technique consists in splitting a portion of an optical signal to check its intensity and quality without obstructing the transmission. The key data provided by this process is the intensity of the power of the signal, measured in decibel-milliwatts (dBm). In standard metro-haul optical networks, the usage of EDFAs to compensate for the insertion loss of optical fibres is preferred. As we have seen in previous Chapters, the ASE noise attributed to an EDFA is one of the main components negatively affecting the Quality of Transmission (QoT) of optical paths. Because of that, it is of high interest to be able to monitor this type of noise in an accurate and fast manner. To date, through the implementation of tasks that are not too expensive nor too complex, it is possible to accurately compute the contribution of ASE noise into the signal power intensity, by actively monitoring the latter only. These two monitoring processes can be performed simultaneously, enabling the extraction of the QoT by means of OSNR, which is the first of two widely accepted metrics of measurement. The second common metric of QoT is the Bit Error Rate (BER), which can only be computed at the dataplane, requiring optical-electrical encodings. While the OSNR given by the signal power intensity and the ASE noise power is an acceptable measurement of QoT, in practice, it is only used to adjust transmission margins but not to eliminate the usage of these. That is because of the occurrence of a third type of noise, the NLI, that contributes to the degradation of QoT but cannot be observed with mainstream monitoring techniques. This type of noise is generated by the interaction of optical paths among themselves and by the interaction of an optical path and the optical fibre medium. The former is known as the Cross-Channel Interference (XCS) and the latter as the Self-Channel Interference (SCI). In the current state-of-the-art, the widely used models of these phenomena are those proposed by Poggiolini *et al.* [219, 221]. Nonetheless, modelling these physical effects is not sufficient to fully assist optical networking functions. Thus, the thrive for OPM devices capable of observing the NLI noise remains latent.

To overcome the limitations imposed by OPM techniques, as it is the application of monitoring processes after the installation of network resources (i.e., wavelength allocation), multiple studies have proposed the inclusion of estimation functions for predicting the communication performance of an optical network [31, 167–171, 186, 225, 230, 231]. While these approaches have given an insight into the physical impairments, this remains an area that could highly benefit from the use of modern technologies (i.e., Machine-Learning (ML) techniques) to improve the reliability of these functions for resource allocation and switching operations. Since it is possible that an estimation is not accurate, margins can be set in order to reduce potential failures. In this Section, we analyse the performance achieved by applying fixed margins to a QoT-E, which considers OSNR signal degradation, in order to achieve pre-allocation of lightpaths and dynamic switching.

While SDN is playing a major role in the control and management of electronic switching resources, its operation in the optical layer is still left to proprietary implementations. Here, we also present a SDN control plane with OPM management capabilities based on the OpenFlow v1.5 recommendations, as an extension to the flow-rule capabilities of this protocol. Additionally, we have

built a SDN-compatible ROADM network simulator to estimate the loss of performance due to the lack of information about the network. The latter was developed using open-source resources such as the Mininet framework [59], and software-switches [232].

4.3.2 System setup

As mentioned above, we used a predecessor system to Mininet-Optical to address our first studies. The architecture of our system is depicted in Figure 4.2. The two bottom layers illustrate the execution of our tests in a single computer, as we extend the Mininet emulator. The latter is shown in the green area of the figure, where we can see the instantiating of the virtual network as isolated TAP interfaces, that are then abstracted by our optical agent (yellow area). The optical agent acts as an OpenFlow translator for the SDN controller SBI, which enables the connection to the control interfaces of the ovs-switch instances. Consequently, the optical agent is the enabler for disaggregation in our systems. Moreover, the optical agent abstracts optical nodes from the packet virtual switches. An example of an optical node architecture is shown in Figure 4.3: each of the ROADM components (Wavelength-Selective Switch (WSS) and EDFA) were emulated using separate virtual switches. With this design it is possible to also abstract the ports of the nodes, which indicate the direction of the traffic. The SDN controller is in charge of handling the traffic. To fully automate the allocation of traffic, we deploy a Mininet application as a REST server that the SDN controller uses to launch packets from individual Linux virtual hosts. Thus, the SDN controller has full control of the network elements that are being emulated, and upon traffic request, can configure the required elements for testing.

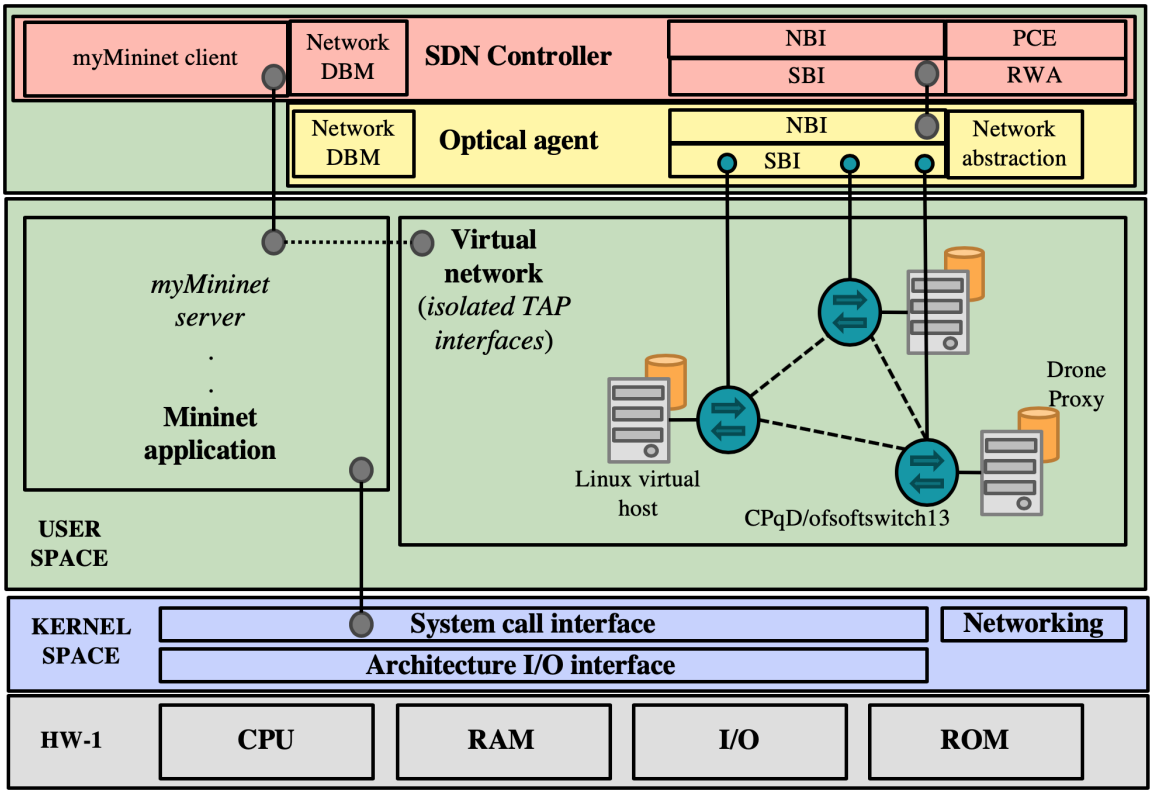

Figure 4.2: System architecture.

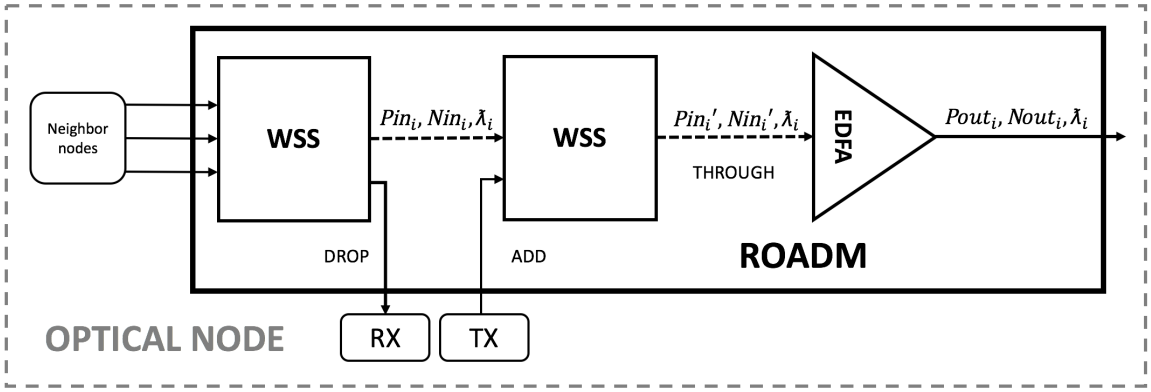

Figure 4.3: Logical representation of the ROADM node.

The network topology we considered is the Telefonica national Spanish telecommunication network model also used by Ruiz *et al.* in [3]. It consists of 21 nodes and 34 inter-city links, with varied distances. For the purposes of analysing large-scale ROADM networks, we incremented the distances in the given Spanish network shown in Figure 4.4 in order to operate on point-to-point connections ranging from 500 km to 4000 km. We have reproduced the topology on the Mininet emulator, developing an abstracted representation of an optical node through the use of OpenFlow software virtual switches from the Centro de Pesquisa e Desenvolvimento em Telecomunicações (CPqD), the CPqD/ofsoftswitch v1.3 user-space software switch [232].

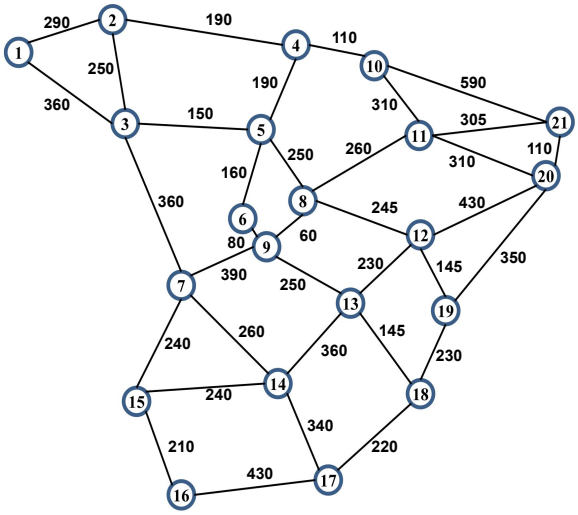

Figure 4.4: Telefonica, national Spanish network (link distances reported in km) [3].

Each output port has a post-amplification EDFA, which compensates for the losses of the WSS in the system. In our abstracted optical network, at each link we installed an additional EDFA for each fibre span of 100 km, and an additional one at the end of a link to operate pre-amplification. In our model, a colourless implementation was achieved by adopting WSS elements for both add and drop ports. The physical transmission and impairments parameters used in our simulations are given in Table 4.1.

Table 4.1: Parameters used for the physical transmission and impairments.

Physical component	Physical impairment
Launch Power	-2 dBm
Fibre Attenuation	0.2 dB/km
WSS Loss	9 dB
EDFA Noise Figure	6
EDFA Gain	20 dB

4.3.3 Model description

To simulate the optical performance of a signal traversing the nodes, we encapsulate optical transmission parameters (e.g., signal power and noise) in customised Ethernet packets to allow the exchange of this information across the virtual switches. Following the SDN paradigm, we are able to monitor the exchanged packets via the OpenFlow protocol calls to the devices. Figure 4.5 depicts the different layers of communication between the entities considered in our model. At the bottom, there is the data plane, which is represented by the virtual network. In between the data and control plane we implemented an optical agent, which is the entity that simulates the optical behaviour of each network element. The optical agent has bidirectional Transport Control Protocol (TCP) connections to both the controller and the data plane. The SDN controller is in charge of the network control and management operations (e.g., path computation, connection control) that could operate over a real ROADM network with support for OpenFlow version 1.5. The agent implementation in our model is used to handle the customised Ethernet packets traversing the network, in order to generate data structures for representing the optical performance, as it uses the values stored in the packet header to keep track of the signal power and noise at each port.

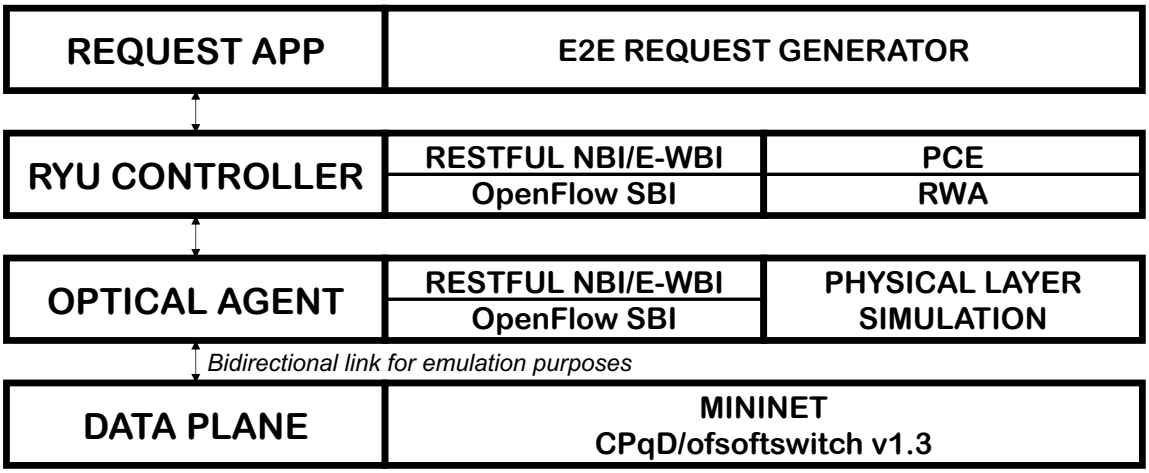

Figure 4.5: Layered architecture of optical SDN system.

The optical agent utilises Equations 4.1 and 4.2 for computing the signal power and noise values at a given port of a path:

$$P_o(P_i, G_t, \lambda) = P_i \times G_t \times f(\lambda) \tag{4.1}$$

$$N_o(N_i, G_t, \lambda) = N_i \times (G_t \times f(\lambda)) + h(\frac{c}{\lambda}) \times ((G_t \times f(\lambda)) - 1) \times NF \times B \tag{4.2}$$

$$OSNR = \frac{P_o}{N_o} \tag{4.3}$$

In Equation 4.1, P_o is the output power out of a given node, P_i the input power, G_t the target gain, and λ the wavelength. We determine the input power as the launched power of the system; target gain is a computed gain per EDFA to maintain the signal power, and $f(\lambda)$ is the ripple function that represents the detailed gain transfer function of the EDFA. In typical systems, a passive Gain Flattening Filter (GFF) is manufactured and applied to the amplifiers to compensate for the EDFA gain wavelength dependence. However, this is optimised for a specific operating point and is not tuned to each individual device, which brings in a certain degree of variability. In addition, the gain characteristics of the device will also vary over time. In order to reproduce this effect, since the optical power control stability problem regards the performance of each amplifier [233–235], we randomly allocated a different gain function to the different EDFAs of the system. This becomes indeed the main unknown variable in the system that affects the performance of the QoT-E. In Figure 4.6, we present the gain functions that are considered for this study. Through hands-on monitoring at the Center for Integrated Access Networks (CIAN) testbed at the University of Arizona, we determined that the signal fluctuation imposed by amplification systems resembles a slowly varying sine function. Then, we shifted these monitored functions to left and right in order to add variability to the signal performance, and maintain the EDFA gain constant.

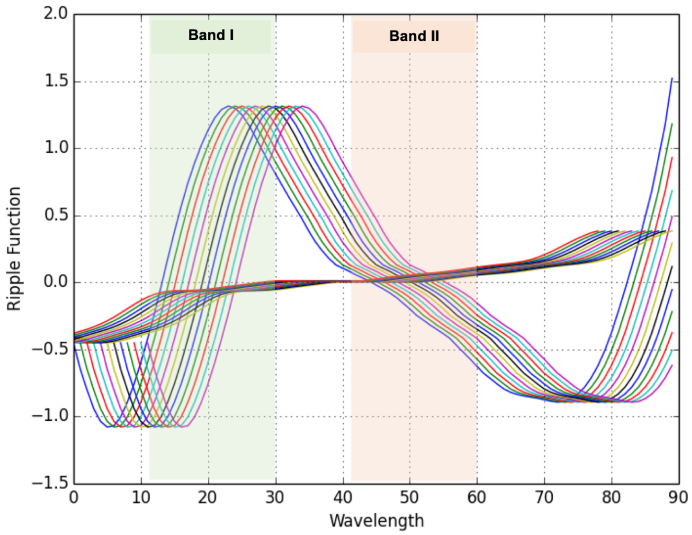

Figure 4.6: EDFAs wavelength-dependent gain modelling.

In Equation 4.2, N_o is the output noise, N_i the input noise and G_t the target gain. We determined the input noise to be the generated noise after each phase, being 0 - or none - at the beginning of a single transmission. The system gain is the average gain of the EDFAs that compose a link. We represent this by adding the ripple variation $f(\lambda)$ to the individual target gains Gt. Then, h is the Planck constant, c is the speed-of-light in an optical fibre, NF is the noise figure of the amplifiers, and B is the bandwidth of a channel in Hertz.

One of the novelties of our study is that we operate the simulations by computing the signal degradation at each node as the packets are traversing the network. Because of the model described in Equations 4.1 and 4.2, the computation of both output power and noise at each node is dependent of the randomisation of ripple behaviour constraint at each optical amplifier.

In the control plane, we implemented a customised controller based on the Ryu framework proposed by NTT labs [23]. Apart from extending the OpenFlow Protocol descriptions to handle optical parameters and interact with our customised Mininet-based simulation system, we included networking functions such as path computation, routing and re-routing, as well as OPM capabilities [133]. These are triggered by external applications to enable point-to-point connectivity, or by monitored data retrieved from the nodes. The NBI of our control plane is developed with RESTful API solutions, allowing for high-level requests from external applications. In addition to the generic networking functions at the control plane, we included an estimation module that performs a prediction of signal degradation given a point-to-point connection. The estimation function implemented in our controller uses the same tools presented in Equations 4.1 and 4.2. However, assuming it has no detailed knowledge of the exact gain transfer function of each amplifier, it does not assume any such variation (e.g., it assumes a flat unitary ripple function). This calculation is triggered whenever there is a point-to-point request, and determines the feasibility of a lightpath to be installed according to the OSNR levels, which are computed using 4.3.

4.3.4 Experiments and results

The traffic generated for this study consisted of 2,000 end-to-end lightpaths of length between 500 and 4,000 km, across the network topology considered in Figure 4.4. The experiments were carried out over two different segments of the C-band, shown in Figure 4.6, in order to take into account the effect of different gain transfer functions.

Similar to Ghobadi *et al.* [225], we analysed the feasibility of all the paths in the monitored traffic to be transmitted at different modulation formats, considering the OSNR signal levels of each transmission channel. For the OSNR thresholds, we have assumed those values above BER pre-Forward Error Correction (FEC) reported in literature, specifically from Ghobadi *et al.* [225], which are based on a symbol rate of 32 Gbaud. The modulation formats are Quadrature Phase Shift Keying (QPSK), 8 Quadrature Amplitude Modulation (8QAM), and 16 Quadrature Amplitude Modulation (16QAM), with OSNR thresholds, respectively, of: 10 dB, 14 dB, and 17 dB. Carrying out an OSNR analysis of each path, we determined in our model that 36.9% of the traffic could be modulated using 16QAM, 50% at 8QAM, and the remaining 13.1% at QPSK for the first band (1534.8 to 1542 nm). For the second band (1546.8 to 1554 nm), 26.6% of the traffic could be modulated at 16QAM, 70% at 8QAM, and 3.4% at QPSK, when we apply no margins. This constitutes the maximum capacity that the selected paths could carry in the network, if the SDN controller had perfect knowledge on the QoT (in this case the OSNR levels) associated with all paths.

The QoT estimator implemented in our controller predicts the OSNR levels of a given signal traversing a path. Because the estimation does not consider the optical power fluctuation caused by the amplifiers (only the noise figure is considered), the only option available to improve the likelihood of succeeding in creating a new path is to apply a margin to all the paths. Intuitively, adopting a more conservative margin also reduces the network capacity, as it reduces the number of paths generated.

We have thus analysed the performance achieved when applying different margins to the prediction of the OSNR levels, in order to verify the maximum capacity achievable. The margins are

applied to the following formula, which is used to determine whether the results of estimation plus margin is above the required OSNR threshold:

$$OSNR_{est} + M > OSNR_{th} \tag{4.4}$$

In Equation 4.4, $OSNR_{est}$ is the estimate OSNR from the controller (which does not know the specific amplifiers Wavelength-Dependent Gain (WDG)), M is the margin applied to the path, and $OSNR_{th}$ the actual required OSNR threshold for setting up the working path. We considered margins from -6 dB (i.e., a conservative approach) to 6 dB (i.e., with an aggressive approach). The results are reported in Figure 4.7. Interestingly, even when margins are omitted (i.e., 0 dB) we do not achieve 100% capacity. This is due to the physical effects modelled in the network, which cause some lightpaths to fail.

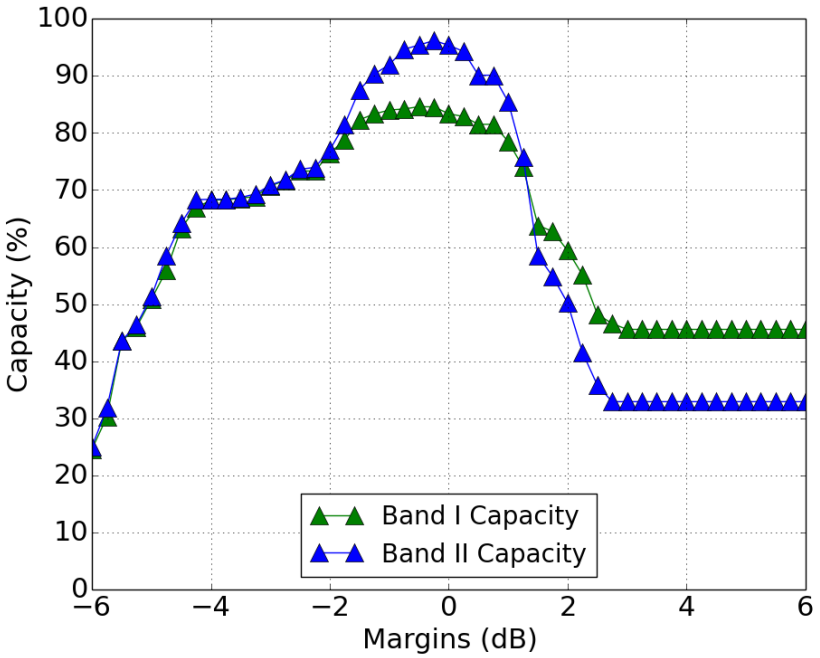

Figure 4.7: Network capacity vs. OSNR margins applied by the control plane.

The maximum capacity of the system is the maximum capacity calculated by our simulation using all the possible paths. This would also be the capacity achieved by the SDN controller if it had exact knowledge of the OSNR levels for every path. The curves show that when implementing a conservative margin, that is, under-estimating the OSNR levels (in the negative region), the QoT-E progressively rejects the allocation of paths, and the overall capacity decreases accordingly. When the QoT-E adopts a more aggressive strategy, that is, over-estimating the OSNR levels (in the positive region), the capacity also decreases progressively, as a higher number of paths does not meet the minimum OSNR threshold for the selected modulation and thus cannot transport data. For the higher values of margin, the QoT-E will assume that all paths can operate at 16QAM, and the achieved capacity settles at the value of 46% and 32%, respectively for the first and second bands of operation, which are related to the percentage of paths that can support the 16QAM modulation, as already mentioned at the beginning of this section. It is imperative to notice that both under-

estimation and over-estimation at the control plane cause discrepancies in the performance of the network because of the misuse of network resources. While constant under-estimation would lead to the non-installation of paths, an over-estimation can lead to the installation of non-feasible paths, hence, installing non-usable resources.

According to our study, the optimal point of the OSNR margin adopted by the controller seem to be around the 0 dB value, for both bands examined. Which directly complies with the need to mitigate the usage of margins. However, even at the optimum, since such margins are adopted equally across all paths, the loss of capacity with respect to the maximum capacity is still of the order of 5%-17%. In Figure 4.8, we show the success rate of two analysis: *(i)* the ratio of number of paths attempted to be installed, with respect to the total number of paths with OSNR levels above BER pre-FEC threshold.

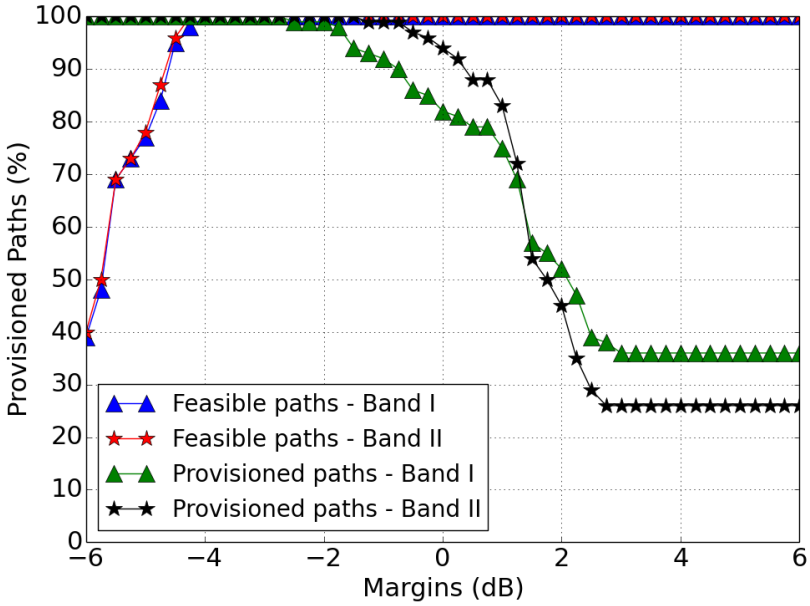

Figure 4.8: Comparison of two analysis: Percentage of feasible paths that are provisioned for both bands vs. Margins (dB) (red and blue curves), and provisioned paths above required OSNR threshold for both bands vs. Margins (dB) (green and black curves).

A more conservative approach would restrict significantly the attempts of installation, whereas a more aggressive prediction would fall into highly optimistic computations, attempting to install 100% of the paths; *(ii)* we analysed the success rate of the established paths. In other words, how the application of different margins to the QoT-E affects the accuracy of feasible lightpaths. Our results suggest that a conservative approach would increase the accuracy of the prediction of feasible paths, but at the expense of restricting network capacity. Contrasted with Figure 4.7, it is noted that when over-estimating the feasibility of lightpaths, the maximum percentage of feasible paths is 36%, allowing for 46% of the network capacity for the first band. Similarly, this analysis determines that for the second band, only 26% of the paths can be successfully allocated, enabling for 32% of the network capacity. Additionally, our results depict maximum provisioning-feasibility when the margins are reduced by 2 and 4 dB. This is due to the effect of the EDFA–WDG functions, which may cause a higher gain at times, explaining the feasibility of lightpaths even when the estimations are low.

4.4 gOSNR-Based QoT Estimation with Active Monitoring

4.4.1 Implications for the use of active-monitoring

As we have been discussing, optical network disaggregation is an area receiving increasing attention, especially from operators, who want to part from legacy vendor lock-in restrictions. In parallel, the use of open interfaces, supported by SDN, has boosted research on control plane algorithms, especially in support of dynamic provisioning. In this regard, one of the main open challenges is that the use of heterogeneous components in disaggregated optical networks increase uncertainty on system performance, which in turn leads to the requirement of larger power and OSNR margins, which adversely affect network efficiency and complicates fault diagnosis.

As we have discussed in Chapters 2 and 3, while analytical models of fiber propagation behaviour are widely available [236], active components can introduce considerable unpredictability into the system. In particular, the WDG of EDFAs can lead to unequal channel power compensation, often referred to as channel power divergence, which are caused by the AGC procedures in EDFAs that reconfigure the mean system gain. Thus, depending on the specific device and working condition, WDG as high as ±0.5-1.0 dB have been measured [220]. This effect generates a power divergence whose uncertainty accumulates in systems with several amplifiers and ROADMs. This has driven the research community to investigate methods to improve accuracy of QoT-E.

In this regard, much progress has been made on the development of accurate analytical signal performance models [190] and, more recently, cognition-based estimators using artificial intelligence algorithms [36, 237]. The main drawback of such approaches is that they require large amounts of data for optical link characterisation, which can be complex and expensive to acquire. An alternative to data-expensive ML models is the use of coherent receivers to estimate lightpath QoT given the characteristics of the optical link, which can effectively provide gOSNR monitoring as well as other power anomaly detection measures through digital backpropagation [145, 146]. This can be part of a larger research area developing control methods that combine real-time data collection with QoT-E and provisioning [147]. This approach involves the use of real-time control plane operations to gather OPM information and run algorithms for the correction of QoT-E functions. Here, we address two key questions for the control and prediction of QoT in disaggregated optical systems, which can be used both for fault management as well as lightpath QoT-E for dynamic wavelength routing. Firstly, we analyze the error that OSNR vs gOSNR monitoring produce in estimating QoT for different numbers of OPMs deployed in an optical link. Secondly, we show how real-time OSNR monitoring information can be used to improve the QoT-E and monitoring functions, even when only OSNR types of OPM are available. For this, we introduce an OSNR monitoring-based channel modelling solution. It should be noted that we do not focus on specific device performance, instead we study monitoring strategies at the network scale and how they can be used effectively to monitor and estimate QoT across the network given uncertainties inherent in the systems.

In particular, we addressed the complication of OSNR monitoring considering that the gOSNR is inversely related to the gOSNR for high transmission power, as shown in Figure 4.9. Thus, for a channel whose power is higher than originally estimated, OSNR monitoring alone would indicate that the QoT is higher than the QoT-E. However, since the nonlinear interference increases with absolute power, at high transmission power (e.g. due to gain ripple power divergence), the presence of nonlinear interference renders the actual QoT lower than its OSNR-based value would indicate.

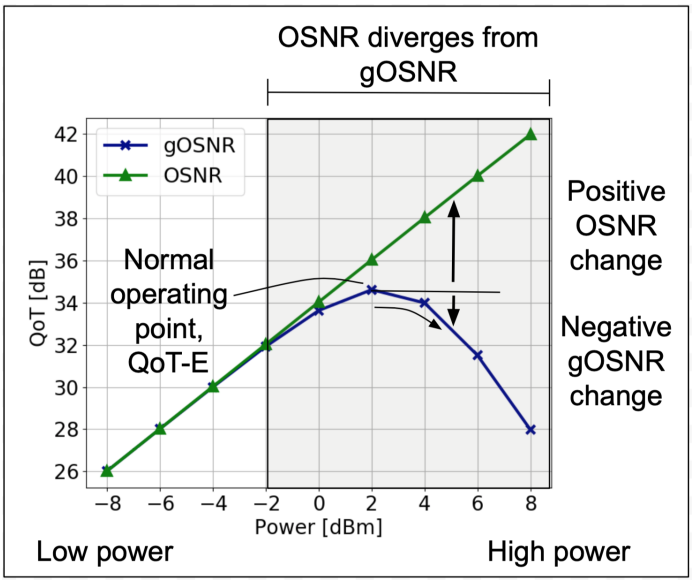

Figure 4.9: Difference between OSNR and gOSNR for increasing power levels, leading to QoT-E inaccuracy.

This is particularly important for monitoring scenarios in which the noise figure of an amplifier can be expected to be relatively constant, but the channel powers will vary based on the loading scenario, which is the main focus of this work.

Thus, we investigated a QoT-E strategy based on active monitoring of lightpaths in an optical SDN environment deployed within Mininet-Optical. Using the Gaussian Noise (GN) model to determine the nonlinear transmission effects [219] along with WDG in the EDFAs and fiber Stimulated Raman Scattering (SRS) [218], we assess the benefits of SDN-based active monitoring to mitigate QoT-E inaccuracies due to wavelength dependent power dynamics in an optical transmission.

4.4.2 Experiments and results: study 1

Our assessment runs over a linear topology, shown in Figure 4.10, of 15 ROADM nodes linearly connected by fiber links of 480 km, made up of 6 x 80 km spans, totaling 6,720 km. To model the WDG behavior, we measured the WDG of 2 real EDFAs [220]. The resulting WDG curves were then randomly assigned to each EDFA, as depicted in Figure 4.10. We also apply channel equalization at each ROADM, by setting the VOAs appropriately. OPM devices are located at the EDFA outputs, and interrogated depending on the monitoring strategy described below.

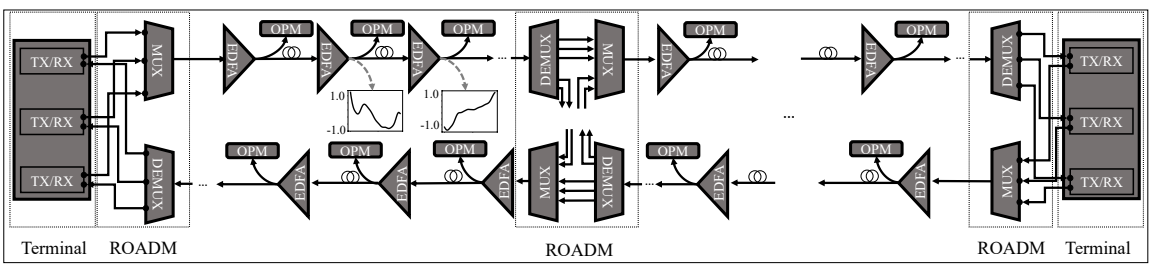

Figure 4.10: Linear topology emulated with Mininet-Optical.

For the transmission system, 3 different C-band traffic loads were considered, corresponding to 10%, 30% and 90% of the system capacity (i.e., 9, 27 and 81 signals, respectively, for a 90-channel transmission system). Two different channel allocation strategies were examined: sequential and random, to account for wavelength loading and configuration dependencies. All channels are transmitted with -2 dBm launch power. To create the optical paths, the SDN controller connects to the control interfaces of the ROADM nodes and installs switching rules into each ROADM. Both the SDN controller and Mininet-Optical were running on an Ubuntu 18.04 virtual machine on an Intel(R) Core(TM) i7-4770HQ CPU @ 2.20GHz processor and 12 GB RAM. For comparison purposes, we adopt a baseline QoT-E model, where the control plane carries out gOSNR estimation by using the same models adopted by the physical layer simulator (i.e., GN model and SRS), but without any knowledge of EDFA-WDG functions or channel power adjustments and without any OPM interrogation. This process was executed for 150 transmission tests for each traffic load and for each channel allocation strategy. The simulation of each individual test required from a few seconds up to 120 seconds to process (depending on the load scenario).

In order to assess the maximum deviation of the controller's QoT-E model from the actual QoT in Mininet-Optical (representing the ground truth), we computed the gOSNR absolute error. Because of the random assignment of WDG functions to the EDFAs, each test case can be considered to be a different optical network system with the same physical topology. The highest absolute error at the output of each amplifier for all tests is shown in Figures 4.11a and 4.11b, respectively, for the sequential and random channel allocation strategies. Here the solid curves represent the error of the baseline QoT-E model described above. As expected, the higher the number of wavelengths used, the worse the baseline QoT-E model performs, due to accumulated nonlinearities and power divergence. These results illustrate an important source of error in QoT-E models, which contributes to the use of larger QoT margins in real systems.

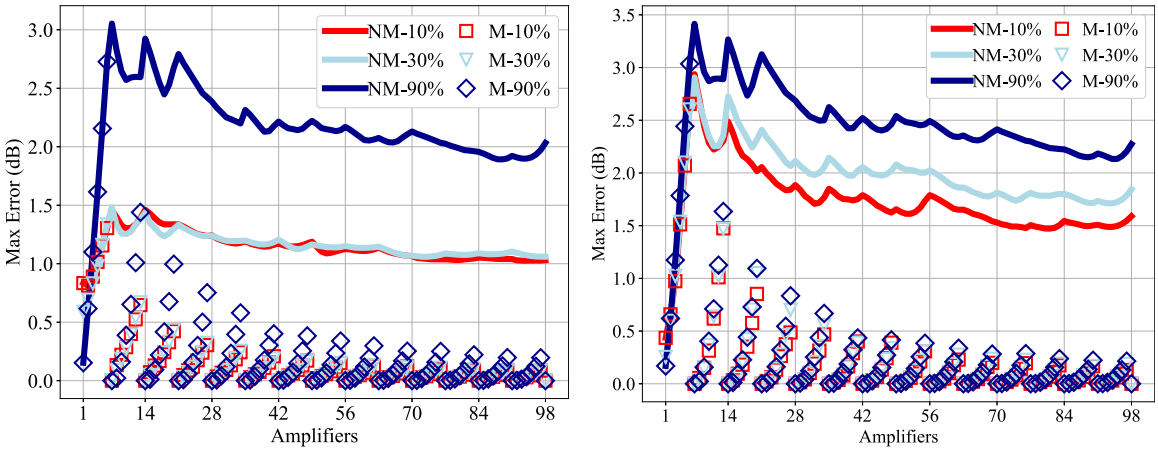

Figure 4.11: Maximum absolute error of gOSNR computations from the QoT-E model with no-monitoring-based corrections (NM-curves) and with monitoring-based corrections (M-markers) at the end of each inter-node link (every 7 amplifiers) for: (a) sequential channel allocation strategy; (b) random channel allocation strategy.

Next, we include the use of OPMs, so that the control plane can assess and correct the QoT-E across the link. This monitoring-based QoT-E method replaces the QoT-E estimated values with monitored values at a number of OPM locations, restarting the estimation process from that point.

The error of this OPM-based method is reported in the figures by the colored empty markers. As a first analysis, OPM nodes were deployed at the end of each inter-node link (every 7-EDFAs). In the figures, at each OPM monitoring point (i.e., every multiple of 7 in the x-axis) the QoT-E error goes to 0. From there, the error starts increasing again, until the next OPM node is reached, at which point the error of the QoT-E model is reset again. It is noticeable that by comparing the unmonitored curves with the monitored data points in Figure 4.11a and Figure 4.11b, retrieving monitoring information can reduce the QoT-E error substantially. At the monitoring point, the error is reduced between 1.5 and 3 dB at short distances and 1 to 2 dB at 2,000km. In addition, after the first 7 amplifiers we have an improvement of at least 0.8 dB and 1.2 dB in the worst case (i.e., just before the monitoring), for the lower loads and higher load, respectively.

We repeated the experiment interrogating OPMs every second inter-node link, i.e. every 14 amplifiers, respectively (using only 8 OPM nodes in our long-haul end-to-end link). Here we found that despite the substantial reduction in number of OPMs, after the first 14 amplifiers, we have an improvement of at least 0.6 dB and 0.8 dB in the worst case, for the lower loads and higher loads, respectively, also after approximately 2000 km. These results are shown in Figures 4.12a and 4.12b.

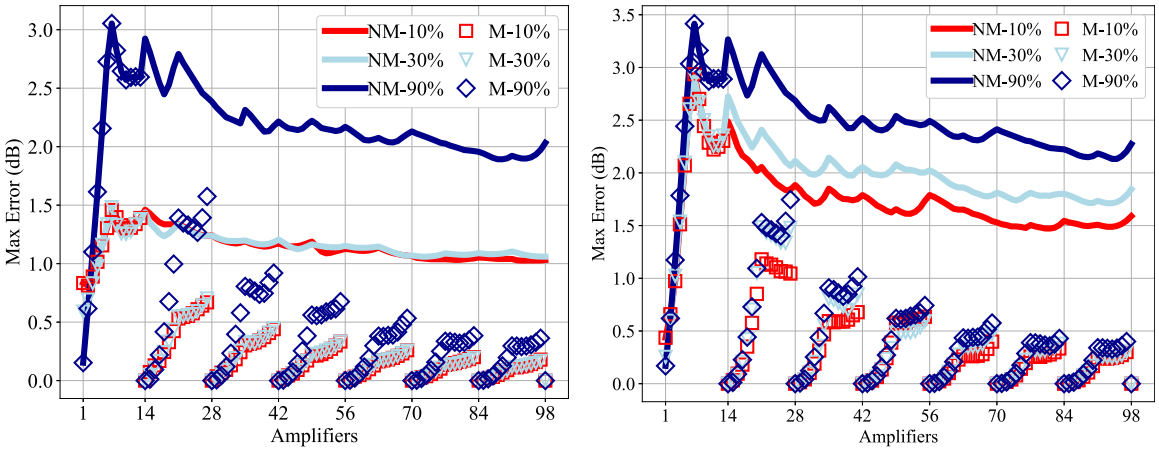

Figure 4.12: Maximum absolute error of gOSNR computations from the QoT-E model with no-monitoring-based corrections (NM-curves) and with monitoring-based corrections (M-markers) at the end of every second inter-node link (every 14 amplifiers) for: (a) sequential channel allocation strategy; (b) random channel allocation strategy.

These results show that an optical system that includes OPM can mitigate the inaccuracies of the baseline QoT-E model, by providing intermediate gOSNR information to an SDN controller. In this study we implemented and tested a real controller that uses the information provided by OPMs, assessing its realistic behaviour over a platform that enables emulation of optical components.

4.4.3 Experiments and results: study 2

In this study, we look at how OPM monitoring at intermediate nodes in a link can help to improve the estimation of gOSNR levels of individual channels along a path. We use the estimated power (P_E), ASE noise (ASE_E) and NLI noise (NLI_E) to compute the estimated gOSNR with $gOSNR_E = P_E/(ASE_E + NLI_E)$. We test three different types of gOSNR estimation models:

- **Model 1**: updates the ASE noise levels from the baseline model estimate based on the expected noise levels given by the OSNR monitoring, where it is available.
- **Model 2**: uses this OSNR monitoring information together with channel monitoring information to build a model for the optical power levels between monitoring points and gOSNR estimates based on these values.
- **Model 3**: uses reference receiver monitors that directly measure gOSNR, which is used to set the QoT values to perform subsequent estimations along the path.

More specifically, in model 1 we replace the P_E and ASE_E values in the QoT-E procedure by the monitored power P_M and ASE noise ASE_M. These updated performance metrics are then used to compute the QoT-E at the subsequent locations in the optical link. Note that such OSNR monitoring is sensitive to uncertainties in the amplifier noise figures, which would be reflected in the ASE noise power measurement. We then propose model 2, where in addition to the operations in model 1, we also compute the difference between P_E and P_M to produce a NLI_E correction factor, p_{corr}, for the gOSNR estimation formula. This measured power difference is then assumed to be uniformly distributed among each span between monitoring locations (i.e. assuming a linear ramp). Thus, at every OPM location i, for every channel ch, we compute $p\_corr_{ch_i} = |Pm_{ch_i}/Pe_{ch_i}|^3$ for the nonlinear noise and ramping it for each span between monitoring locations. Then we apply this correction factor to NLI_E, resulting in a corrected NLI noise (NLI_C), which is used to compute an updated $gOSNR_E$. Last, model 3 replaces all estimated metrics by direct gOSNR measurements, effectively resetting the QoT-E to a new starting value at that node for use in subsequent estimation along the path, which is the procedure evaluated in the previous study. Naturally, model 3 provides the most accurate results and requires more expensive reference receivers. Thus, it is important to understand the relative merits of different monitoring strategies to balance against their potential costs.

With Mininet-Optical we model the Cost239 European Network topology with 11 nodes and 26 links. For this analysis, we focus on the London to Copenhagen link, measuring 1000 km, composed of 20x50km fibre spans. We assume that all spans are optically compensated by EDFAs with target gains of 11 dB. Then, our optical SDN controller configures the transponders to set the wavelength channels and launch power. Also, the controller must configure the ROADM nodes to switch lightpaths appropriately. We include a boost amplifier after every ROADM, compensating for an overall insertion loss of 17 dB. We also include channel power equalisation procedures at the ROADM nodes and at every 6th span in the links, carried out through VOAs in the ROADMs or equivalent channel gain equalisers.

Our first goal is to analyse the performance of the three models described above to assist gOSNR estimation. For this, we configured a 15-channel transmission configuration to traverse the link. The 15-channel set was randomly allocated in the C-band channels (191.6 - 195.6 THz), with channel spacing of 50GHz and launch power of 0 dBm per channel. In Figure 4.13a we show the performance of the three models when OPMs are co-located with channel leveling locations (every 6th span), in addition to each intermediate location between these. Thus, we consider 8 OPM nodes out of 21 possible locations (evenly-spaced across the link). In the figure, the green solid curve represents the maximum error produced by the baseline QoT-E model (when we do not monitor at any location). This maximum QoT error is computed considering the estimations for all 15 channels, predicted at each potential monitoring location. The light-blue curves correspond to the performance of model 1 described above, the red curves to model 2, and the dark-blue curves to model 3. We can see

that simply correcting data points with OSNR information (model 1) reduces the error compared to the unmonitored scenario. However, peak errors are still similar. Here we consider peak errors as the main indicator of estimator performance, as these will affect most the required system margins. The key finding is that our proposed model 2 (red curve) is able to lower the peak error by over 0.5 dB, using the exact same amount of OSNR information. Indeed it is capable of reducing peak errors considerably.

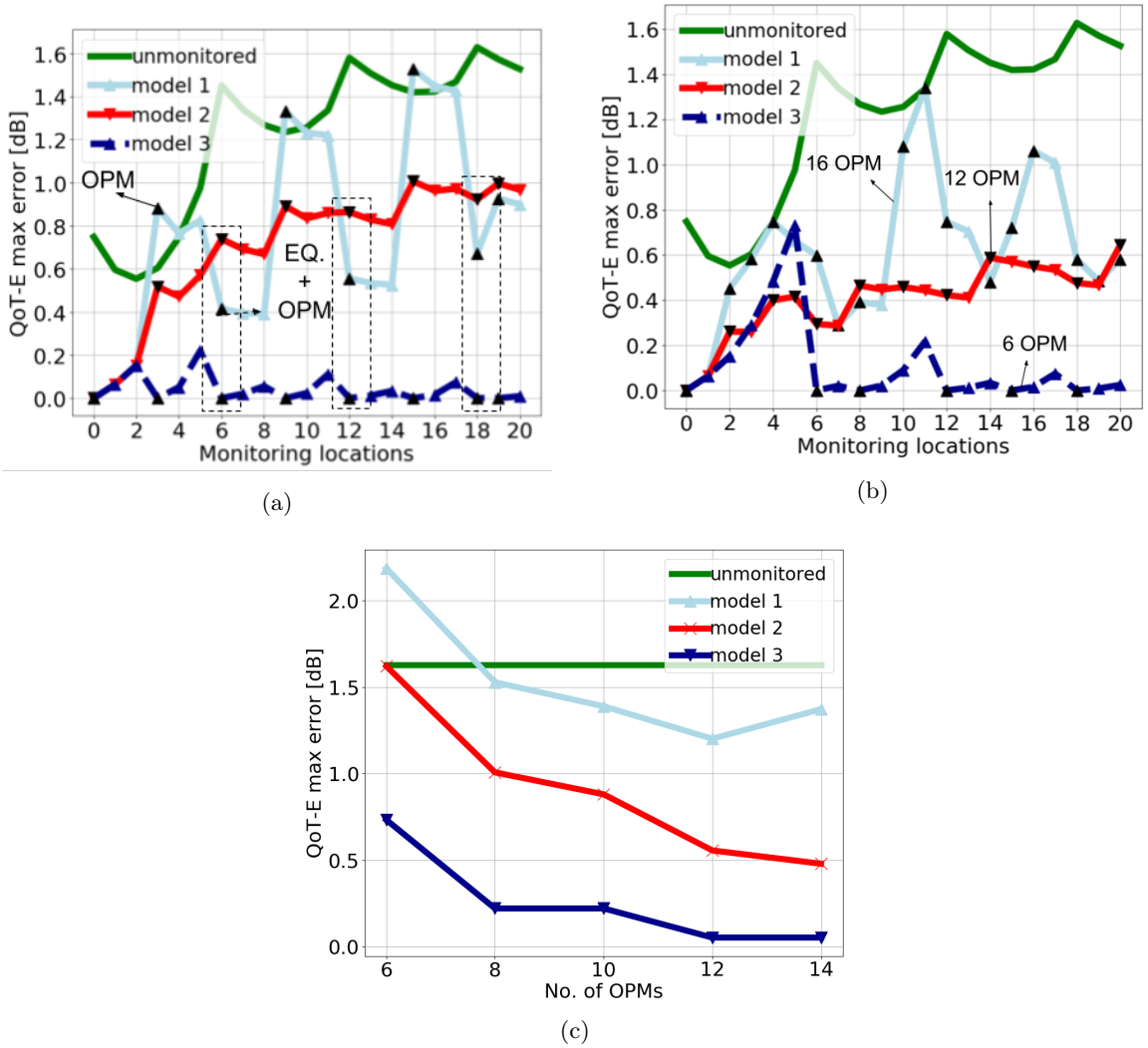

Figure 4.13: (a) Comparison of different QoT-E correction models with 8 OPMs. (b) Comparison of model 1 with 16 OPMs, model 2 with 12 and model 3 with 6. (c) Comparison of the impact of increasing the number of OPM locations for the three models.

Figure 4.13b focuses on the trade-off between the model used and the number of OPM locations. Here we can see that even with a higher number of OPM locations (16 out of 21 locations), simply correcting OSNR data points (model 1) is not effective in reducing the peak estimation error, which remains similar to the unmonitored curve at location 11. Our proposed model 2 can instead reduce the peak error by 0.7 dB, even using a smaller number of OPMs (12 are considered here). Comparing the red and dark blue curve, we can also notice that we can trade simple OSNR monitors with more complex gOSNR solutions, if we increase their number. When coupled with our proposed model 2, using 12 ONSR monitors provides comparable peak error (0.1 dB lower) than using 6 gOSNR

monitors. The comparison between the three models as a function of the number of OPM locations, is finally reported in Figure 4.13c, which reports the peak error for each scenario. We can observe that model 2 outperforms model 1 by up to 1 dB. In addition, for increasing number of OPM locations, the discrepancy with model 3 is reduced to less than 0.5 dB.

4.5 Summary

In this Chapter, we have analysed the internal composition of optical control systems in the context of disaggregated optical networks. In particular, we have presented a customised architecture of an optical control plane, including the modules: UI, DBM, PCE/RWA, OPM, QoT-E, NBI and SBI. We have also demonstrated the integration of these modules within customised SDN controllers, which we have enabling dynamic lightpath provisioning on top of emulated optical network systems modelled with Mininet-Optical. For the latter, we have presented a series of studies addressing the impact of receiver margins in the network capacity provisioning, the impact of active monitoring and its potential to assist QoT-E modules.

First, we presented a study on the network under-utilisation issue brought by the absence of detailed knowledge on the behaviour of EDFA gain functions across wavelengths and over time. We used the Ryu SDN controller framework to build a customised control system that operated over an extended-Mininet emulation of the Telefonica Spanish national network. With this network, we have investigated the impact on margin utilisation imposed by the differences in QoT-E processes in network capacity between an optimal situation, where the gain function of the cascaded EDFAs is known in advance, and the real situation, where the controller only uses a flat gain function. By comparing the outcome of the ground-truth model (physical layer simulation) with the prediction of the controller, we could calculate how the use of different margin values for the OSNR affect network capacity. We showed that an aggressive margin strategy, that would tend to over-estimate the available OSNR, reduces the performance, as it favors the adoption of higher modulation rates, leading to situations where the paths created could not operate below the BER threshold. On the other hand, a too conservative strategy that tends to under-estimate the OSNR, would lead to a situation where the controller operates over lower modulation rates, and in some cases declines the creation of wavelength paths, which would instead have worked correctly, according to the Mininet simulation. According to our study, the optimal point of the OSNR margin adopted by the controller seem to be around the 0 dB value, for both bands examined. However, even at the optimum, since such margins are adopted equally across all paths, the loss of capacity with respect to the maximum capacity is still of the order of 5%-17%.

Moreover, we have investigated the uses of active optical performance monitoring to enhance QoT-E processes. We have shown that it is possible to trade the use of complex (and more expensive) monitoring equipment (i.e., coherent receivers capable of estimating full gOSNR) with OSNR monitors that make use of the individual channel power data to adjust the estimation of NLI noise. Furthermore, we have studied the impact of EDFA-WDG functions on the SDN controller QoT-E model, and assessed the estimation accuracy variation with distance from actively monitoring the performance of optical signals at distributed locations along an end-to-end long-haul link, enabling the evaluation of QoT-E also at intermediate locations of the optical link. Our approach enable testing the correctness of control plane operations, so that it can be deployed on a real network, where improvement of QoT-E can reduce margins, thus improving the overall network efficiency.

Furthermore, we plan to emulate the use of sparse OPM in the network to gain knowledge on the wavelength and time-varying behaviour of other EDFAs, and feeding the data to machine-learning based techniques to improve the per-path estimation of the OSNR, thus increasing the network utilisation.

5 Cognitive-Assisted Control

5.1 Introduction

As discussed in Chapter 4, non-disaggregated and disaggregated optical control systems face multiple challenges that constrain the capacity of optical network resources. These can be tackled with cognitive-assisted (i.e., Machine-Learning (ML)) control planes capable of dealing with uncertainty in the optical domain [70]. For example, a control system can potentially learn from the interactions of channels in a transmission in order to predict the behaviour of unestablished optical paths [65] in order to allocate those that meet a required Quality of Transmission (QoT). The end goal is to maximise the usage of optical networks resources without exceeding costs.

As a result, the development of cognitive-assisted control systems is of major interest to everyone involved in the optical networks research area, from infrastructure providers to network engineers. In this Chapter, we address a series of studies considering the inclusion of "cognition" into control plane functions such as routing and wavelength-assignment, wavelength-switching, and real-time device configuration, by means of the centralisation and softwareisation of the control and all network management functions following the Software-Defined Networking (SDN) paradigm. First, we need to define the current limitations of control systems in terms of active monitoring and data collection availability. There is a common trade-off when deploying monitoring equipment in optical networks which is that larger and more accurate data availability requires highly complex and expensive resources (see Chapters 2 and 4). To mitigate this, there is a current interest of compensating for the defective quality of the data that cheaper monitoring equipment can provide. The nature of the defective data in this type of monitoring equipment is due to the limitations in monitoring sensitivity of the materials. The aim is to use this data to help predict the behaviour of optical paths before their installation. Thus, optimising the use of resources. This has been commonly addressed by means of Quality of Transmission Estimation (QoT-E) procedures [146, 196, 201], which are considered to be implemented as modules of control planes capable of assisting networking functions such as wavelength-switching. We have shown in Chapter 4 that these QoT-E modules can be implemented in an online and offline manner when using data from monitoring equipment after a transmission has taken place. However, data processing tasks could benefit from cognitive algorithms [65, 70].

In this Chapter, we present a performance analysis on supervised-learning algorithms as QoT-E modules. We begin with the analysis of the Support Vector Machine (SVM) algorithm, and how optical domain data can become readily available for it. We explain how the algorithm could be a potential candidate only if the data collection processes can ever become faster. Then, we perform an analysis of other supervised-learning algorithms by looking at their time complexity and accuracy when handling optical networks data. We show how a basic correlation among certain algorithms is

formed and how there continues to be a trade-off of time complexity (i.e., how long it takes to train and build learning models) vs. computing resources (i.e., what CPU/GPU and RAM is required). Finally, we present a series of conclusions and forthcoming work.

5.1.1 Scope and contributions

The scope of this Chapter is limited to the study of supervised-learning algorithms, which provide relatively fast estimation and prediction models with low degrees of complexity, making them ideal candidates to operate within real-time optical networking scenarios. Although unsupervised-learning algorithms have also been reviewed in recent years [238], the unstructured nature of the data commonly used for this type of algorithm does not align well with the composition of optical networks. This is mainly because optical networks are closed-systems, where all the elements and their functionalities are correlated. We intend to solely investigate the feasibility of their application into the optical domain, meaning that the mathematical optimisation of these is beyond the scope of this thesis. The focus is instead on analysing the optical network data requirements for this type of algorithms to achieve optimal performance. That is, understanding the data that can be collected from optical networks in a static manner (i.e., device-configuration specifications) and in a dynamic manner (i.e., active device monitoring). Our focus is on the latter, addressing the multiple possibilities of the information that could be generated by actively monitoring optical networks components.

As reviewed in Chapter 4, the quality of the monitored data is entirely dependant on the level of sophistication of the monitoring devices, which at the same time determines their costs. Because of that, it is important to understand how the management of these type of resources can be optimised to minimise costs and improve overall performance. In order to build a strategy to optimise the management of monitoring resources, we want to first understand the nature of the parameters that we want to observe and the methods to obtain it. Thus, within this area of research, we analyse how optical signals can be observed and what type of data can be extracted. Then, we use this knowledge to process the monitored data to create information that we can subsequently feed to the supervised-learning algorithms that would enable the prediction of the QoT of lightpaths that have not been installed.

The main contributions of this Chapter are:

- Analysis of the different types of data that is available in optical access networks, the processes required to retrieve these and the nature of the processing tasks.
- Performance analysis of the SVM algorithm when handling offline optical networking data, including static and dynamic parameters, such as the number of nodes in a network and the number of channels in a transmission.
- Proposal of using channel allocation and channel loading information to build a relevant feature to assist the training process of supervised-learning algorithms.
- Proposal of an algorithm for data generation with the Mininet-Optical system and an evaluation of its usage with ML algorithms.
- Evaluation of the offline usage of supervised-learning algorithms to predict optical signal behaviour considering uncertain networking scenarios due to the wavelength-dependent operation of optical network components.

5.2 Problem definition

Heuristic models assisted with optimal Optical Performance Monitor (OPM) placement can significantly mitigate the utilisation of optical transmission margins by 1-3 dB, which enables an optimisation of the management of network capacity [225, 239]. Unfortunately, the available number of such devices is typically limited due to the increase in costs that these devices contribute, which is in the tens of thousands for individual devices (see Chapters 2 and 4). In addition, state-of-the-art OPM devices do not support the performance speed foreseen for disaggregated control systems, which will require sub-millisecond operation rates for basic networking functions (i.e., wavelength switching). The latter also imposes a limitation for the development of cognitive-assisted control systems, since the algorithms considered to be embedded in the optical control plane require fast and vast data availability.

5.2.1 Cognitive-Assisted Control

In the context of software-defined optical networks, the composition of the optical control systems vary according to the specific needs of each network and the components that have enabled disaggregation. As such, inputs to the control system arrive from different sources at different times. For instance, traffic requests can arrive through the Northbound Interface (NBI) at the same time that alarms are triggered at its Southbound Interface (SBI). Despite the parallel occurrence of events, the control system must be capable of handling them in the fastest possible time. As a result, the inclusion of cognition to assist networking functions at the control plane must comply with the sub-millisecond operations time required for common networking functions such as wavelength switching. However, ML algorithms can operate at different time rates to build their models, entirely dependent on the size of the data used for these processes. Once the models are built, classification and estimation tasks can be performed fast. Hence, it is necessary to understand what type of optical networks data can ML algorithms handle at the fastest rates with the best performance.

5.2.2 Data Composition

The key element determining optimal performance of ML algorithms is data. In an optical network, data becomes available from different sources, at different times and is of different composition. For instance, we can categorise data in the optical domain in two classes: static and dynamic. On one hand, static data refers to elements of the network that do not change over time, as it is the number of nodes in a path, the length of a path, etc. On the other hand, dynamic data appears when traffic is launched into the network. Examples of this type of data are the channels launched in a given transmission, the adjusted gain of the Erbium-Doped Fibre Amplifiers (EDFAs) in long links, the fluctuating power levels of the channels, etc. Furthermore, in optical network systems some data remains ever hidden to the control plane. This is due to the complex randomised physical behaviour of the network components that cannot be inferred and can only be observed at specific times and under specific configurations. An example of these would be the Wavelength-Dependent Gain (WDG) of the EDFAs, which has been the main feature of interest throughout this thesis. Intuitively, the heterogeneity of the sources and nature of the data within optical network systems imposes several engineering challenges. In this Chapter, the main challenge that we tackle is that of feature extraction.

5.2.3 System setup

We have discussed that in-field optical data generation is a complex and time consuming task. Furthermore, the variation of the topology configuration and the system setup parameters may be limited to the available equipment at the time. Despite the use of synthetic data cannot give a definite answer on how a ML algorithm will perform once applied in the field, it enables low cost, fast analysis and understanding of the algorithms, allowing comparisons of their potentials. Afterwards, real data is necessary for validating these tools.

For the studies presented in this Chapter, Mininet-Optical was used to generate multiple end-to-end linear topologies as depicted in Figure 5.1, considering multiple combinations of the parameters listed in Table 5.1. These linear topologies are composed of optically-amplified links and Reconfigurable Add/Drop Multiplex (ROADM) nodes, equipped with Wavelength-Selective Switches (WSSs) and Automatic Gain Control (AGC)-EDFAs for pre-/post-signal amplification. Additionally, end-to-end transmission is enabled for up to 90 wavelength channels in the C-band (1529.6 nm - 1565.2 nm).

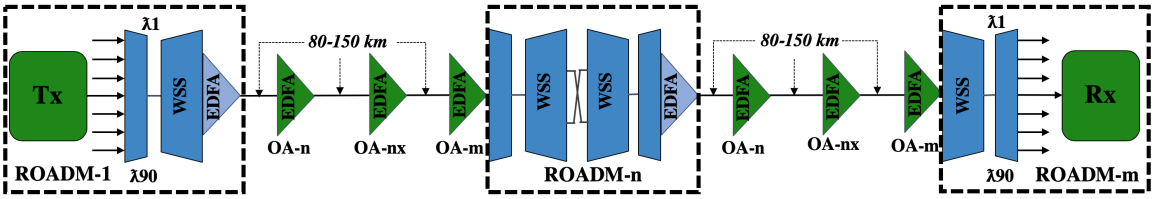

Figure 5.1: Linear topology with varying configurations as per features in Table 5.1.

Table 5.1: Topology configuration parameters.

Feature	Value
Number of ROADMs	2 to 8
Number of fiber spans	2 to 6
Length of fiber span	80 to 150 km
Launch channel power	-10 to 4 dBm
EDFA Preamp gain	Fiber compensation adjustment dB

For all system setups, a WSS insertion loss of 9 dB is assumed and compensated by in-line (post-amp) EDFA. The ROADM nodes are interconnected by links composed of several spans. For each linear topology, spans are set to the same length. EDFA in-line amplifiers are configured to compensate for the span loss. For example, as depicted in Figure 5.1, Mininet-Optical can be used to generate a 3-ROADM network linearly connected with links of 2-spans of 80 km with in-line EDFA system gain set to 17.6 dB. In the case of the booster EDFAs the system gain is set to a fixed value of 9 dB, since they are deployed to compensate for the mean ROADM insertion loss. Finally, upon transmission, a launch power level for all signals is selected. The latter will be further explained in the subsequent sections.

Additionally, we assumed that Gain Flattening Filters (GFFs) are used at line amp sites for EDFA gain equalisation. However, similarly to the studies presented in Chapter 4, we are capable of modelling residual WDG-EDFA, causing undesirable power excursions during wavelength switching (add-drop). Therefore, WDG curves are randomly assigned to each EDFA in all topology

configurations, considering different gain settings. An example is shown in Figure 5.2, where a booster EDFA is assigned a curve with an amplitude range of -/+ 1.5 dB, and a preamp EDFA is assigned a curve with an amplitude range of -/+ 0.4 dB. All subsequent line amplifiers would have similar characteristics, with WDG functions varying in spectral shape and amplitude, as described in Chapter 4. Gain curves were experimentally retrieved from a physical testbed, and then synthetically assigned to the EDFAs as we have presented in previous Chapters. Moreover, the power excursions which result from the interaction of WDG and AGC were modeled following the work in Junio *et al.* [240], considering the switching functions (add-drop) and the wavelength channel load and the channel configuration (i.e. which channels are active).

We have shown that the detection of the feasible modulation format to transmit an unestablished lightpath would enhance the overall network capacity. Because of that, we use OPM nodes to monitor the QoT of the transmitted channels for all tests. The deployment of OPM nodes was considered at the receiver end of all topologies, allowing us to retrieve the power and Amplified Spontaneous Emission (ASE) noise levels for each received wavelength channel. With this data, we were able to compute the Optical Signal to Noise Ratio (OSNR) following the well-known formula $OSNR = \frac{P}{P_{ASE}}$.

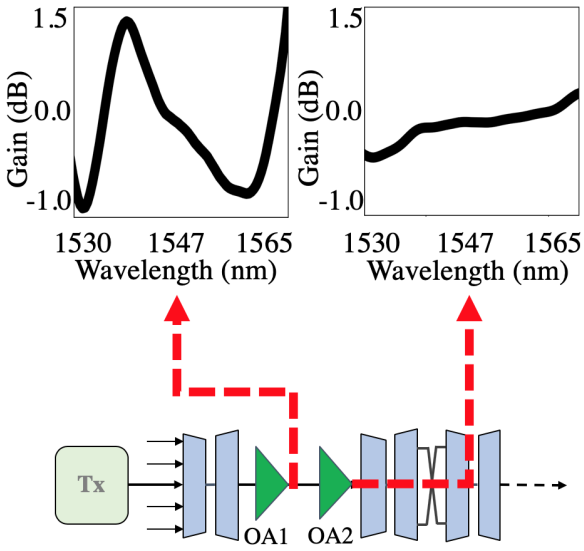

Figure 5.2: Different EDFA wavelength-dependent gain functions. Post-amp EDFA is assigned a curve with an amplitude range of -/+ 1.5 dB, and a preamp EDFA is assigned a curve with an amplitude range of -/+ 0.4 dB.

5.2.4 Feature extraction and data generation

Feature extraction refers to a process in ML that consists in analysing all the data available in the population of interest (i.e., optical networks) and creating subsets from the combination of the different data points, in order to generate relevant features that would improve the learning process of the supervised-learning algorithms. We focus first on the role of static data sources (i.e., number of nodes in a network) and study under which scenarios its usage becomes relevant. Additionally, we consider the generation of features by combining dynamic features (i.e., number of channels in a transmission).

As mentioned above, we use Mininet-Optical to model the WDG of EDFAs to generate data that accounts for the power excursions induced by this phenomenon. In contrast to the topological parameters encountered in Table 5.2, these physical effects cannot be labeled and fed into the SVM learning model even though they significantly affect the transmission performance. That is because the wavelength-dependent operation of the optical network components always remains unknown to the control plane. To overcome this learning impairment, we propose to analyse the interaction of channels under different topological configurations, so the model can indirectly learn from their performance.

Our approach consists in extending the system parameters used to train the ML models, to not only consider network topological settings (i.e., number of nodes, number of links, etc.) as it is the common case, but to also include the number of active channels and their position in the spectrum before installing a new channel. This allow us to collect relevant data with regard to the WDG of EDFAs. For the latter, we introduce the concept of a 1x10 data-array, which represents 10 segments of the transmission spectrum (i.e., the C-band in our study). In a 90 channel WDM network, each slot (bin) of the 1x10 data-array would correspond to a number of active channels in the range 1-10, as shown in Figure 5.3.

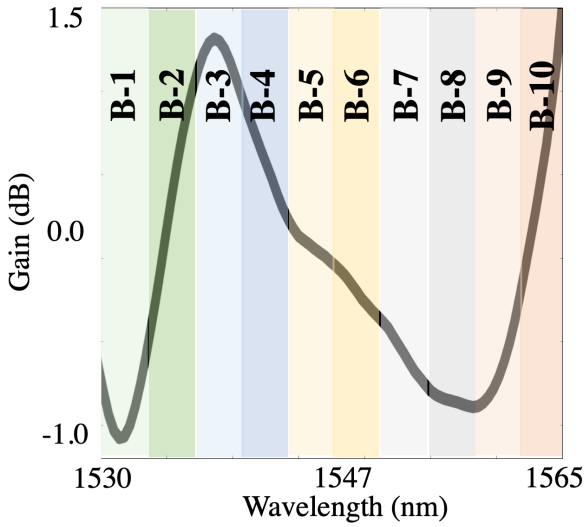

Figure 5.3: Segmented spectrum of EDFA wavelength-dependent gain.

The interaction of lightpaths across transmissions is highly variable. This results in different effects on individual wavelength channels with respect to the number of active channels and their position in the spectral band. We focus on the performance of a newly established lightpath into a system with a given Wavelength Load (WL). That is, setting up a new lightpath when there are N active wavelength channels. For instance, in a 90 C-band channels, for the training data sets we only consider WL-scenarios for n active channels: $\{n|n \in \{1, 5, 10, 15, 20, 25, 30, 35, 40, 45, 50, 55, 60, 65, 70\}\}$. Subsequently, we register the labeled OSNR levels of the (n+1)-channel to be installed. On the opposite, for the testing data set we consider WL-scenarios where n can take any value so that $\{n|n \in \{1 - 90\}\}$. Hence, the classifiers would attempt to predict the OSNR levels of the (n+1)-channel, which it may have not been trained for before.

The input labeled data used to train our models consisted in: the wavelength (measure in nm) of the monitored channel, the topology configuration settings depicted in Table 5.1, and the 1x10

segmented spectrum data-array described above, accounting for 16 parameters in total. The data generation process with Mininet-Optical consist in the following steps:

- Set a linear WDM network topology and configuration settings by randomly selecting a combination of values from Table 5.1.
- Randomly select n-channels to add to the network as per WL case, and add them to the network.
- Randomly select another (n+1)-channel and add it to the network.
- For the (n+1)-channel, monitor power and noise levels, compute the OSNR levels, and generate a register (labeled sample).

Following these steps we can study the effects of the various topological and network configuration settings perceived on the transmitted channels. Also, because the deployed networks may be significantly different from one another, the generated data used to train the ML classifiers enable the performance analysis of such estimation tools in generic use cases. In our case, we attempt for the classifiers to learn about the physical effects resulting of the interaction of the channels (i.e., power excursions) and the correlation that exists between the number of channels active in the system, their position in the signal spectrum, and the transmission performance.

5.3 On the use of Support Vector Machines

The SVM algorithm is a ML algorithm suitable for classification and regression problems. Because it is based on grouping sets of data based on similarity of features, it is mostly used for classification [241]. In the optical domain, the application of this algorithm has been studied by Tremblay *et al.* [201], Bouda *et al.* [146], Mata *et al.* [198] and Morais *et al.* [202]. While all these studies share a common verdict on the performance of SVM and its suitability for handling optical networks data, they mostly used static data to assess their experiments without deepening in feature extraction. Thus, we further inquired the applicability of this algorithm in the optical domain when handling dynamic data and by combining data points to create relevant features. In this section, we present a study that includes the active WL as a feature for a QoT-E module using the SVM as the estimation model. The study assesses the algorithm in a multi-class classification use case, requiring it to predict the OSNR of unestablished lightpaths. Our implementation of SVM achieved a 96.2% classification accuracy.

5.3.1 Overview

Because of the irregular nature of nonlinearities encountered in optical networks, controlling the physical effects introduced by these phenomena is rather challenging. As explained above, cognitive control will play an important role in learning from the power dynamics in optical transmission systems to mitigate the undesired performance impact in the QoT. Proposals of cognitive control in the optical domain have been surveyed by Mata *et al.* [65] and Musumesci *et al.* [70]. Conceptual analyses have demonstrated the favorable potential of statistical tools to predict, estimate and classify the QoT of lightpaths in optical transmission systems [196–203]. Small in-field experimental studies have also exhibited positive cognition capabilities implemented in software-defined optical control systems [205, 206, 228, 240]. In general, a common trade-off exists between learning model accuracy, amount of required data, algorithm complexity, and computational time.

To date, work done with learning models consisted mainly in offline training approaches, whereas only few live demonstrations of cognitive control systems have been performed [205, 206, 228, 240]. This is mainly due to the technical limitations imposed by networking components to generate large collections of optical data in a fast and dynamic manner. Also, the fact that mainstream monitoring tools are usually allocated only at strategic (low number of) points in a network, limits the perspective of analysis towards the interaction of multiple transmissions.

In addition, given the implementation dependent performance of the optical network elements (i.e., routers, amplifiers), learning models tend not to be robust enough to assist *all* control systems, but would only perform reasonably well for those systems they were trained for. As a result, we consider relevant the analysis of multiple network features and their role in enhancing QoT-E. In particular, here we focus on the power dynamics of amplified transmission systems. We present an analysis of the power excursion phenomenon due to the presence of AGC EDFA in Wavelength Division Multiplexing (WDM) networks equipped with ROADMs. AGC operates by maintaining a constant gain averaged across all wavelength channels in a link.

As a use case, we aim to determine the most suitable modulation format to transmit a wavelength channel upon lightpath provisioning. In this Chapter, we present an insight of the capabilities of SVM classifiers to perform multi-class optical parameter-based prediction of QoT. Our SVM model was deployed with the Scikit-learn Machine Learning Python Application Programming Interface (API) [242], and was trained to predict the OSNR levels of a wavelength channel upon installation.

5.3.2 Classifier Description

For our experiments, we used the toolkit developed by Pedregosa *et al.* [242], which consists in an open-source API for ML models in Python. We have implemented the SVM classifier for the multi-class scenario that can be described as:

$$\begin{gathered} \min_{w,b,\zeta} \frac{1}{2} w^T w + C \sum_{i=1}^{n} \zeta_i \\ \text{subject to } y_i(w^T \phi(x_i) + b) \geq 1 - \zeta_i, \\ \zeta_i \geq 0, i = 1, ..., n \end{gathered} \tag{5.1}$$

For the given training vectors $x_i \in \mathbb{R}^p, i = 1, ..., n$ in two classes, and a set of labeled training patterns $y \in \{1, -1\}^n$.

Then, the dual of this formulation is described as:

$$\begin{gathered} \min_{\alpha} \frac{1}{2} \alpha^T M \alpha - e^T \alpha \\ \text{subject to } y^T \alpha = 0 \\ 0 \leq \alpha_i \leq C, i = 1, ..., n \end{gathered} \tag{5.2}$$

where e is a vector of all ones, M is an n-by-n positive semi-definite matrix, $M_{ij} \equiv y_i y_j K(x_i, x_j)$, where $K(x_i, x_j) = \phi(x_i)^T \phi(x_j)$ is the kernel function.

Last, the decision function is described as:

$$sgn(\sum_{i=1}^{n} y_i \alpha_i K(x_i, x) + \rho) \tag{5.3}$$

where ρ is an independent parameter. The main regularisation parameter of this implementation of SVM is C, which controls the cost of misclassification on the training data. Additionally, the performance is tightly dependent on the kernel function and the kernel coefficient γ. Because it is hard to select an appropriate set of parameters and avoid over-/under-fitting the classifier model, the SVM-API [242] extends a feature for an exhaustive search over specified parameter values for an estimator. This allows for multiple parameters to be trained in parallel (i.e., multiple values of C), to use those that best fit to the final model, enabling higher SVM classification accuracy.

5.3.3 Experiments and results

We follow up on the use case where we explore the potential of a QoT-E to determine the feasible modulation format to be used for unestablished lightpaths. In Ghobadi *et al.* [225], such flexibility of performance has proven to improve the usage of network capacity and its resources. Four QoT classes are considered in that study: OSNR $\geq$ 17 dB, $\geq$ 14 dB, $\geq$ 10 dB, corresponding to the feasible modulation formats of 16 Quadrature Amplitude Modulation (16QAM), 8 Quadrature Amplitude Modulation (8QAM) and Quadrature Phase Shift Keying (QPSK), respectively. For OSNR $<$ 10 dB we assume the path is below the Bit Error Rate (BER) threshold. We established the minimum OSNR threshold to 10 dB, hence, below this value we consider that no lightpath is feasible and label it as the “none" class.

Considering the feature extraction and data generation processes presented in section 5.2.4, we have generated 30,588 training samples, for which we balanced the distribution of the training set among the four QoT classes to avoid learning bias. For the test samples, we followed a similar approach, only that this time we considered random WL scenarios (i.e., N is allowed to take any number between 1 and 90). In this way, we were able to analyse the potential of the multi-class SVM classifier to predict OSNR-QoT levels of any WL, without having trained the system for all cases. This gives an insight of the significance of active wavelength channels in a system to predict the QoT of unestablished lightpaths. We generated 7,380 test samples. The total data set adds up to 37,968 samples, which have been separated for training and test data with an 80-20% ratio.

The SVM implementation with the Python Scikit-learn API allows for an exhaustive search over specified parameter values for an estimator, allowing for multiple parameters to be trained in parallel, so the model can pick those that give the higher performance accuracy. We have trained the model with the values: $\gamma = 0.001, 0.0001, 1e-05$, $C = 10, 100, 1000$, and two kernel functions: Radial Basis Function (RBF) and a polynomial function. Then, we have also used a 5-fold cross-validation for the splitting strategy. For details of the code implementation, refer to the Scikit-learn documentation [242].

The multi-class SVM classifier is assessed for the four QoT classes; the receiver operating characteristic (ROC) curve and confusion matrix are shown in Figure 5.4 and 5.5, respectively. ROC depicts two metrics of assessment, *i)* contrasting the true positive rate (TPR) against the false positive rate (FPR) of the attempts to predict any of the four QoT classes, and *ii)* the area under the curve (AUC), which uses the value of 1 as the highest possible classification performance. Our results demonstrate an exceptional performance for the case of QoT classes corresponding to

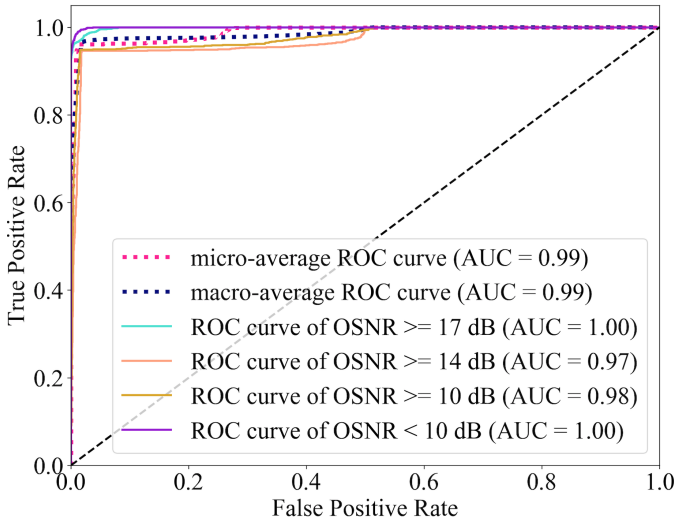

Figure 5.4: Receiver operating characteristic.

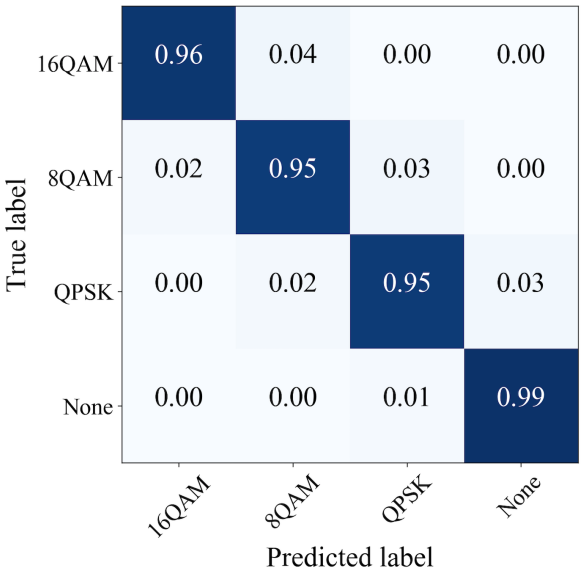

Figure 5.5: Confusion Matrix.

16QAM and below OSNR threshold, whereas a lesser performance is achieved for 8QAM and QPSK. Separately, the confusion matrix depicts the percentage of accurately classified OSNR levels for the four classes, 16QAM, 8QAM, QPSK, and below OSNR threshold (none), respectively. The overall accuracy obtained with this tool for the multi-class classification use case was 96.2%. It is important to note that these results consider generalised prediction capabilities, given that the network system topologies used to train and test the learning model were different.

Although the classification accuracy demonstrated exceptional performance, a significant pitfall of this implementation of the multi-class SVM classifier is the computational time required to train the model, given its complexity $O(n^3)$. Because we enabled the exhaustive parameter search function in our implementation, the training process was even longer, taking about 10 minutes in a Linux x86_64 server with 15-core Intel(R) Xeon(R) CPU E5-2699 v4 @ 2.20 GHz processors. However, we are keen in continuing exploring SVM in the future, given that this time the classifier was used in

the multi-class classification use case, for system setups with widely varied topological configuration settings. Hence, we still consider relevant the study of the multiple relevant features in an optical network concerning the power dynamics, to decrease the computational time required for SVM.

5.4 On the use of other supervised-learning algorithms

This time, we analyse the performance of various classification algorithms when considering both topological features (e.g., number of nodes, fibre distance, amplifier span, etc.) and also the WL, similarly to what we did in the previous section. With regard to the comparison of the ML models, two crucial metrics are considered: the accuracy at classifying different classes of traffic (based on OSNR levels), and the computational time required to train (build) the models, together with the size of the data samples. For the execution of the experiments, we also used the Scikit-learn: Machine Learning in Python tool [242].

5.4.1 Classification algorithms and optimisation techniques

This section describes the classification algorithms analysed in this study, where only supervised learning-based algorithms were used. We have reviewed 11 algorithms, which we have split in two classes: normal and ensemble-based. The normal class is composed by K-Nearest Neighbour (KNN), Linear-Support Vector Machine (L-SVM), Radial Basis Function SVM (RBF-SVM), Logistic Regression (LR), Decision Tree (DT), Artificial Neural Network (ANN), Naive Bayes (NB), and Linear Discriminant Analysis (LDA). The ensemble-based class is composed by Random Forest (RF), AdaBoost, and Bagging. We briefly describe the main components of each algorithm and their functionality, for details of the models we redirect to the documentation.

Furthermore, we wish to understand the scalability performance of the ML classifiers. For this we used six sets of independent data samples of different size, following the data generation process described in section 5.2.4. In total, we generated 294,343 data samples, which we split as 22.7 K, 42.3 K, 45 K, 51 K, 57.7 K, 75.6 K, for the six sets, respectively. Also, we balanced the input data in order to mitigate misperformance of the classifiers.

Normal Classifiers

Normal classifiers consist in a group of well-known algorithms that are vastly used in the area of ML. These act as individual processes, as opposed to optimisation strategies (ensemble algorithms) which will be explained later in this section. The implementation of normal classifiers varies according to the specific application needs. However, it is possible to generalise their individual performance and compare them by looking at their time complexity. Following, we list the classifiers as:

K-Nearest Neighbours

This algorithm attempts to classify values in multiple classes by clustering the data and comparing individual values to their K number of immediate neighbours.

Time complexity: $O(kn^2)$, for k-nearest-neighbours.

Linear-Support Vector Machine

This algorithm attempts to learn from the input data by categorising and building different classes (*hyperplanes*), which are subsequently used for future classification. It relies on regularisation parameters C and gamma to avoid misclassification and correlation of individual points, respectively. It also transforms the problem with linear algebra - kernel functions.

Time complexity: $O(n_{features}n^2_{samples})$, with linear kernel function.

Radial Basis Function SVM

Same as before.

Time complexity: $O(n_{features}n^2_{samples})$, with radial basis kernel function.

Logistic Regression

This algorithm utilises a logistic function to build a model of dependent variables, more commonly used for binary scenarios. However, by applying optimisation algorithms it is possible to use logistic regression for classifying multiple classes. Our implementation considers the Limited-memory Broyden-Fletcher-Goldfarb-Shanno (L-BFGS) optimisation algorithm.

Time complexity: $O(n^2)$, with L-BGFS.

Decision Tree

This algorithm consists in identifying relations between the input parameters and their output values building comparison points (tree branches), to subsequently perform as a binary tree.

Time complexity: $O(n_{features}n_{samples}log(n_{samples}))$.

Artificial Neural Networks

This algorithm is based on a multi-layer perceptron, which learns correlations between inputs and outputs and generates 'weights' for future inputs that are used for minimising the error of classification.

Time complexity: $O(nmh^koi)$, for n training samples, m features, h neurons per layer, k hidden layers, o output neurons, and i number of iterations.

Naive Bayes

This algorithm considers the assumption of conditional independence between the multiple features given the values of the various classes. Our implementation of this algorithm considered the likelihood of the sample features to be Gaussian.

Time complexity: $O(nK)$, for K number of classes.

Linear Discriminant Analysis

This algorithm operates by finding linear correlations of the input features.

Time complexity: $O(n^2_{features} n_{samples})$.

Ensemble Classifiers

These types of classifiers are the result of the combination of various classifiers altogether. These can be understood as optimisation techniques for algorithms that do not perform well for given use cases, such as overfitting the data or performing weakly due to the lack of data. For the purposes of this study, we reviewed the ensemble classifiers of Random Forests, Boosting and Bagging. The time complexity of these methods is directly related to the classifiers being considered for the ensemble composition.

Random Forest

This ensemble learning method for classification consists in the combination of multiple decision trees at training time, and operates the classification of various classes by selecting the classification/prediction mode among the decision trees.

Ada Boost

This algorithm, adaptive boosting (AdaBoost), operates by combining multiple “weak" classifiers in order to create a much stronger/accurate tool.

Bagging

This algorithm, bootstrap aggregation (bagging), operates by bootstrapping (random sampling with replacement) multiple models in parallel, and come up with hypothesis of more accurate classifications, making a decision based on the most accurate hypothesis.

5.4.2 Experiments and results

In order to speed up the execution time, our experiments were run on a Linux x86_64 server with 10 Intel(R) Xeon(R) CPU E5-2699 v4 @ 2.20 GHz processors. For instance, it enables the declaration of multiple parameters for training the models. Additionally, it enables a dynamic search of the best possible parameters to train specific models for given use cases with the *GridSearchCV* function. Thus, after a wide search of such parameters for our use case, we found those that enhanced a mean tolerable prediction accuracy among the various classifiers, which are depicted in Table 5.2.

The visual representation of the results of the normal classifiers are presented in Figures 5.6a and 5.6b, showing the training computational time and the F1-score against the multiple sample sizes, respectively. We can demonstrate the trade-off between high classification accuracy and high training computational time, which is a well-known feature among these type of classifiers.

Table 5.2: Parameters used for training the algorithms.

Algorithm	Model Parameters
K-Nearest Neighbours	K:1
Linear SVM	kernel:linear, gamma:100, C:0.0001
RBF SVM	kernel:rbf, gamma:100, C:0.0001
Logistic Regression	solver:lbfgs, multiclass:multinomial, random_state:1
Decision Tree	max depth:5
Artificial Neural Network	alpha:1, max iter:10000
Naive Bayes	default
Random Forest	max depth:5, estimators no.:10, max features:1
AdaBoost	estimators no.:10
Bagging	estimators no.:100, max samples:0.8, max features:0.8

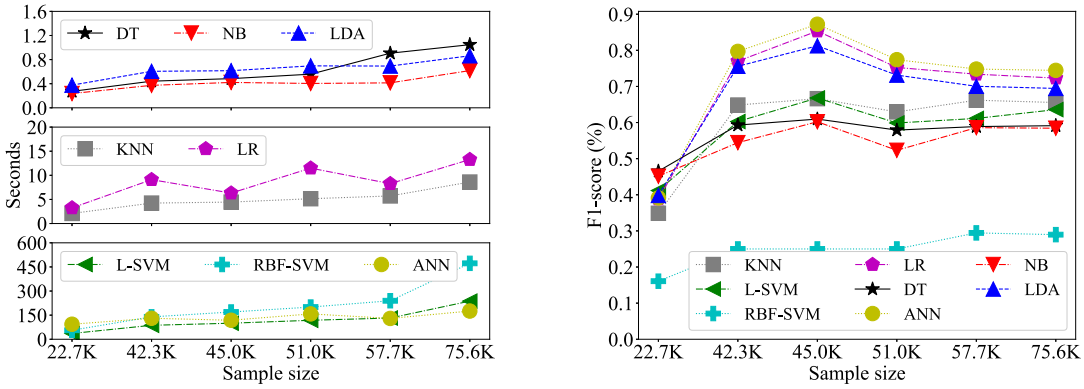

(a) (b)

Figure 5.6: (a) Training time of each classifier. (b) F1-score of each classifier.

However, the novelty of this analysis focuses on the ability for these statistical tools to learn from our selected optical domain features (i.e., active WL) and the topological configurations (i.e., number of nodes and fiber spans) together. Taken these under consideration, the comparison shows that some algorithms perform better than the others, in some cases achieving up to 90% F1-score. While in the literature we can find similar results achieving higher prediction accuracy [203], [201], [196], our analysis considers EDFA power excursions and nonlinearities (i.e., Stimulated Raman Scattering (SRS)) that introduce power dynamics that are harder to predict. Thus, we believe the results can be further improved in the future by better depicting the physical layer parameters for training the algorithms.

In addition, there are two main patterns we can identify in Figure 5.6a. *i)* Contrary to an expected passive incremental accuracy performance as the volume of the sample size increases, our results show a decreased performance in the classifiers that can achieve the highest accuracy after 45,000 samples, and an increased/convergent performance in the classifiers that achieve a higher accuracy up to 70%. *ii)* In the figure, we can also perceive a group-like behaviour among some of the classifiers. Neglecting the RBF-SVM model (due to its deficient performance), we can see two groups, one consisting of the classifiers KNN, L-SVM, DT and NB; and the second with LR, ANN and LDA. While the F1-score achieved by the former does not go higher than 70% in our experiments, the latter group show an F1-score performance of almost 90%. By our last sample data (75.6K), all

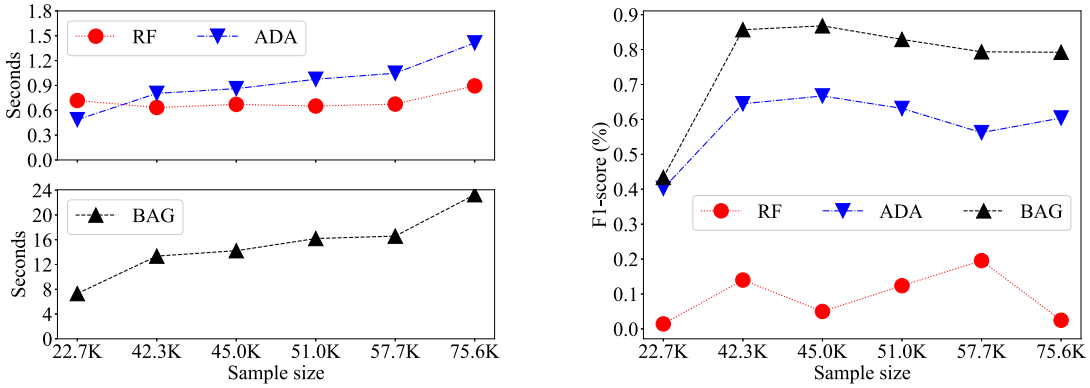

(a) (b)

Figure 5.7: (a) Training time of each ensemble classifier. (b) F1-score of each ensemble classifier.

of the classifiers seem to begin convergence. Intrinsically, each of these are mathematically-defined in different forms, however, we require further exploration that could justify a correlation with the manipulation of the input data to each of them and their performance when attempting to predict unestablished lightpaths as in our use case.

The performance of the ensemble classifiers are depicted in Figure 5.7a and 5.7b. As for the normal classifiers, we can also see a trade-off between training computational time and the classification performance. While the results from the AdaBoost and the Bagging models were expected, the low performance of the Random Forest algorithm was not such. However, these results claim to be implementation-dependent, and due to the reasonable performance of the Decision Tree classifier in the previous analysis, we would further explore the implementation of Random Forest. We have summarised these results in Table 5.4.

	KNN		**L-SVM**		**RBF-SVM**		**LR**	
***SS**	***F1-S (%)***	***TT***	***F1-S (%)***	***TT***	***F1-S (%)***	***TT***	***F1-S (%)***	***TT***
22,723	0.34	2.09s	0.41	36.03s	0.16	56.05s	0.38	3.24s
42,320	0.64	4.24s	0.6	1.44m	0.25	2.32m	0.76	9.1s
44,952	0.66	4.45s	0.66	1.66m	0.25	2.82m	0.85	6.31s
50,984	0.62	5.14s	0.59	1.96m	0.25	3.33m	0.75	11.49s
57,740	0.66	5.72s	0.61	2.20m	0.29	3.99m	0.73	8.26s
75,624	0.65	8.6s	0.63	3.95m	0.29	7.87m	0.72	13.27s

	DT		**ANN**		**NB**		**LDA**	
***SS**	***F1-S (%)***	***TT***	***F1-S (%)***	***TT***	***F1-S (%)***	***TT***	***F1-S (%)***	***TT***
22,723	0.46	0.27s	0.39	1.55m	0.45	0.23s	0.39	0.37s
42,320	0.59	0.44s	0.79	2.17m	0.54	0.37s	0.75	0.60s
44,952	0.6	0.48s	0.87	1.97m	0.6	0.42s	0.81	0.61s
50,984	0.57	0.55s	0.77	2.62m	0.52	0.40s	0.73	0.69s
57,740	0.58	0.90s	0.74	2.16m	0.58	0.41s	0.7	0.69s
75,624	0.59	1.04s	0.74	2.92m	0.58	0.61s	0.69	0.86s

Table 5.3: Results of the F1-score and training computation time for each classifier against the sample sizes. **Note: SS: sample size; F1-S: F1-score; TT: training time.*

5.5 Summary

We have analysed the feasibility of supervised-learning algorithms to assist QoT-E modules as part of optical control systems. We presented a study focusing on the SVM algorithm where we addressed its definition, weaknesses and strengths, as well as a performance analysis of its capabilities for handling static and dynamic optical domain data. In addition, we presented another study where we analysed the performance of multiple supervised-learning algorithms handling the same data as with the previous study. In that work, we presented each algorithm with their implementation time complexity and examples of configurations.

In the work related to the usage of the SVM algorithm. We have studied the potential of deploying QoT-E tools with a multi-class SVM classifier to assist the routing and wavelength assignment module of future optical control systems, in order to improve the management of network resources. Our experiments demonstrated high performance accuracy when using information of the active wavelength channels in a network to train the classifier. Concretely, our algorithm performed with an overall accuracy of 96.2% for the multi-class classification use case. Interestingly, the assessment considered dynamic data in the form of the active WL, and we combined different features to create significant inputs to the classifier. We have also given an insight to the potential of this type of learning model to be trained and tested for systems consisting in different topological configurations, overcoming the limitations of system dependent models. Nonetheless, our system still required a number of data samples above 30 thousand, which poses implementation challenges in a physical testbed. Because of that, our future work will concentrate in reducing the number of data samples by analysing the potential of other optical network features, which would enhance the reduction of data samples.

In the work related to the performance analysis of multiple ML algorithms, we assessed each algorithm to compute the prediction of OSNR levels of newly established lightpaths in optical networks with different configuration settings and dimensions. We have found that a group of the investigated algorithms was capable of performing with an F1-score of almost 90%. This group was conformed by the Logistic Regression (LR), ANN and LDA. However, we have also identified a group conformed by the KNN, L-SVM, DT and NB, which did not achieve an acceptable performance, with an overall accuracy not higher than 70%.

Our results suggest that the implementation of such algorithms to complement the decision-making processes of control systems is promising, but requires further analysis of the physical layer features in the optical domain. This is mainly due to the incapacity for the learning models reviewed to handle the unexpected behaviours and nonlinearities encountered in optical network systems. Finer tuning of the performance parameters is also required.

Furthermore, we have found an interesting behavioural correlation between some of the classifiers that we will further explore in the future. Also, while in our implementation none of the classifiers achieved a F1-score performance above 90%, we believe that through finer tuning and with the implementation of more complex techniques, such as deep-/reinforcement-/transfer-learning, we could achieve better performance and find a better suitability for the metro-access transport networks scenario.

6 Conclusions and Future Directions

6.1 General conclusions

In this thesis, we have introduced a novel software system, Mininet-Optical, that enhances the development, testing and prototyping of control plane procedures (e.g., algorithms and systems) in optical disaggregated networks. We have explained the software architecture of the system and the algorithms that enable the simulation of Optical Line Systems (OLSs) performance. For the latter, we have described the mathematical models that describe the multiple physical effects occurring in an optical transmission, complying with state-of-the-art OLS equipment, and, we have shown the validation procedures against both analytical models and testbeds, showing that Mininet-Optical performs comparably to those systems. Mininet-Optical is the first tool that enables real optical control plane assessment in a virtual environment. As a consequence, we expect that the system will play an important role in the next years of the evolution of disaggregated optical networks. Throughout this thesis, we have used Mininet-Optical to model the network systems that we used to assess our optical control plane research.

We focused primarily on the study and development of intelligent Quality of Transmission Estimation (QoT-E) systems as integrated systems of the optical control plane. Thus, we have demonstrated the effectiveness of different techniques to develop these tools. Firstly, we developed a QoT-E system based on well-known analytical models of the physical effects occurring in optical networks, and studied the impact on QoT-E for lightpath installation due to the component-dependent performance (e.g., wavelength-dependent gain of EDFAs). We have shown that lightpath provisioning procedures assisted with QoT-E can help reduce the application of OSNR margins. In addition, we have shown that the inaccurate estimation of these transmission margins can constrain the network capacity utilisation. In particular, we have shown that when we follow a conservative margin strategy (pessimistic strategy), the installation of lightpaths get compromised, reducing lightpath utilisation. On the other hand, an aggressive margin strategy (optimistic strategy) can result in the over-provisioning of resources that are not suitable for transmission, resulting in a misuse of network resources. In our studies, we have found that even at the optimum with QoT-E-assisted control planes, the loss of capacity due to the use of transmission margins, with respect to the maximum capacity, could still be of the order of 5 - 17%.

Moreover, we have also demonstrated the performance of three Generalized Optical Signal to Noise Ratio (gOSNR) QoT-E strategies relying on active monitoring to optimise prediction accuracy, integrated within a real optical control system evaluated with Mininet-Optical. The first strategy relied on using Optical Signal to Noise Ratio (OSNR) monitors to examine the power and Amplified Spontaneous Emission (ASE) noise levels to adjust the QoT-E estimations; the second strategy relied

on OSNR monitors also, but this time we made use of the power level monitored data to compute a more accurate approximation of the Nonlinear Interference (NLI) noise; and the third strategy relied on reference receivers capable of recovering gOSNR estimates. Then, we have examined the impact of placing the different monitoring nodes at different locations of an optical link. In fact, we have shown that by placing either type of OPM node at periodic locations of an optical link we can reduce QoT-E errors by 0.3 - 2.0 dB. However, we have concluded that OSNR monitors provide limited information for correct estimation of QoT.

In addition to our analytical modelling-based QoT-E systems, we have also shown performance evaluations of Machine-Learning (ML) algorithms to predict Quality of Transmission (QoT). We have used Mininet-Optical to generate large amounts of synthetic data that was used to train and test multiple algorithms. First, we have shown that combining basic physical layer information, such as the number of nodes in a link, with the wavelength or frequency description of the active channels in a point-to-point connection, it is possible to achieve gOSNR estimation accuracy of 96.2% with a Support Vector Machine (SVM) algorithm. Then, we have also shown a performance evaluation of other ML algorithms when handling physical layer information of optical networks, and presented an analysis of the suitability of these to be implemented in optical control planes. We evaluated the algorithms: K-NN, L-SVM, RBF-SVM, Logistic Regression, Decision Trees, Artificial Neural Network (ANN), Naive Bayes, Linear Discriminant Analysis, Random Forest, Ada-Boost and Bagging techniques. In our studies, we have found that as these algorithms require large amounts of data, their development and deployment is constrained to testbeds capable of collecting the data. Although, if it is possible to collect large amounts of data from an OLS, these systems can outperform analytical models. Moreover, we have concluded that due to the fast times of model development, algorithms like Decision Trees, Naive Bayes, Logistic Regression and K-NN could be of use if implemented appropriately.

We conclude that the optical control plane can indeed take advantage of analytical and cognition-based modelling systems of the physical layer, in order to improve the management of network resources through better fault management solutions and dynamic lightpath provisioning. Additionally, the inclusion of monitoring capabilities at intermediate locations of an optical link is being proven to enhance the performance of QoT-E systems, thus it should be of interest the development of monitoring systems within disaggregated optical components. Nonetheless, there are still many open challenges and discussions.

6.1.1 Continuation of studies

Mininet-Optical is becoming an open-source project that continues to grow. Accordingly, we will continue to develop features that enhance the development, testing and prototyping of optical control plane procedures. For instance, we will develop compatible Southbound Interface (SBI) interfaces with state-of-the-art models such as OpenROADM, T-API and NETCONF. In addition, we want to study the integration of other virtualised networking functions in our control plane, such as multi-layer (e.g., electronic and optical) dynamic switching. From an internal system (software) composition, we will enable the modularisation of optical network components, to enable performance tests of different internal node compositions (i.e., defining multiple ROADM models). Consequently, Mininet-Optical could be used as a sandbox to create virtual twins of real testbeds, enhancing the evaluation of control plane tests. Moreover, we want to further integrate our system

with popular SDN controller frameworks such as Open Network Operating System (ONOS). And lastly, we also want to continue to validate Mininet-Optical against additional hardware systems.

Furthermore, we will continue to investigate the development of QoT-E systems assisted with both active monitoring capabilities and ML algorithms. For the former, we want to better understand the real economical implications for enabling active monitoring of optical transmissions in the context of disaggregated optical networks, and also further investigate what information is more relevant to monitor in order to improve QoT-E performance. For the latter, we want to investigate sophisticated ML methods such as transfer and reinforcement learning to combine Mininet-Optical data with physical data, to enhance our QoT-E algorithms.

6.2 Future directions

Moving forward, it is necessary to continue to validate and develop communication protocols enabling SBI connections between the optical Software-Defined Networking (SDN) control plane and white-box optical equipment. That is, further validation of the models OpenFlow, OpenROADM, OpenConfig, T-API, Transponder Abstraction Interface (TAI). Moreover, while ONOS has been widely accepted as the standard Network Operating System (NOS) system due to its closeness to the Optical Network Foundation (ONF), the integration of optical disaggregated equipment with other systems such as OpenDayLight will need to be further evaluated.

Also, the development of cognition-assisted QoT-E systems is an area of research that requires further investigation looking at the integration of these within the optical control plane. This also needs to be evaluated in the context of central offices re-architected as a data centre, considering the convergence of networking layers.

Bibliography

[1] Cisco-Visual-Networking, "White paper: Forecast and methodology 2016-2021," *San Jose, CA, USA*, 2016.

[2] TIP, "GNPy Project." [Online]. Available: https://github.com/Telecominfraproject/gnpy

[3] M. Ruiz, O. Pedrola, L. Velasco, D. Careglio, J. Fernández-Palacios, and G. Junyent, "Survivable IP/MPLS-over-WSON multilayer network optimization," *Journal of Optical Communications and Networking*, vol. 3, no. 8, pp. 629–640, 2011.

[4] NGMNAlliance, "5G White Paper, February 2015," *URL https://www. ngmn. org/uploads/media/NGMN_ 5G_ White_ Paper_ V1_ 0. pdf*, 2017.

[5] L. Peterson, A. Al-Shabibi, T. Anshutz, S. Baker, A. Bavier, S. Das, J. Hart, G. Palukar, and W. Snow, "Central office re-architected as a data center," *IEEE Communications Magazine*, vol. 54, no. 10, pp. 96–101, 2016.

[6] "Open Networking Foundation (ONF)," https://www.opennetworking.org/.

[7] "CORD (Central Office Re-architected as a Datacenter)," https://opennetworking.org/cord/.

[8] IHS, "Routing, nfv & packet-optical strategies service provider survey - 2017," 2017.

[9] M. Ruffini and D. C. Kilper, "From Central Office Cloudification to Optical Network Disaggregation," in *2018 IEEE Photonics Society Summer Topical Meeting Series (SUM)*, 2018, pp. 153–154.

[10] M. Ruffini and F. Slyne, "Moving the Network to the Cloud: The Cloud Central Office Revolution and Its Implications for the Optical Layer," *Journal of Lightwave Technology*, vol. 37, no. 7, pp. 1706–1716, 2019.

[11] E. Riccardi, P. Gunning, O. G. de Dios, M. Quagliotti, V. Lopez, and A. Lord, "An Operator view on the Introduction of White Boxes into Optical Networks," *Journal of Lightwave Technology*, vol. 36, no. 15, pp. 3062–3072, 2018.

[12] "Optical Networking and Communication Market," https://www.psmarketresearch.com/market-analysis/-optical-networking-and-communication-market.

[13] "Telecom Infra Project (TIP)," https://telecominfraproject.com/.

[14] V. Lopez, O. G. de Dios, and J. P. Fernandez-Palacios, "Whitebox Flavors in Carrier Networks," in *2019 Optical Fiber Communications Conference and Exhibition (OFC)*, 2019, pp. 1–3.

[15] B. Gartner, "Cisco to Drive Disaggregation Across Optical Vendor Ecosystem as Part of the Telecom Infra Project Phoenix Initiative," February 2021. [Online]. Available: https://blogs.cisco.com/news/cisco-to-drive-disaggregation-across-optical-vendor-ecosystem-as-part-of-the-telecom-infra-\project-phoenix-initiative

[16] S. Dianto, "Fujitsu Joins Tier 1 Operators and the Telecom Infra Project to Advance 400G Transponder Disaggregation," February 2021. [Online]. Available: https://www.fujitsu.com/us/about/resources/news/press-releases/2021/fnc20210202.html

[17] "TIP-OOPT," https://telecominfraproject.com/oopt/.

[18] N. McKeown, T. Anderson, H. Balakrishnan, G. Parulkar, L. Peterson, J. Rexford, S. Shenker, and J. Turner, "OpenFlow: Enabling Innovation in Campus Networks," vol. 38, no. 2, 2008. [Online]. Available: https://doi.org/10.1145/1355734.1355746

[19] "OpenROADM," http://www.openroadm.org/home.html.

[20] "OpenConfig," http://www.openconfig.net/.

[21] "T-API," https://github.com/OpenNetworkingFoundation/TAPI.

[22] "Transponder Abstraction Interface," https://github.com/Telecominfraproject/oopt-tai.

[23] "Ryu Controller," https://osrg.github.io/ryu/.

[24] "OpenDayLight," https://www.opendaylight.org/.

[25] "Open Network Operating Systems," https://onosproject.org/.

[26] R. Munõz, R. Vilalta, R. Casellas, R. Martínez, F. Francois, M. Channegowda, A. Hammad, S. Peng, R. Nejabati, D. Simeonidou, N. Yoshikane, T. Tsuritani, V. López, and A. Autenrieth, "Experimental assessment of ABNO-based network orchestration of end-to-end multi-layer (OPS/OCS) provisioning across SDN/OpenFlow and GMPLS/PCE control domains," in *2014 The European Conference on Optical Communication (ECOC)*, 2014, pp. 1–3.

[27] A. Aguado, V. López, J. Marhuenda, O. González de Dios, and J. P. Fernández-Palacios, "ABNO: A feasible SDN approach for multi-vendor IP and optical networks," in *OFC 2014*, 2014, pp. 1–3.

[28] T. Das, V. Sridharan, and M. Gurusamy, "A Survey on Controller Placement in SDN," *IEEE Communications Surveys Tutorials*, vol. 22, no. 1, pp. 472–503, 2020.

[29] A. Mayoral, V. López, M. López-Bravo, D. García-Montes, O. Gonzalez-de-Dios, A. Aguado, R. Szwedowski, K. Mrówka, F. Marques, Z. Stevkovski, D. Verchere, Q. Pham-Van, L. Tancevski, and J. . Fernandez-Palacios, "Multi-Layer Service Provisioning Over Resilient Software-Defined Partially Disaggregated Networks," *Journal of Lightwave Technology*, vol. 38, no. 2, pp. 546–552, 2020.

[30] N. Sambo, "Locally automated restoration in SDN disaggregated networks," *IEEE/OSA Journal of Optical Communications and Networking*, vol. 12, no. 6, pp. C23–C30, 2020.

[31] M. Filer, J. Gaudette, M. Ghobadi, R. Mahajan, T. Issenhuth, B. Klinkers, and J. Cox, "Elastic optical networking in the Microsoft cloud," *IEEE/OSA Journal of Optical Communications and Networking*, vol. 8, no. 7, pp. A45–A54, 2016.

[32] D. W. Boertjes, M. Reimer, and D. Cote, "Practical considerations for near-zero margin network design and deployment [invited]," *J. Opt. Commun. Netw.*, vol. 11, no. 9, pp. C25–C34, Sep 2019.

[33] D. Azzimonti, C. Rottondi, and M. Tornatore, "Reducing probes for quality of transmission estimation in optical networks with active learning," *IEEE/OSA Journal of Optical Communications and Networking*, vol. 12, no. 1, pp. A38–A48, 2020.

[34] M. Klinkowski, P. Ksieniewicz, M. Jaworski, G. Zalewski, and K. Walkowiak, "Machine Learning Assisted Optimization of Dynamic Crosstalk-Aware Spectrally-Spatially Flexible Optical Networks," *Journal of Lightwave Technology*, vol. 38, no. 7, pp. 1625–1635, 2020.

[35] Z. Gao, S. Yan, J. Zhang, M. Mascarenhas, R. Nejabati, Y. Ji, and D. Simeonidou, "ANN-Based Multi-Channel QoT-Prediction Over a 563.4-km Field-Trial Testbed," *Journal of Lightwave Technology*, vol. 38, no. 9, pp. 2646–2655, 2020.

[36] A. D'Amico, S. Straullu, A. Nespola, I. Khan, E. London, E. Virgillito, S. Piciaccia, A. Tanzi, G. Galimberti, and V. Curri, "Using machine learning in an open optical line system controller," *IEEE/OSA Journal of Optical Communications and Networking*, vol. 12, no. 6, pp. C1–C11, 2020.

[37] A. Mahajan, K. Christodoulopoulos, R. Martínez, S. Spadaro, and R. Munõz, "Modeling EDFA Gain Ripple and Filter Penalties With Machine Learning for Accurate QoT Estimation," *Journal of Lightwave Technology*, vol. 38, no. 9, pp. 2616–2629, 2020.

[38] S. Aladin, A. V. S. Tran, S. Allogba, and C. Tremblay, "Quality of Transmission Estimation and Short-Term Performance Forecast of Lightpaths," *Journal of Lightwave Technology*, vol. 38, no. 10, pp. 2807–2814, 2020.

[39] Y. Zhou, Q. Sun, and S. Lin, "Link State Aware Dynamic Routing and Spectrum Allocation Strategy in Elastic Optical Networks," *IEEE Access*, vol. 8, pp. 45 071–45 083, 2020.

[40] T. Panayiotou, G. Savva, I. Tomkos, and G. Ellinas, "Decentralizing machine-learning-based QoT estimation for sliceable optical networks," *IEEE/OSA Journal of Optical Communications and Networking*, vol. 12, no. 7, pp. 146–162, 2020.

[41] L. R. R. D. Santos and T. AbrÃ£o, "Heuristic Chaotic Hurricane-Aided Efficient Power Assignment for Elastic Optical Network," *IEEE Access*, vol. 8, pp. 83 359–83 374, 2020.

[42] R. Di Marino, C. Rottondi, A. Giusti, and A. Bianco, "Assessment of Domain Adaptation Approaches for QoT Estimation in Optical Networks," in *2020 Optical Fiber Communications Conference and Exhibition (OFC)*, 2020, pp. 1–3.

[43] C. Liu, X. Chen, R. Proietti, and S. J. Ben Yoo, "Evol-TL: Evolutionary Transfer Learning for QoT Estimation in Multi-Domain Networks," in *2020 Optical Fiber Communications Conference and Exhibition (OFC)*, 2020, pp. 1–3.

[44] Q. Fan, J. Lu, G. Zhou, D. Zeng, C. Guo, L. Lu, J. Li, C. Xie, C. Lu, F. N. Khan, and A. P. T. Lau, "Experimental Comparisons between Machine Learning and Analytical Models for QoT Estimations in WDM Systems," in *2020 Optical Fiber Communications Conference and Exhibition (OFC)*, 2020, pp. 1–3.

[45] J. Pesic, M. Lonardi, N. Rossi, T. Zami, E. Seve, and Y. Pointurier, "How Uncertainty on the Fiber Span Lengths Influences QoT Estimation using Machine Learning in WDM Networks," in *2020 Optical Fiber Communications Conference and Exhibition (OFC)*, 2020, pp. 1–3.

[46] D. Azzimonti, C. Rottondi, A. Giusti, M. Tornatore, and A. Bianco, "Active vs Transfer Learning Approaches for QoT Estimation with Small Training Datasets," in *2020 Optical Fiber Communications Conference and Exhibition (OFC)*, 2020, pp. 1–3.

[47] E. Seve, J. Pesic, and Y. Pointurier, "Accurate QoT Estimation by Means of a Reduction of EDFA Characteristics Uncertainties with Machine Learning," in *2020 International Conference on Optical Network Design and Modeling (ONDM)*, 2020, pp. 1–3.

[48] A. Mahajan, K. Christodoulopoulos, R. Martinez, S. Spadaro, and R. Munoz, "Improving QoT Estimation Accuracy with DGE Monitoring using Machine Learning," in *2020 International Conference on Optical Network Design and Modeling (ONDM)*, 2020, pp. 1–6.

[49] A. D'Amico, E. London, E. Virgillito, A. Napoli, and V. Curri, "Quality of Transmission Estimation for Planning of Disaggregated Optical Networks," in *2020 International Conference on Optical Network Design and Modeling (ONDM)*, 2020, pp. 1–3.

[50] E. Virgillito, S. Straullu, A. Castoldi, R. Pastorelli, and V. Curri, "Non-Linear SNR Degradation of Mixed 10G/100G Transmission Over Dispersion-Managed Networks," in *2020 22nd International Conference on Transparent Optical Networks (ICTON)*, 2020, pp. 1–4.

[51] I. Khan, M. Bilal, M. Siddiqui, M. Khan, A. Ahmad, M. Shahzad, and V. Curri, "QoT Estimation for Light-path Provisioning in Un-Seen Optical Networks using Machine Learning," in *2020 22nd International Conference on Transparent Optical Networks (ICTON)*, 2020, pp. 1–4.

[52] I. Khan, M. Bilal, and V. Curri, "Advanced Formulation of QoT-Estimation for Un-established Lightpaths Using Cross-train Machine Learning Methods," in *2020 22nd International Conference on Transparent Optical Networks (ICTON)*, 2020, pp. 1–4.

[53] R. Ayassi, A. Triki, M. Laye, N. Crespi, R. Minerva, and C. Catanese, "An Overview on Machine Learning-Based Solutions to Improve Lightpath QoT Estimation," in *2020 22nd International Conference on Transparent Optical Networks (ICTON)*, 2020, pp. 1–4.

[54] R. M. Morais and B. Pereira, "Machine Learning in Optical Communication Systems and Networks," in *2020 IEEE Workshop on Signal Processing Systems (SiPS)*, 2020, pp. 1–1.

[55] A. Triki, E. L. Rouzic, O. Renais, G. Lambert, G. Thouenon, C. Betoule, E. Delfour, S. Vachhani, and B. Bathula, "Open-Source QoT Estimation for Impairment-Aware Path Computation in OpenROADM Compliant Network," in *2020 European Conference on Optical Communications (ECOC)*, 2020, pp. 1–3.

[56] J. Pesic, M. Lonardi, E. Seve, N. Rossi, and T. Zami, "Transfer Learning from Unbiased Training Data Sets for QoT Estimation in WDM Networks," in *2020 European Conference on Optical Communications (ECOC)*, 2020, pp. 1–4.

[57] D. E. Comer, *Automated network management systems.* Pearson India, 2006.

[58] N. Fujimoto, T. Ishihara, A. Taniguchi, H. Yamashita, and K. Yamaguchi, "Experimental broadband drop/insert/cross-connect system: 1.8 Gbit/s optical shuttle bus," in *IEEE Global Telecommunications Conference and Exhibition. Communications for the Information Age*, 1988, pp. 954–959 vol.2.

[59] "Mininet," http://mininet.org/.

[60] B. Lantz, B. Heller, and N. McKeown, "A network in a laptop: rapid prototyping for software-defined networks," in *Proceedings of the 9th ACM SIGCOMM Workshop on Hot Topics in Networks*, 2010, pp. 1–6.

[61] "ACM SIGCOMM Test of Time Paper Award," https://www.sigcomm.org/awards/test-of-time-paper-award.

[62] M. Ruffini, "Multidimensional Convergence in Future 5G Networks," *J. Lightwave Technol.*, vol. 35, no. 3, pp. 535–549, Feb 2017. [Online]. Available: http://jlt.osa.org/abstract.cfm?URI=jlt-35-3-535

[63] R. Hui, "Chapter 10 - Modulation formats for optical communications," in *Introduction to Fiber-Optic Communications*, R. Hui, Ed. Academic Press, 2020, pp. 439 – 495. [Online]. Available: http://www.sciencedirect.com/science/article/pii/B978012805345400010X

[64] M. Angelou, Y. Pointurier, D. Careglio, S. Spadaro, and I. Tomkos, "Optimized Monitor Placement for Accurate QoT Assessment in Core Optical Networks," *IEEE/OSA Journal of Optical Communications and Networking*, vol. 4, no. 1, pp. 15–24, 2012.

[65] J. Mata, I. de Miguel, R. J. Durán, N. Merayo, S. K. Singh, A. Jukan, and M. Chamania, "Artificial intelligence (AI) methods in optical networks: A comprehensive survey," *Optical Switching and Networking*, vol. 28, pp. 43 – 57, 2018. [Online]. Available: http://www.sciencedirect.com/science/article/pii/S157342771730231X

[66] F. Musumeci, C. Rottondi, A. Nag, I. Macaluso, D. Zibar, M. Ruffini, and M. Tornatore, "An Overview on Application of Machine Learning Techniques in Optical Networks," *IEEE Communications Surveys Tutorials*, vol. 21, no. 2, pp. 1383–1408, 2019.

[67] J. Xie, F. R. Yu, T. Huang, R. Xie, J. Liu, C. Wang, and Y. Liu, "A Survey of Machine Learning Techniques Applied to Software Defined Networking (SDN): Research Issues and Challenges," *IEEE Communications Surveys Tutorials*, vol. 21, no. 1, pp. 393–430, 2019.

[68] T. Tanimura, "Machine Learning Techniques in Optical Physical-Layer Monitoring," in *2018 IEEE Photonics Society Summer Topical Meeting Series (SUM)*, 2018, pp. 55–56.

[69] W. S. Saif, M. A. Esmail, A. M. Ragheb, T. A. Alshawi, and S. A. Alshebeili, "Machine Learning Techniques for Optical Performance Monitoring and Modulation Format Identification: A Survey," *IEEE Communications Surveys Tutorials*, vol. 22, no. 4, pp. 2839–2882, 2020.

[70] F. Musumeci, C. Rottondi, A. Nag, I. Macaluso, D. Zibar, M. Ruffini, and M. Tornatore, "A Survey on Application of Machine Learning Techniques in Optical Networks," *CoRR*, vol. abs/1803.07976, 2018. [Online]. Available: http://arxiv.org/abs/1803.07976

[71] Y. Lu and H. Gu, "Flexible and Scalable Optical Interconnects for Data Centers: Trends and Challenges," *IEEE Communications Magazine*, vol. 57, no. 10, pp. 27–33, 2019.

[72] P. Pavon-Marino and J.-L. Izquierdo-Zaragoza, "Net2plan: an open source network planning tool for bridging the gap between academia and industry," *IEEE Network*, vol. 29, no. 5, pp. 90–96, 2015.

[73] "ONF - ODTN," https://opennetworking.org/odtn.

[74] "Cloud Enhanced Open Software Defined Mobile Wireless Testbed for City-Scale Deployment, COSMOS," https://www.cosmos-lab.org. [Online]. Available: https://www.cosmos-lab.org

[75] Nokia-Communications, "Nokia finalizes its acquisition of Alcatel-Lucent, ready to seize global connectivity opportunities," November 2016. [Online]. Available: https://www.nokia.com/about-us/news/releases/2016/11/02/nokia-finalizes-its-acquisition-of-alcatel-lucent-ready-to-seize-global-connectivity-opportunities/

[76] D. Kreutz, F. M. V. Ramos, P. E. Veríssimo, C. E. Rothenberg, S. Azodolmolky, and S. Uhlig, "Software-Defined Networking: A Comprehensive Survey," *Proceedings of the IEEE*, vol. 103, no. 1, pp. 14–76, 2015.

[77] Y. Li and M. Chen, "Software-Defined Network Function Virtualization: A Survey," *IEEE Access*, vol. 3, pp. 2542–2553, 2015.

[78] A. S. Thyagaturu, A. Mercian, M. P. McGarry, M. Reisslein, and W. Kellerer, "Software defined optical networks (SDONs): A comprehensive survey," *IEEE Communications Surveys & Tutorials*, vol. 18, no. 4, pp. 2738–2786, 2016.

[79] "Software-Defined Networking Market," https://www.marketsandmarkets.com/Market-Reports/software-defined-networking-sdn-market-655.html.

[80] "Internet Engineering Task Force," https://www.ietf.org/.

[81] International Telecommunication Unit, "Architecture for SDN control of transport networks," https://www.itu.int/rec/T-REC-G.7702/en.

[82] "Optical Internetworking Forum," https://www.oiforum.com.

[83] "The Linux Foundation," https://www.linuxfoundation.org.

[84] "Open Compute Project (OCP)," https://www.opencompute.org.

[85] "ONF - Stratum," https://opennetworking.org/stratum.

[86] "ONF - Trellis," https://opennetworking.org/trellis.

[87] "ONF - NG-SDN," https://opennetworking.org/ng-sdn.

[88] "P4 Project," https://opennetworking.org/p4/.

[89] "ONF - XOS," https://opennetworking.org/xos.

[90] "ONF - OTCC," https://opennetworking.org/open-transport.

[91] "ONF - Information Modeling," https://opennetworking.org/open-information-model-tooling.

[92] N. Robinson, "Design and Deployment of Optical White Box," in *2018 Optical Fiber Communications Conference and Exposition (OFC)*, 2018, pp. 1–3.

[93] H. Schmidtke, I. Lyubomirsky, and B. Taylor, "Packet-optical integration and trend towards white boxes," in *2017 Optical Fiber Communications Conference and Exhibition (OFC)*, 2017, pp. 1–3.

[94] A. Sgambelluri, A. Giorgetti, D. Scano, F. Cugini, and F. Paolucci, "OpenConfig and OpenROADM Automation of Operational Modes in Disaggregated Optical Networks," *IEEE Access*, vol. 8, pp. 190 094–190 107, 2020.

[95] A. Sgambelluri, P. Velha, C. J. Oton, A. Giorgetti, A. D'Errico, S. Stracca, and F. Cugini, "OpenROADM-Controlled White Box Encompassing Silicon Photonics Integrated Reconfigurable Switch Matrix," in *2020 Optical Fiber Communications Conference and Exhibition (OFC)*, 2020, pp. 1–3.

[96] "G.707: Network node interface for the synchronous digital hierarchy (SDH)," https://www.itu.int/rec/T-REC-G.707-200701-I/en.

[97] "G.709: Interfaces for the optical transport network," https://www.itu.int/rec/T-REC-G.709/en.

[98] "Generalized Multi-Protocol Label Switching (GMPLS) Architecture," https://tools.ietf.org/html/rfc3945.

[99] S. Das, G. Parulkar, and N. McKeown, "Why OpenFlow/SDN can succeed where GMPLS failed," in *2012 38th European Conference and Exhibition on Optical Communications*, 2012, pp. 1–3.

[100] "Requirements Analysis for Transport OpenFlow/SDN," https://opennetworking.org/wp-content/uploads/2013/04/onf2014.227_Optical_Transport_Requirements.pdf.

[101] "Optical Transport Protocol Extensions," https://opennetworking.org/wp-content/uploads/2014/10/Optical_Transport_Protocol_Extensions_V1.0.pdf.

[102] "Network Configuration Protocol (NETCONF)," https://tools.ietf.org/html/rfc6241.

[103] F. Zhang, D. Li, H. Li, S. Belotti, and D. Ceccarelli, "Framework for GMPLS and PCE Control of G.709 Optical Transport Networks," https://tools.ietf.org/html/rfc7062, 2009.

[104] "Path Computation Element (PCE) Communication Protocol Generic Requirements," https://tools.ietf.org/html/rfc4657, 2006.

[105] D. King and A. Farrell, "RFC 7491: A PCE-based Architecture for Application-based Network Operations," https://tools.ietf.org/html/rfc7491, 2012.

[106] L. Gifre, F. Paolucci, L. Velasco, A. Aguado, F. Cugini, P. Castoldi, and V. López, "First Experimental Assessment of ABNO-Driven In-Operation Flexgrid Network Re-Optimization," *Journal of Lightwave Technology*, vol. 33, no. 3, pp. 618–624, 2015.

[107] Y. Yoshida, A. Maruta, K. Kitayama, M. Nishihara, T. Tanaka, T. Takahara, J. C. Rasmussen, N. Yoshikane, T. Tsuritani, I. Morita, S. Yan, Y. Shu, Y. Yan, R. Nejabati, G. Zervas, D. Simeonidou, R. Vilalta, R. Munõz, R. Casellas, R. Martínez, A. Aguado, V. López, and J. Marhuenda, "SDN-Based Network Orchestration of Variable-Capacity Optical Packet Switching Network Over Programmable Flexi-Grid Elastic Optical Path Network," *Journal of Lightwave Technology*, vol. 33, no. 3, pp. 609–617, 2015.

[108] A. Aguado, S. Peng, M. V. Alvarez, V. Lopez, T. Szyrkowiec, A. Autenrieth, R. Vilalta, R. Munõz, R. Casellas, R. Martínez, N. Yoshikane, T. Tsuritani, R. Nejabati, and D. Simeonidou, "Dynamic virtual network reconfiguration over SDN orchestrated multi-technology optical transport domains," in *2015 European Conference on Optical Communication (ECOC)*, 2015, pp. 1–3.

[109] L. Liu, D. Zhang, T. Tsuritani, R. Vilalta, R. Casellas, L. Hong, I. Morita, H. Guo, J. Wu, R. Martinez, and R. Munoz, "Field Trial of an OpenFlow-Based Unified Control Plane for Multilayer Multigranularity Optical Switching Networks," *Journal of Lightwave Technology*, vol. 31, no. 4, pp. 506–514, 2013.

[110] H. Y. Choi, L. Liu, T. Tsuritani, and I. Morita, "Demonstration of BER-Adaptive WSON Employing Flexible Transmitter/Receiver With an Extended OpenFlow-Based Control Plane," *IEEE Photonics Technology Letters*, vol. 25, no. 2, pp. 119–121, 2013.

[111] L. Liu, H. Y. Choi, R. Casellas, T. Tsuritani, I. Morita, R. Martínez, and R. Munõz, "Demonstration of a dynamic transparent optical network employing flexible transmitters/receivers controlled by an OpenFlow-stateless PCE integrated control plane [invited]," *IEEE/OSA Journal of Optical Communications and Networking*, vol. 5, no. 10, pp. A66–A75, 2013.

[112] A. Farrel, J.-P. Vasseur, and J. Ash, "A path computation element (PCE)-based architecture," 2006.

[113] R. Casellas, R. Martínez, R. Munõz, R. Vilalta, L. Liu, T. Tsuritani, and I. Morita, "Control and management of flexi-grid optical networks with an integrated stateful path computation element and OpenFlow controller [invited]," *IEEE/OSA Journal of Optical Communications and Networking*, vol. 5, no. 10, pp. A57–A65, 2013.

[114] R. Casellas, R. Munõz, R. Martínez, and R. Vilalta, "Applications and status of path computation elements [invited]," *IEEE/OSA Journal of Optical Communications and Networking*, vol. 5, no. 10, pp. A192–A203, 2013.

[115] R. Munõz, R. Casellas, R. Martínez, and R. Vilalta, "PCE: What is It, How Does It Work and What are Its Limitations?" *Journal of Lightwave Technology*, vol. 32, no. 4, pp. 528–543, 2014.

[116] N. Sambo, G. Meloni, F. Paolucci, F. Cugini, M. Secondini, F. Fresi, L. Potì, and P. Castoldi, "Programmable Transponder, Code and Differentiated Filter Configuration in Elastic Optical Networks," *Journal of Lightwave Technology*, vol. 32, no. 11, pp. 2079–2086, 2014.

[117] C. Chen, X. Chen, M. Zhang, S. Ma, Y. Shao, S. Li, M. S. Suleiman, and Z. Zhu, "Demonstrations of Efficient Online Spectrum Defragmentation in Software-Defined Elastic Optical Networks," *Journal of Lightwave Technology*, vol. 32, no. 24, pp. 4701–4711, 2014.

[118] Z. Zhu, C. Chen, X. Chen, S. Ma, L. Liu, X. Feng, and S. J. B. Yoo, "Demonstration of Cooperative Resource Allocation in an OpenFlow-Controlled Multidomain and Multinational SD-EON Testbed," *Journal of Lightwave Technology*, vol. 33, no. 8, pp. 1508–1514, 2015.

[119] R. Casellas, R. Munõz, R. Martínez, R. Vilalta, A. Mayoral, L. Liu, T. Tsuritani, and I. Morita, "Overarching Control of Flexi Grid Optical Networks: Interworking of GMPLS and OpenFlow Domains," *Journal of Lightwave Technology*, vol. 33, no. 5, pp. 1054–1062, 2015.

[120] Z. Zhu, X. Chen, C. Chen, S. Ma, M. Zhang, L. Liu, and S. J. B. Yoo, "OpenFlow-assisted online defragmentation in single-/multi-domain software-defined elastic optical networks [invited]," *IEEE/OSA Journal of Optical Communications and Networking*, vol. 7, no. 1, pp. A7–A15, 2015.

[121] N. Sambo, F. Paolucci, G. Meloni, F. Fresi, and t. y. v. n. p. d. L. Poti and P. Castoldi, journal=IEEE/OSA Journal of Optical Communications and Networking.

[122] J. Oliveira, J. Oliveira, E. Magalhaes, J. Januário, M. Siqueira, R. Scaraficci, M. Salvador, L. Mariote, N. Guerrero, L. Carvalho, F. van't Hooft, G. Santos, and M. Garrich, "Toward terabit autonomic optical networks based on a software defined adaptive/cognitive approach [invited]," *IEEE/OSA Journal of Optical Communications and Networking*, vol. 7, no. 3, pp. A421–A431, 2015.

[123] M. Svaluto Moreolo, J. M. Fabrega, L. Nadal, F. J. Vílchez, A. Mayoral, R. Vilalta, R. Munõz, R. Casellas, R. Martínez, M. Nishihara, T. Tanaka, T. Takahara, J. C. Rasmussen, C. Kottke, M. Schlosser, R. Freund, F. Meng, S. Yan, G. Zervas, D. Simeonidou, Y. Yoshida, and K. Kitayama, "SDN-Enabled Sliceable BVT Based on Multicarrier Technology for Multiflow Rate/Distance and Grid Adaptation," *Journal of Lightwave Technology*, vol. 34, no. 6, pp. 1516–1522, 2016.

[124] Y. Ou, S. Yan, A. Hammad, B. Guo, S. Peng, R. Nejabati, and D. Simeonidou, "Demonstration of Virtualizeable and Software-Defined Optical Transceiver," *Journal of Lightwave Technology*, vol. 34, no. 8, pp. 1916–1924, 2016.

[125] F. Pederzolli, M. Gerola, A. Zanardi, X. Forns, J. F. Ferran, and D. Siracusa, "YAMATO: The First SDN Control Plane for Independent, Joint, and Fractional-Joint Switched SDM Optical Networks," *Journal of Lightwave Technology*, vol. 35, no. 8, pp. 1335–1341, 2017.

[126] R. Casellas, R. Vilalta, R. Martínez, and R. Munõz, "Highly available SDN control of flexi-grid networks with network function virtualization-enabled replication," *IEEE/OSA Journal of Optical Communications and Networking*, vol. 9, no. 2, pp. A207–A215, 2017.

[127] F. Paolucci, A. Sgambelluri, F. Cugini, and P. Castoldi, "Network Telemetry Streaming Services in SDN-Based Disaggregated Optical Networks," *Journal of Lightwave Technology*, vol. 36, no. 15, pp. 3142–3149, 2018.

[128] R. Munõz, R. Vilalta, R. Casellas, R. Martínez, F. Francois, M. Channegowda, A. Hammad, S. Peng, R. Nejabati, D. Simeonidou, N. Yoshikane, T. Tsuritani, V. López, and A. Autenrieth, "Transport Network Orchestration for End-to-End Multilayer Provisioning Across Heterogeneous SDN/OpenFlow and GMPLS/PCE Control Domains," *Journal of Lightwave Technology*, vol. 33, no. 8, pp. 1540–1548, 2015.

[129] R. Munoz, R. Vilalta, R. Casellas, R. Martinez, T. Szyrkowiec, A. Autenrieth, V. Lopez, and D. Lopez, "Integrated SDN/NFV management and orchestration architecture for dynamic deployment of virtual SDN control instances for virtual tenant networks [invited]," *IEEE/OSA Journal of Optical Communications and Networking*, vol. 7, no. 11, pp. B62–B70, 2015.

[130] R. Casellas, R. Martinez, R. Munoz, R. Vilalta, and L. Liu, "Control and orchestration of multidomain optical networks with GMPLS as inter-SDN controller communication [Invited]," *IEEE/OSA Journal of Optical Communications and Networking*, vol. 7, no. 11, pp. B46–B54, 2015.

[131] R. Vilalta, R. Munoz, R. Casellas, R. Martinez, S. Peng, R. Nejabati, D. Simeonidou, N. Yoshikane, T. Tsuritani, I. Morita, V. Lopez, T. Szyrkowiec, and A. Autenrieth, "Multidomain network hypervisor for abstraction and control of openflow- enabled multitenant multitechnology transport networks [Invited]," *IEEE/OSA Journal of Optical Communications and Networking*, vol. 7, no. 11, pp. B55–B61, 2015.

[132] R. Vilalta, A. Mayoral, R. Munõz, R. Casellas, and R. Martínez, "Multitenant Transport Networks With SDN/NFV," *Journal of Lightwave Technology*, vol. 34, no. 6, pp. 1509–1515, 2016.

[133] Y. Li, W. Mo, S. Zhu, Y. Shen, J. Yu, P. Samadi, K. Bergman, and D. C. Kilper, "tSDX: enabling impairment-aware all-optical inter-domain exchange," *Journal of Lightwave Technology*, vol. 36, no. 1, pp. 142–154, 2017.

[134] S. Oda, M. Miyabe, S. Yoshida, T. Katagiri, Y. Aoki, J. C. Rasmussen, M. Birk, and K. Tse, "A Learning Living Network for Open ROADM Networks," in *ECOC 2016; 42nd European Conference on Optical Communication*, 2016, pp. 1–3.

[135] S. Oda, M. Miyabe, S. Yoshida, T. Katagiri, Y. Aoki, T. Hoshida, J. C. Rasmussen, M. Birk, and K. Tse, "A Learning Living Network With Open ROADMs," *Journal of Lightwave Technology*, vol. 35, no. 8, pp. 1350–1356, 2017.

[136] J. Kundrát, J. Vojtech, P. Skoda, R. Vohnout, J. Radil, and O. Havlis, "YANG/NETCONF ROADM: Evolving Open DWDM Toward SDN Applications," *Journal of Lightwave Technology*, vol. 36, no. 15, pp. 3105–3114, 2018.

[137] L. Velasco, A. Sgambelluri, R. Casellas, L. Gifre, J. Izquierdo-Zaragoza, F. Fresi, F. Paolucci, R. Martínez, and E. Riccardi, "Building Autonomic Optical Whitebox-Based Networks," *Journal of Lightwave Technology*, vol. 36, no. 15, pp. 3097–3104, 2018.

[138] A. Campanella, H. Okui, A. Mayoral, D. Kashiwa, O. G. de Dios, D. Verchere, Q. Pham Van, A. Giorgetti, R. Casellas, R. Morro, and L. Ong, "ODTN: Open Disaggregated Transport Network. Discovery and Control of a Disaggregated Optical Network through Open Source Software and Open APIs," in *2019 Optical Fiber Communications Conference and Exhibition (OFC)*, 2019, pp. 1–3.

[139] "Edge-core," https://www.edge-core.com/.

[140] J. Kundrát, O. Havlis, and t. y. v. n. p. d. J. Jedlinský and J. Vojtech, journal=Journal of Lightwave Technology.

[141] "Lumentum ROADM Graybox," https://www.lumentum.com/en/products/dci-roadm-graybox.

[142] A. Kushwaha, S. Sharma, N. Bazard, T. Das, and A. Gumaste, "A 400 Gb/s Carrier-Class SDN White-Box Design and Demonstration: The Bitstream Approach," *Journal of Lightwave Technology*, vol. 36, no. 15, pp. 3115–3130, 2018.

[143] V. Lopez, W. Ishida, A. Mayoral, T. Tanaka, O. G. de Dios, and J. P. Fernandez-Palacios, "Enabling fully programmable transponder white boxes [Invited]," *J. Opt. Commun. Netw.*, vol. 12, no. 2, pp. A214–A223, Feb 2020. [Online]. Available: http://jocn.osa.org/abstract.cfm?URI=jocn-12-2-A214

[144] A. Campanella, B. Yan, R. Casellas, A. Giorgetti, V. Lopez, Y. Zhao, and A. Mayoral, "Reliable Optical Networks With ODTN: Resiliency and Fail-Over in Data and Control Planes," *Journal of Lightwave Technology*, vol. 38, no. 10, pp. 2755–2764, 2020.

[145] T. Tanimura, S. Yoshida, K. Tajima, S. Oda, and T. Hoshida, "Fiber-Longitudinal Anomaly Position Identification Over Multi-Span Transmission Link Out of Receiver-end Signals," *Journal of Lightwave Technology*, vol. 38, no. 9, pp. 2726–2733, 2020.

[146] M. Bouda, S. Oda, O. Vassilieva, M. Miyabe, S. Yoshida, T. Katagiri, Y. Aoki, T. Hoshida, and T. Ikeuchi, "Accurate prediction of quality of transmission based on a dynamically configurable optical impairment model," *IEEE/OSA Journal of Optical Communications and Networking*, vol. 10, no. 1, pp. A102–A109, Jan 2018.

[147] F. Meng, A. Mavromatis, Y. Bi, R. Wang, S. Yan, R. Nejabati, and D. Simeonidou, "Self-learning monitoring on-demand strategy for optical networks," *IEEE/OSA Journal of Optical Communications and Networking*, vol. 11, no. 2, pp. A144–A154, 2019.

[148] Y. Pointurier, M. Coates, and M. Rabbat, "Active monitoring of all-optical networks," in *2008 10th Anniversary International Conference on Transparent Optical Networks*, vol. 1, 2008, pp. 169–172.

[149] Y. Pointurier, M. Coates, and M. Rabbat, "Cross-Layer Monitoring in Transparent Optical Networks," *IEEE/OSA Journal of Optical Communications and Networking*, vol. 3, no. 3, pp. 189–198, 2011.

[150] M. Angelou, Y. Pointurier, S. Azodolmolky, D. Careglio, S. Spadaro, and I. Tomkos, "A novel monitor placement algorithm for accurate performance monitoring in optical networks," in *2011 Optical Fiber Communication Conference and Exposition and the National Fiber Optic Engineers Conference*, 2011, pp. 1–3.

[151] I. Sartzetakis, K. Christodoulopoulos, and E. Varvarigos, "Improving QoT estimation accuracy through active monitoring," in *2017 19th International Conference on Transparent Optical Networks (ICTON)*, 2017, pp. 1–4.

[152] N. Sambo, P. Giardina, I. Sartzetakis, A. Sgambelluri, F. Fresi, M. Dallaglio, G. Meloni, G. Bernini, K. Christodoulopoulos, P. Castoldi, and E. Varvarigos, "Experimental Demonstration of Network Automation based on QoT Estimation and Monitoring in both Single- and Multi-Domains," in *2017 European Conference on Optical Communication (ECOC)*, 2017, pp. 1–3.

[153] S. Yan, A. Aguado, Y. Ou, R. Wang, R. Nejabati, and D. Simeonidou, "Multilayer network analytics with SDN-based monitoring framework," *IEEE/OSA Journal of Optical Communications and Networking*, vol. 9, no. 2, pp. A271–A279, 2017.

[154] L. Gifre, J. Izquierdo-Zaragoza, M. Ruiz, and L. Velasco, "Autonomic disaggregated multilayer networking," *IEEE/OSA Journal of Optical Communications and Networking*, vol. 10, no. 5, pp. 482–492, 2018.

[155] E. Seve, J. Pesic, C. Delezoide, A. Giorgetti, A. Sgambelluri, N. Sambo, S. Bigo, and Y. Pointurier, "Automated Fiber Type Identification in SDN-Enabled Optical Networks," *Journal of Lightwave Technology*, vol. 37, no. 7, pp. 1724–1731, 2019.

[156] P. Pavon-Marino, M. Bueno-Delgado, and J. Izquierdo-Zaragoza, "Evaluating internal blocking in noncontentionless flex-grid ROADMs [invited]," *IEEE/OSA Journal of Optical Communications and Networking*, vol. 7, no. 3, pp. A474–A481, 2015.

[157] J. I. Zaragoza and P. Pavon-Marino, "Assessing IP vs optical restoration using the open-source Net2Plan tool," in *2014 16th International Telecommunications Network Strategy and Planning Symposium (Networks)*, 2014, pp. 1–6.

[158] J. Pedreno-Manresa, J. Izquierdo-Zaragoza, and P. Pavon-Marino, "Joint fault tolerant and latency-aware design of multilayer optical networks," in *2016 International Conference on Optical Network Design and Modeling (ONDM)*, 2016, pp. 1–6.

[159] J. Izquierdo-Zaragoza, J. Pedreno-Manresa, P. Pavon-Marino, O. G. de Dios, and V. Lopez, "Dynamic operation of an IP/MPLS-over-WDM network using an open-source active stateful BGP-LS-enabled multilayer PCE," in *2016 18th International Conference on Transparent Optical Networks (ICTON)*, 2016, pp. 1–4.

[160] J. Izquierdo-Zaragoza, A. Fernandez-Gambin, J. Pedreno-Manresa, and P. Pavon-Marino, "Leveraging Net2Plan planning tool for network orchestration in OpenDaylight," in *2014 International Conference on Smart Communications in Network Technologies (SaCoNeT)*, 2014, pp. 1–6.

[161] M. Filer, M. Cantono, A. Ferrari, G. Grammel, G. Galimberti, and V. Curri, "Multi-Vendor Experimental Validation of an Open Source QoT Estimator for Optical Networks," *Journal of Lightwave Technology*, vol. 36, no. 15, pp. 3073–3082, 2018.

[162] A. Ferrari, K. Balasubramanian, M. Filer, Y. Yin, E. Le Rouzic, J. Kundrat, G. Grammel, G. Galimberti, and V. Curri, "Assessment on the in-field lightpath QoT computation including connector loss uncertainties," *IEEE/OSA Journal of Optical Communications and Networking*, vol. 13, no. 2, pp. A156–A164, 2021.

[163] S. Barzegar, M. Ruiz, and L. Velasco, "Soft-Failure Localization and Time-Dependent Degradation Detection for Network Diagnosis," in *2020 22nd International Conference on Transparent Optical Networks (ICTON)*, 2020, pp. 1–4.

[164] G. Borraccini, S. Straullu, A. Ferrari, E. Virgillito, S. Bottacchi, S. Swail, S. Piciaccia, G. Galimberti, G. Grammel, and V. Curri, "Using QoT-E for Open Line Controlling and Modulation Format Deployment: an Experimental Proof of Concept," in *2020 European Conference on Optical Communications (ECOC)*, 2020, pp. 1–4.

[165] J. Kundrát, A. Campanella, E. L. Rouzic, A. Ferrari, O. Havlis, and t. y. v. n. p. d. M. Hazlinský and G. Grammel and G. Galimberti and V. Curri, booktitle=2020 Optical Fiber Communications Conference and Exhibition (OFC).

[166] A. Campanella *et al.*, "Reliable optical networks with ODTN: Resiliency and fail-over in data and control planes," *Journal of Lightwave Technology*, vol. 38, no. 10, pp. 2755–2764, 2020.

[167] T. Zami, A. Morea, and N. Brogard, "Impact of routing on the transmission performance in a partially transparent optical network," in *National Fiber Optic Engineers Conference*. Optical Society of America, 2008, p. JThA50.

[168] A. Morea, N. Brogard, F. Leplingard, J.-C. Antona, T. Zami, B. Lavigne, and D. Bayart, "QoT function and A* routing: an optimized combination for connection search in translucent networks," *Journal of Optical Networking*, vol. 7, no. 1, pp. 42–61, 2008.

[169] F. Leplingard, T. Zami, A. Morea, N. Brogard, and D. Bayart, "Determination of the impact of a quality of transmission estimator margin on the dimensioning of an optical network," in *Optical Fiber Communication Conference*. Optical Society of America, 2008, p. OWA6.

[170] F. Leplingard, A. Morea, T. Zami, and N. Brogard, "Interest of an adaptive margin for the quality of transmission estimation for lightpath establishment," in *Optical Fiber Communication Conference*. Optical Society of America, 2009, p. OWI6.

[171] A. Morea, T. Zami, and F. Leplingard, "Introduction of confidence levels for transparent network planning," in *2009 35th European Conference on Optical Communication*. IEEE, 2009, pp. 1–2.

[172] N. Sambo, C. Pinart, E. Le Rouzic, F. Cugini, L. Valcarenghi, and P. Castoldi, "Signaling and multi-layer probe-based schemes for guaranteeing QoT in GMPLS transparent networks," in *2009 Conference on Optical Fiber Communication*, 2009, pp. 1–3.

[173] C. Pinart, N. Sambo, E. Rouzic, F. Cugini, and P. Castoldi, "Probe Schemes for Quality-of-Transmission-Aware Wavelength Provisioning," *IEEE/OSA Journal of Optical Communications and Networking*, vol. 3, no. 1, pp. 87–94, 2011.

[174] Y. Pointurier, S. Azodolmolky, M. Angelou, and I. Tomkos, "Issues and challenges in physical-layer aware optically switched network design and operation," in *2009 International Conference on Photonics in Switching*, 2009, pp. 1–1.

[175] N. Sambo, Y. Pointurier, F. Cugini, L. Valcarenghi, P. Castoldi, and I. Tomkos, "Lightpath Establishment Assisted by Offline QoT Estimation in Transparent Optical Networks," *IEEE/OSA Journal of Optical Communications and Networking*, vol. 2, no. 11, pp. 928–937, 2010.

[176] F. Paolucci, N. Sambo, F. Cugini, A. Giorgetti, and P. Castoldi, "Experimental Demonstration of Impairment-Aware PCE for Multi-Bit-Rate WSONs," *IEEE/OSA Journal of Optical Communications and Networking*, vol. 3, no. 8, pp. 610–619, 2011.

[177] S. Azodolmolky, Y. Pointurier, M. Angelou, J. Solé-Pareta, and I. Tomkos, "Routing and wavelength assignment for transparent optical networks with QoT estimation inaccuracies," in *2010 Conference on Optical Fiber Communication (OFC/NFOEC), collocated National Fiber Optic Engineers Conference*, 2010, pp. 1–3.

[178] S. Azodolmolky, Y. Pointurier, M. Angelou, D. Careglio, J. Solé-Pareta, and I. Tomkos, "A Novel Impairment Aware RWA Algorithm With Consideration of QoT Estimation Inaccuracy," *IEEE/OSA Journal of Optical Communications and Networking*, vol. 3, no. 4, pp. 290–299, 2011.

[179] Y. Qin, Y. Pointurier, E. Escalona, S. Azodolmolky, M. Angelou, I. Tomkos, K. Ramantas, K. Vlachos, R. Nejabati, and D. Simeonidou, "Hardware accelerated impairment aware control plane," in *2010 Conference on Optical Fiber Communication (OFC/NFOEC), collocated National Fiber Optic Engineers Conference*, 2010, pp. 1–3.

[180] Y. Qin, K. C. S. Cheng, J. Triay, E. Escalona, G. S. Zervas, G. Zarris, N. Amaya-Gonzalez, C. Cervelló-Pastor, R. Nejabati, and D. Simeonidou, "Demonstration of C/S based hardware accelerated QoT estimation tool in dynamic impairment-aware optical network," in *36th European Conference and Exhibition on Optical Communication*, 2010, pp. 1–3.

[181] I. Tomkos, S. Azodolmolky, D. Klonidis, M. Aggelou, and K. Margariti, "Dynamic impairment aware networking for transparent mesh optical networks: Activities of EU project DICONET," in *2008 10th Anniversary International Conference on Transparent Optical Networks*, vol. 1, 2008, pp. 6–12.

[182] T. Zami, A. Morea, and F. Leplingard, "A new method to plan more realistic optical transparent networks," *Bell Labs Technical Journal*, vol. 14, no. 4, pp. 213–226, 2010.

[183] B. Garcia-Manrubia, P. Pavon-Marino, R. Aparicio-Pardo, M. Klinkowski, and D. Careglio, "Offline Impairment-Aware RWA and Regenerator Placement in Translucent Optical Networks," *Journal of Lightwave Technology*, vol. 29, no. 3, pp. 265–277, 2011.

[184] G. Bottari, G. Bruno, D. Caviglia, and D. Ceccarelli, "Evolutive lightpath assessment in GMPLS-controlled transparent optical networks," in *2011 Optical Fiber Communication Conference and Exposition and the National Fiber Optic Engineers Conference*, 2011, pp. 1–3.

[185] t. y. v. n. p. d. J. Perelló and S. Spadaro and F. Agraz and M. Angelou and S. Azodolmolky and Y. Qin and R. Nejabati and D. Simeonidou and P. Kokkinos and E. Varvarigos and S. Al Zahr and M. Gagnaire and I. Tomkos, booktitle=2011 Optical Fiber Communication Conference and Exposition and the National Fiber Optic Engineers Conference.

[186] T. Zami, "Physical impairment aware planning of next generation WDM backbone networks," in *Optical Fiber Communication Conference*. Optical Society of America, 2012, pp. OW3A–3.

[187] I. Sartzetakis, K. Christodoulopoulos, C. Tsekrekos, D. Syvridis, and E. Varvarigos, "Quality of transmission estimation in WDM and elastic optical networks accounting for space–spectrum dependencies," *IEEE/OSA Journal of Optical Communications and Networking*, vol. 8, no. 9, pp. 676–688, 2016.

[188] M. Bouda, S. Oda, O. Vasilieva, M. Miyabe, S. Yoshida, T. Katagiri, Y. Aoki, T. Hoshida, and T. Ikeuchi, "Accurate prediction of quality of transmission with dynamically configurable optical impairment model," in *2017 Optical Fiber Communications Conference and Exhibition (OFC)*, March 2017, pp. 1–3.

[189] T. Panayiotou, S. P. Chatzis, and G. Ellinas, "Performance analysis of a data-driven quality-of-transmission decision approach on a dynamic multicast-capable metro optical network," *Journal of Optical Communications and Networking*, vol. 9, no. 1, pp. 98–108, 2017.

[190] M. Cantono, D. Pilori, A. Ferrari, C. Catanese, J. Thouras, J. Augé, and V. Curri, "On the Interplay of Nonlinear Interference Generation With Stimulated Raman Scattering for QoT Estimation," *Journal of Lightwave Technology*, vol. 36, no. 15, pp. 3131–3141, 2018.

[191] C. Delezoide, P. Ramantanis, and P. Layec, "Weighted Filter Penalty Prediction for QoT Estimation," in *2018 Optical Fiber Communications Conference and Exposition (OFC)*, 2018, pp. 1–3.

[192] T. Zhang, A. Samadian, A. Shakeri, B. Mirkhanzadeh, C. Shao, M. Razo, M. Tacca, A. Ferrari, M. Cantono, V. Curri, G. Martinelli, G. M. Galimberti, T. Xia, G. Wellbrock, and A. Fumagalli, "A WDM Network Controller With Real-Time Updates of the Physical Layer Abstraction," *Journal of Lightwave Technology*, vol. 37, no. 16, pp. 4073–4080, 2019.

[193] J. Zhao, B. Bao, H. Yang, E. Oki, and B. C. Chatterjee, "Holding-time- and impairment-aware shared spectrum allocation in mixed-line-rate elastic optical networks," *IEEE/OSA Journal of Optical Communications and Networking*, vol. 11, no. 6, pp. 322–332, 2019.

[194] R. J. Vincent, D. J. Ives, and S. J. Savory, "Scalable Capacity Estimation for Nonlinear Elastic All-Optical Core Networks," *Journal of Lightwave Technology*, vol. 37, no. 21, pp. 5380–5391, 2019.

[195] E. Virgillito, A. D'Amico, A. Ferrari, and V. Curri, "Observing and Modeling Wideband Generation of Non-Linear Interference," in *2019 21st International Conference on Transparent Optical Networks (ICTON)*, 2019, pp. 1–4.

[196] L. Barletta, A. Giusti, C. Rottondi, and M. Tornatore, "QoT estimation for unestablished lighpaths using machine learning," in *2017 Optical Fiber Communications Conference and Exhibition (OFC)*, March 2017, pp. 1–3.

[197] C. Rottondi, L. Barletta, A. Giusti, and M. Tornatore, "Machine-learning method for quality of transmission prediction of unestablished lightpaths," *IEEE/OSA Journal of Optical Communications and Networking*, vol. 10, no. 2, pp. A286–A297, Feb 2018.

[198] J. Mata, I. de Miguel, R. J. Durán, J. C. Aguado, N. Merayo, L. Ruiz, P. Fernández, R. M. Lorenzo, and E. J. Abril, "A SVM approach for lightpath QoT estimation in optical transport networks," in *2017 IEEE International Conference on Big Data (Big Data)*, Dec 2017, pp. 4795–4797.

[199] J. Mata, I. d. Miguel, R. J. Durán, J. C. Aguado, N. Merayo, L. Ruiz, P. Fernández, R. M. Lorenzo, E. J. Abril, and I. Tomkos, "Supervised Machine Learning Techniques for Quality of Transmission Assessment in Optical Networks," in *2018 20th International Conference on Transparent Optical Networks (ICTON)*, July 2018, pp. 1–4.

[200] S. Aladin and C. Tremblay, "Cognitive Tool for Estimating the QoT of New Lightpaths," in *2018 Optical Fiber Communications Conference and Exposition (OFC)*, March 2018, pp. 1–3.

[201] C. Tremblay and S. Aladin, "Machine Learning Techniques for Estimating the Quality of Transmission of Lightpaths," in *2018 IEEE Photonics Society Summer Topical Meeting Series (SUM)*, July 2018, pp. 237–238.

[202] R. M. Morais and J. Pedro, "Evaluating Machine Learning Models for QoT Estimation," in *2018 20th International Conference on Transparent Optical Networks (ICTON)*, July 2018, pp. 1–4.

[203] R. M. Morais and J. Pedro, "Machine learning models for estimating quality of transmission in DWDM networks," *IEEE/OSA Journal of Optical Communications and Networking*, vol. 10, no. 10, pp. D84–D99, Oct 2018.

[204] F. Meng, S. Yan, R. Wang, Y. Ou, Y. Bi, R. Nejabati, and D. Simeonidou, "Robust Self-Learning Physical Layer Abstraction Utilizing Optical Performance Monitoring and Markov Chain Monte Carlo," in *2017 European Conference on Optical Communication (ECOC)*, Sept 2017, pp. 1–3.

[205] G. Liu, K. Zhang, X. Chen, H. Lu, J. Guo, J. Yin, R. Proietti, Z. Zhu, and S. J. Ben Yoo, "The First Testbed Demonstration of Cognitive End-to-End Optical Service Provisioning with Hierarchical Learning across Multiple Autonomous Systems," in *2018 Optical Fiber Communications Conference and Exposition (OFC)*, 2018, pp. 1–3.

[206] W. Mo, C. L. Gutterman, Y. Li, S. Zhu, G. Zussman, and D. C. Kilper, "Deep-neural-network-based wavelength selection and switching in ROADM systems," *IEEE/OSA Journal of Optical Communications and Networking*, vol. 10, no. 10, pp. D1–D11, Oct 2018.

[207] E. Seve, J. Pesic, C. Delezoide, S. Bigo, and Y. Pointurier, "Learning process for reducing uncertainties on network parameters and design margins," *IEEE/OSA Journal of Optical Communications and Networking*, vol. 10, no. 2, pp. A298–A306, 2018.

[208] R. Proietti, X. Chen, A. Castro, G. Liu, H. Lu, K. Zhang, J. Guo, Z. Zhu, L. Velasco, and S. J. B. Yoo, "Experimental Demonstration of Cognitive Provisioning and Alien Wavelength Monitoring in Multi-domain EON," in *2018 Optical Fiber Communications Conference and Exposition (OFC)*, 2018, pp. 1–3.

[209] R. Proietti, X. Chen, K. Zhang, G. Liu, M. Shamsabardeh, A. Castro, L. Velasco, Z. Zhu, and S. J. Ben Yoo, "Experimental demonstration of machine-learning-aided qot estimation in multi-domain elastic optical networks with alien wavelengths," *IEEE/OSA Journal of Optical Communications and Networking*, vol. 11, no. 1, pp. A1–A10, 2019.

[210] R. Proietti, X. Chen, K. Zhang, G. Liu, M. Shamsabardeh, A. Castro, L. Velasco, Z. Zhu, and S. J. Ben Yoo, "Experimental demonstration of machine-learning-aided qot estimation in multi-domain elastic optical networks with alien wavelengths," *IEEE/OSA Journal of Optical Communications and Networking*, vol. 11, no. 1, pp. A1–A10, 2019.

[211] M. Salani, C. Rottondi, and M. Tornatore, "Routing and Spectrum Assignment Integrating Machine-Learning-Based QoT Estimation in Elastic Optical Networks," in *IEEE INFOCOM 2019 - IEEE Conference on Computer Communications*, 2019, pp. 1738–1746.

[212] I. Sartzetakis, K. K. Christodoulopoulos, and E. M. Varvarigos, "Accurate quality of transmission estimation with machine learning," *IEEE/OSA Journal of Optical Communications and Networking*, vol. 11, no. 3, pp. 140–150, 2019.

[213] V. Curri, A. D'Amico, and S. Straullu, "Synergetical Use of Analytical Models and Machine-Learning for Data Transport Abstraction in Open Optical Networks," in *2019 21st International Conference on Transparent Optical Networks (ICTON)*, 2019, pp. 1–4.

[214] R. Casellas, R. Martínez, R. Vilalta, and R. Muñoz, "Control, management, and orchestration of optical networks: evolution, trends, and challenges," *Journal of Lightwave Technology*, vol. 36, no. 7, pp. 1390–1402, 2018.

[215] J. Bai, Y. Shen, C. Xu, and G. Gao, "Influence of inter-channel nonlinear interference on the QoT estimation for elastic optical fiber networks," in *2019 18th International Conference on Optical Communications and Networks (ICOCN)*, 2019, pp. 1–3.

[216] M. Tornatore, "Machine Learning Applications in Optical Networks," in *2019 24th Opto-Electronics and Communications Conference (OECC) and 2019 International Conference on Photonics in Switching and Computing (PSC)*, 2019, pp. 1–1.

[217] D. C. Kilper and Y. Li, "Optical Physical Layer SDN: Enabling Physical Layer Programmability through Open Control Systems," in *Optical Fiber Communication Conference*. Optical Society of America, 2017, p. W1H.3. [Online]. Available: http://www.osapublishing.org/abstract.cfm?URI=OFC-2017-W1H.3

[218] M. Zirngibl, "Analytical model of Raman gain effects in massive wavelength division multiplexed transmission systems," *Electronics Letters*, vol. 34, no. 8, pp. 789–790, April 1998.

[219] P. Poggiolini, Y. Jiang, A. Carena, and F. Forghieri, "Analytical modeling of the impact of fiber non-linear propagation on coherent systems and networks," *Enabling Technologies for High Spectral-Efficiency Coherent Optical Communication Networks*, 2016.

[220] W. Mo, S. Zhu, Y. Li, and D. C. Kilper, "Dual-wavelength source based optical circuit switching and wavelength reconfiguration in multi-hop ROADM systems," *Opt. Express*, vol. 25, no. 22, pp. 27 736–27 749, 2017.

[221] P. Poggiolini, G. Bosco, A. Carena, V. Curri, Y. Jiang, and F. Forghieri, "A detailed analytical derivation of the GN model of non-linear interference in coherent optical transmission systems," *arXiv preprint arXiv:1209.0394*, 2012.

[222] J. Junio, D. C. Kilper, and V. W. Chan, "Channel power excursions from single-step channel provisioning," *IEEE/OSA Journal of Optical Communications and Networking*, vol. 4, no. 9, pp. A1–A7, 2012.

[223] C. Gutterman, A. Minakhmetov, J. Yu, M. Sherman, T. Chen, S. Zhu, I. Seskar, D. Raychaudhuri, D. Kilper, and G. Zussman, "programmable optical x-haul network in the cosmos testbed," in *2019 IEEE 27th International Conference on Network Protocols (ICNP)*.

[224] J. Yu, T. Chen, C. Gutterman, S. Zhu, G. Zussman, I. Seskar, and D. Kilper, "COSMOS: Optical Architecture and Prototyping," in *2019 Optical Fiber Communications Conference and Exhibition (OFC)*, 2019, pp. 1–3.

[225] M. Ghobadi, J. Gaudette, R. Mahajan, A. Phanishayee, B. Klinkers, and D. Kilper, "Evaluation of elastic modulation gains in microsoft's optical backbone in North America," in *2016 Optical Fiber Communications Conference and Exhibition (OFC)*, March 2016, pp. 1–3.

[226] B. Lantz, A. A. Díaz-Montiel, J. Yu, C. Rios, M. Ruffini, and D. Kilper, "Demonstration of software-defined packet-optical network emulation with Mininet-Optical and ONOS," in *Optical Fiber Communication Conference*. Optical Society of America, 2020, pp. M3Z–9.

[227] R. Muńoz, R. Casellas, and t. y. v. n. p. k. d. I. m. R. Martínez, booktitle=2011 37th European Conference and Exhibition on Optical Communication.

[228] F. Meng, Y. Ou, S. Yan, K. Sideris, M. D. G. Pascual, R. Nejabati, and D. Simeonidou, "Field Trial of a Novel SDN Enabled Network Restoration Utilizing In-Depth Optical Performance Monitoring Assisted Network Re-Planning," in *Optical Fiber Communication Conference*. Optical Society of America, 2017, p. Th1J.8. [Online]. Available: http://www.osapublishing.org/abstract.cfm?URI=OFC-2017-Th1J.8

[229] K. Christodoulopoulos, I. Sartzetakis, P. Soumplis, and E. Varvarigos, "Cross-layer and dynamic network orchestration based on optical performance monitoring," in *2017 International Conference on Optical Network Design and Modeling (ONDM)*, May 2017, pp. 1–6.

[230] O. Gerstel, M. Jinno, A. Lord, and S. B. Yoo, "Elastic optical networking: A new dawn for the optical layer?" *IEEE Communications Magazine*, vol. 50, no. 2, pp. s12–s20, 2012.

[231] Y. Yin, L. Liu, R. Proietti, and S. B. Yoo, "Software defined elastic optical networks for cloud computing," *IEEE Network*, vol. 31, no. 1, pp. 4–10, 2016.

[232] "CPqD Software Switch," https://github.com/CPqD/ofsoftswitch13.

[233] D. Gorinevsky and G. Farber, "System analysis of power transients in advanced WDM networks," *Journal of lightwave technology*, vol. 22, no. 10, p. 2245, 2004.

[234] L. Pavel, "Dynamics and stability in optical communication networks: a system theory framework," *Automatica*, vol. 40, no. 8, pp. 1361–1370, 2004.

[235] D. Kilper, S. Chandrasekhar, and C. White, "Transient gain dynamics of cascaded erbium doped fiber amplifiers with re-configured channel loading," in *Optical Fiber Communication Conference*. Optical Society of America, 2006, p. OTuK6.

[236] R. Wang, S. Bidkar, F. Meng, R. Nejabati, and D. Simeonidou, "Load-aware nonlinearity estimation for elastic optical network resource optimization and management," *IEEE/OSA Journal of Optical Communications and Networking*, vol. 11, no. 5, pp. 164–178, 2019.

[237] F. Locatelli, K. Christodoulopoulos, M. S. Moreolo, J. M. FÃ brega, and S. Spadaro, "Machine Learning-Based in-Band OSNR Estimation From Optical Spectra," *IEEE Photonics Technology Letters*, vol. 31, no. 24, pp. 1929–1932, 2019.

[238] T. Liao, L. Xue, W. Hu, and L. Yi, "Unsupervised Learning for Neural Network-Based Blind Equalization," *IEEE Photonics Technology Letters*, vol. 32, no. 10, pp. 569–572, 2020.

[239] A. A. Díaz-Montiel, J. Yu, W. Mo, Y. Li, D. C. Kilper, and M. Ruffini, "Performance analysis of QoT estimator in SDN-controlled ROADM networks," in *2018 International Conference on Optical Network Design and Modeling (ONDM)*, May 2018, pp. 142–147.

[240] J. Junio, D. C. Kilper, and V. W. S. Chan, "Channel Power Excursions From Single-Step Channel Provisioning," *J. Opt. Commun. Netw.*, vol. 4, no. 9, pp. A1–A7, Sep 2012. [Online]. Available: http://jocn.osa.org/abstract.cfm?URI=jocn-4-9-A1

[241] J. Cervantes, F. Garcia-Lamont, L. Rodríguez-Mazahua, and A. Lopez, "A comprehensive survey on support vector machine classification: Applications, challenges and trends," *Neurocomputing*, vol. 408, pp. 189 – 215, 2020. [Online]. Available: http://www.sciencedirect.com/science/article/pii/S0925231220307153

[242] F. Pedregosa, G. Varoquaux, A. Gramfort, V. Michel, B. Thirion, O. Grisel, M. Blondel, P. Prettenhofer, R. Weiss, V. Dubourg, J. Vanderplas, A. Passos, D. Cournapeau, M. Brucher, M. Perrot, and E. Duchesnay, "Scikit-learn: Machine Learning in Python," *Journal of Machine Learning Research*, vol. 12, pp. 2825–2830, 2011.